공학석사 학위논문

선박용 강재의 도장면 제거를 위한 Q-스위칭 파이버 레이저 클리닝에 관한 기초 연구

A Fundamental Study on Q-switching Fiber Laser Cleaning Process for Removing Paint Layer of Steel Surface for Shipbuilding

지도교수 김 종 도

2020년 2월

한국해양대학교 해양과학기술전문대학원

해양과학기술융합학과

김 지 언

본 논문을 김지연의 공학석사 학위논문으로 인준함.

위원장 이 명 훈 (인)

위 원 강 준 (인)

위 원 김 종 도 (인)

2019년 12월 17일

한국해양대학교 해양과학기술전문대학원

Contents

List of Tables

List of Figures

선박용 강재의 도장면 제거를 위한 Q-스위칭 파이버 레이저 클리닝에 관한 기초 연구

김지언

한국해양대학교 해양과학기술전문대학원
해양과학기술융합학과

초록

현재 조선해양 산업 현장에서 도장 전처리 작업은 그라인딩 및 쇼트 방식을 채택하고 있으나 동력 공구에 의한 작업자의 위험성 및 분진 비산에 의한 환경오염과 작업자의 건강문제가 지속적으로 야기되고 있다. 또한 현재의 전처리 방법으로는 협소구역의 접근이 난해하고 모서리 등의 개소와 복잡한 형상에 대한 작업이 어려우며 모재의 손상을 유발하고 표면의 균일한 클리닝이 어렵다는 단점을 가지고 있다. 반면, 레이저 열원을 이용한 표면 클리닝 기술은 공정 중 환경오염 물질의 배출이 거의 없는 친환경 기술이다. 레이저의 우수한 제어 특성으로 인하여 표면의 오염층만을 선택적으로 제거할 수 있으며 국부적인 표면 클리닝이 가능하기 때문에 작업 시간이 단축되고 모재의 손상을 최소화 할 수 있다. 또한 비 접촉식 공정으로 다양한 표면 형상에 적용이 가능하다는 장점이 있다. 이러한 장점으로 인하여 문화재 복원 사업은 물론이며 금형, 전기・전자 및 반도체 산업에서 레이저 클리닝 기술은 이미 실용화 단계에 접어들었다. 또한 최근에는 대면적의 표면 전처리 공정에 레이저 클리닝을 도입하고자 하는 수요가 증가하면서 조선해양 산업, 항공

우주 산업 및 자동차 산업 등에 실용화가 기대되고 있다. 특히 조선해양 산업에서 레이저를 이용한 클리닝 기술 수준은 초기 단계이며 기존의 클리닝 기술을 대체하고자 다양한 연구가 진행중이다. 따라서 국내 기술수요에 적극 대처하고 향후 작업효율과 작업환경의 개선을 통해서 조선해양 산업 도장 전처리의 패러다임을 변화하기 위해 레이저 클리닝 기술을 확보하는 것이 시급하다.

본 연구에서는 평균 출력 100 W의 Q-스위칭 파이버 레이저를 이용하여 강재 표면의 도장면 및 산화층을 제거하기 위해 레이저 클리닝 실험을 진행하였다. 기초실험으로써 실제 조선해양 산업에 적용되는 에폭시 및 숍프라이머 도장면과 국부적인 발청 수준인 얇은 산화층에 대해 스캔횟수, 펄스 중첩률, 패스 중첩률 및 에너지 밀도에 따른 레이저 클리닝을 실시하였다. 이와 같이 다양한 변수에서 얻어진 클리닝부의 특성을 분석하였으며, 레이저 클리닝 효율을 계산하여 최적의 조건을 도출하였다. 결과적으로 모재의 손상 및 열영향부 없는 우수한 클리닝 부를 얻을 수 있었다.

키워드: 레이저 클리닝 프로세스;
친환경 기술;
에폭시 도장면;
숍프라이머 도장면;
레이저 클리닝부;
레이저 클리닝 효율;

Chapter 1 Introduction

1.1 Research background and purpose

With a growing awareness of the need to address environmental problems such as air pollution, the abundance of fine plastics, and climate change, numerous efforts are being made to reduce environmental pollution in various industries[1, 2]. Therefore, the shipbuilding and marine industries have been increasingly showing interest in environmentally friendly surface pretreatment technologies, which can replace the current welding and painting pretreatment methods that contribute to environmental pollution. Unlike the general manufacturing industry, shipyards must utilize a number of outdoor activities that are difficult or impossible to conduct in the confines of a pollution reducing facility. Environmental complaints are frequently raised the vicinity of ship-related manufacturing sites, where paint dust generated during the paint removal process is spread into the surrounding area. The fine dust generated in an enclosed area is detrimental to worker health and delays the work time owing to a contamination of the surrounding high-cost equipment and inter-process interference. It is therefore necessary to develop a surface pretreatment technology using an eco-friendly laser cleaning technology as an alternative to the current pretreatment technology[3 ~ 7].

Laser cleaning is a process for selectively evaporating and removing only surface contaminants without damaging the base metal by irradiating a high density laser beam onto the surface of the material, as shown in Fig. 1.1 (a). Current surface pretreatment technologies such as mechanical and chemical cleaning, shown in Fig. 1 (b) and (c), have a disadvantage in that they damage the base metal through a deformation or corrosion during the cleaning process, making it difficult to clean the surface in a uniform manner.

In addition, the generation of secondary pollutants such as fine dust and chemical solvents lowers worker safety and creates environmental pollution. In particular, such treatment approaches have difficulty accessing narrow areas and complex shapes. Laser cleaning, by contrast, is a dry cleaning technology with little pollutant emissions. In addition, owing to the excellent controllability of the laser, a selective and local cleaning is possible, which reduces the work time and minimizes damage to the base metal[8 ~ 17].

Owing to the advantages of the above-mentioned laser cleaning technology, such an approach has been applied to the removal of corrosives and oxides remaining on the surfaces of iron and bronze artifacts[18 ~ 22]. In addition, Trelenberg et al. applied laser cleaning to a semiconductor material[23], and Dumitru et al. and Beaudoin et al. both studied a laser cleaning technology applying the laser ablation mechanism of carbon thin films and silicon used in electrical and electronic components[24, 25]. The use of a short pulse laser has also significantly improved the product quality, and laser cleaning technology has already been put into practical use in such industries. Various industries have recently begun reviewing the applicability of this technique owing to an increase in demand for introduction of laser cleaning to large-area surface treatment procedures. Mohammad et al. attempted to introduce laser cleaning to remove the coating on the surface of automobile plates[8]. AlShaer et al. significantly reduced defects by applying laser cleaning as a welding pretreatment process to improve the weldability of aluminum materials, which are most actively used as lightweight materials in the automotive industry[9]. Extensive research has been carried out in the aerospace industry, including the removal of sulfide layers deposited on impeller blades and the application of laser cleaning to titanium, the main material used in gas turbines[7, 16, 26]. Finally, D'Addona et al. reported an improved weld quality by applying laser cleaning to a welding pretreatment during the shipbuilding process[5]. In addition, if the current surface pretreatment technology is replaced with laser cleaning in these various industrial fields, the costs will be significantly reduced, as shown in Table 1.1[15, 26 ~ 29]. Furthermore, research on conventional laser cleaning from the viewpoint of experimental materials has mainly focused on the removal of surface contaminants such as oil, grease, dust and coating layers, as well as surface oxide layers such as aluminum, titanium and copper[15-17, 26, 28].

As described above, studies on the pretreatment of welds and the removal of oxide layers and contaminants on metal materials have been continuously conducted in various industrial fields. However, in the shipbuilding and offshore industries, there have been few studies on the removal of paint, particularly on a steel surface used for shipbuilding. Therefore, in this study, research on the removal of the paint and oxide layer on the steel for shipbuilding was carried out. Using a laser, which is an eco-friendly energy source, we can overcome the limitations of current technologies and secure a high-quality and high-efficiency surface treatment applicable to the shipbuilding and offshore industries. In addition, this fundamental study will supply an important data on the application of a laser cleaning technology, the interest of which has increased in various industries.

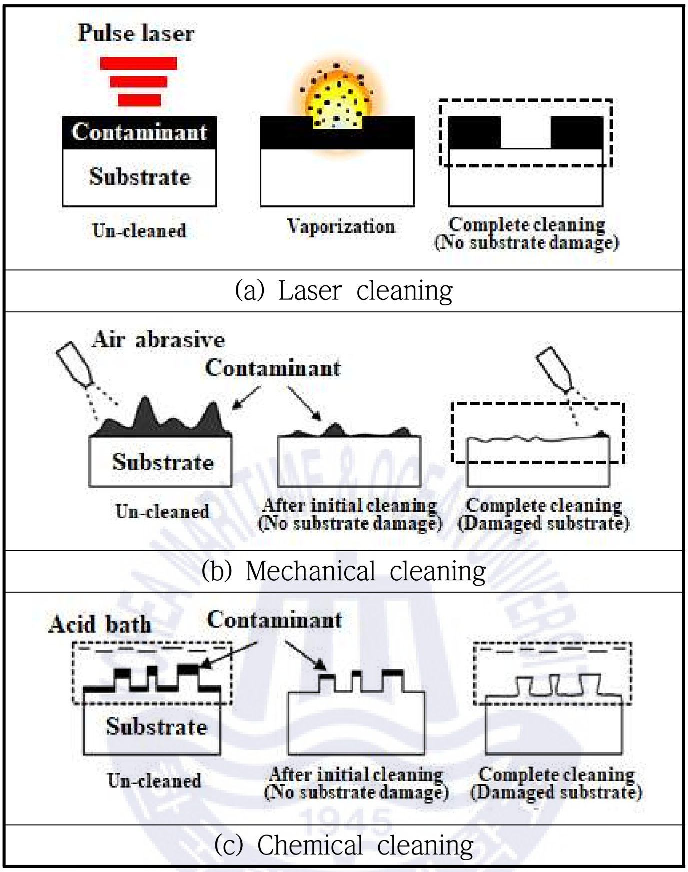

Fig. 1.1 Types of surface pre-treatment processes

Table 1.1 Percentage of cost comparison between current technology and laser cleaning techniques of four available applications

No.	Available cleaning application	Current cleaning technology	Cost of cleaning with Current technology	Cost of cleaning with laser technology
1	Storage tank	Sand blasting	95 % – 100 %	42.79 %
2	Navy parts	Burn-off oven	100 %	126.3 %
3	Aircraft	Chemical cleaning	100 %	71.36 %
4	Ground vehicles	Media blasting	100 %	54.9 %

1.2 Research contents

The steel used in ships is easily exposed to corrosive environments such as seawater, and thus becomes rusted when exposed to such environments for a lengthy period of time. Contaminants such as rust, paint, grease and dust on the surface of a steel material lower the efficiency and quality during the welding and painting processes and should be removed through a surface cleaning technology. Laser cleaning applied to a surface can remove contaminants in an environmentally friendly manner without damaging the base metal. The laser cleaning of the paint and oxide layer on the surface of a metal material involves both laser ablation and thermal process mechanisms, and thus the laser cleaning results are clearly different depending on the process parameters applied. The main process parameters can be largely divided into laser and material parameters. Therefore, this study aims to derive the optimum efficiency achievable by analyzing the laser cleaning results according to the process parameters used for epoxy and shop primer paints with different properties.

The details of this study are as follows.

(1) Characteristics of laser cleaned surface according to the process parameters

The characteristics of a laser cleaned surface according to the process parameters were determined by comparing and analyzing the shape of the surface and the cross-section and roughness of the cleaned surface formed when changing the number of scans, the overlap rate of the laser beam and the energy density, which are the main process parameters used for laser cleaning on epoxy and shop primer painted steel plates.

(2) Component analysis of the laser cleaned surface

To determine whether the paint and oxide layer remain on the surface of a laser cleaned surface under each condition, a component analysis of a laser cleaned surface was conducted using EDS and XRD.

(3) Analysis of laser cleaning efficiency

Through laser cleaning experiments applied according to the process parameters, the optimum conditions were derived by comparing one scan time of a 15 mm × 15 mm area under each condition with the laser cleaning efficiency calculated from the thickness of the paint and oxide layer removed at that scan time.

(4) Comparison of evaporation characteristics based on paint type

To analyze the effect of the material parameters on the laser cleaning results, the evaporation characteristics of epoxy and shop primer paints with different evaporation points were compared.

(5) Evaluation of mechanical characteristics of laser cleaned area

To determine the mechanical characteristics of the cleaned area according to the heat input into the base metal, the hardness was measured in the longitudinal direction of the laser cleaned surface under optimum efficiency and maximum heat input conditions, and then compared with the base metal.

(6) Evaluation of microstructure characteristics of laser cleaned area

The microstructure of the cleaned area was compared and analyzed using an optical microscope and a scanning electron microscope under optimum efficiency and maximum heat input conditions to identify the damage of the base material, the melted zone and the heat affected zone.

Chapter 2 Theoretical Background

2.1 Paint types and coating characteristics

2.1.1 Composition of paint

(1) Epoxy resin

Epoxy resin is a representative thermosetting resin that has a 3D network structure through curing process. It was first commercialized in the 1940's and is an industrially critical material of which the consumption is increasing every year because of its excellent properties such as heat resistance, corrosion resistance, adhesion and insulation, as well as diverse uses and applications including coating, adhesives, electric and electronic materials and composite materials. In particular, epoxy resin is a representative resin used in anticorrosive paint.

Epoxy resin reacts with polymers containing di- and poly-functional active hydrogens such as polyamines, polyamides, polyacids, polymercaptans and polyphenol to produce hard, robust thermosetting network polymers. Furthermore, epoxy resin undergoes less shrinkage deformation during curing reaction than other thermosetting resins. In terms of processing characteristics, epoxy resin has a long life, does not produce byproducts, and transfer molding is possible. However, despite these advantages, epoxy resin has such defects as poor high-temperature wetting characteristics and inappropriateness as top coat because gloss and color are degraded when it receives direct sunlight. Furthermore, the applications of epoxy resin are limited because it is easily fractured even by light impact due to high density crosslinking.

Widely used types of epoxy resin include bisphenol A epoxy resin, which is produced by reacting bisphenol A with epichlorohydrine, bisphenol F epoxy resin, flame-retardant epoxy resin and novolac epoxy resin.

(2) Pigment

Pigment determines the decorative effect of coating such as color, hiding power, gloss and light resistance. It is a colored powder that does not dissolve in water and most organic solvents. Pigments are set in objects with the help of a sealant or finely dispersed and colored in objects. Pigments are largely divided into inorganic and organic pigments. Inorganic pigments metal compounds including lead, pearl and copper, and have excellent light resistance and heat resistance. By contrast, organic pigments do not have excellent heat resistance but are characterized by a wide variety of colors, and hydrogen carbonate compounds belong to them. Furthermore, pigments can be also classified by the use, and various types can be selected depending on the surrounding environment of coating. Because resin alone cannot play sufficient anticorrosion role, an appropriate anticorrosion pigments can be used to maximize anticorrosion effect.

(3) Solvent

Solvent is a substance having the property of dissolving alone, and generally refers to a liquid mixed in an undiluted paint. Solvents are mainly used to dilution for viscosity control of paints. Thinners mainly used for the viscosity composition of paints are composed of a mixture of solvents. Furthermore, solvents are also used to control drying speed considering the temperature and humidity of the surrounding environment.

(4) Additive

There are many complex and diverse types of additives that are used in paint manufacturing. Additives are indispensable for the improvement of properties and stability of paints[8, 30 ~ 31].

a. Thinner : This is a volatile liquid added to reduce the viscosity of paint. It does not exist in the paint film because it evaporates during the drying process.

b. Dispersant: This additive disperses pigments uniformly and stably in a resin. It is also called surfactant or wetting agent.

c. Anti-precipitation agent: This additive prevents pigments from precipitating to the bottom of the container during storage of paints.

d. Film-forming inhibitor: This additive prevents the formation of a film on the dry surface in the container during paint storage.

e. Binder: This substance forms paint film by binding with a pigment and gives absorbability to the metal substrate.

f. Plasticizer: This plays the role of a reinforcing agent and is used to give flexibility, durability and cold resistance to paints.

g. Anti-foaming agent: This additive is used to suppress air bubbles during paint manufacturing or coating.

h. Anti-flooding agent: This additive prevents color change caused by aggregation of dispersed pigments during paint storage.

2.1.2 Zinc dust paint

Zinc dust paint is a paint that contains zinc dust and prevents corrosion using the ionization tendency of metals. In the electrolyte, that is, the ship, electrons flow from zinc to iron due to the formation of local cells in the seawater. Using a zinc dust paint is an active corrosion preventive method to corrode zinc and protect iron. This is different from coating the surface or passivating iron like conventional anticorrosion paints.

Zinc dust paints can be classified into organic and inorganic types depending on the type of binders. The paint that binds with an organic resin such as epoxy resin, is an organic zinc dust paint and pigments such as Al, ZnO and Fe_2O_3 may be used in addition to the zinc dust in some cases. The paint bound with ethyl silicate is called an inorganic zinc dust paint. Zinc dust paints are divided into ethyl silicate type(solvent type) and alkali silicate type (water soluble type). Therefore, not only organic solvents, but also water can be used as solvent. Inorganic zinc dust paints are mainly used in iron structures(e.g., chimney, steel equipment, oil storage tanks and nuclear facilities) that require heat and corrosion resistance[5, 30 ~ 37].

2.1.3 Paints used on ship

(1) Importance of ship painting

Ships are always immersed in seawater and marine organisms such as sea animals and seaweeds including green and brown algae are attached to the ships and multiply, thus accelerating the aging of the hull. The exterior part of the ship also receives impacts from waves and sea breezes while repeatedly being immersed in seawater and then exposed to the air. The interior part of the ship is in poor ventilation, high temperature and humid conditions. Thus, the entire ship is exposed to corrosive environment. Corrosions require repair and repainting process, resulting in economic loss. Therefore, ship painting is a critical means to prevent these damage and loss by removing corrosion and speed reducing factors and to preserve the performance of each mechanism and decorate the ship.

(2) Types of paints by ship part

a. Paints for bottom part

Anti-fouling paints are used for anticorrosion of the bottom, pipe line for water and exterior parts. In the past, vinyl-based paints were the mainstream, but nowadays, epoxy paints are mainly used.

Furthermore, anti-fouling paints reinforced with anti-fouling agents are used to prevent the attachment of marine organisms to the hull shell. Anti-fouling paints are composed of a binder, which gives coating strength, rosin that promotes the release of anti-fouling agent and anti-fouling agent. For binder, chlorinated rubber and vinyl-based products are generally used. For anti-fouling agents, mercury and arsenic were used in the past, but they are not used now due to hazards and pollution problems. To meet the demand for tin-free anti-fouling paints, self-polishing copolymer anti-fouling paints of which the polymer dissolves in water by hydrolysis on the surface in seawater are mainstream.

b. Paints for boot-top and top side

The boot-tp area alternate between dry and wet conditions and require anti-fouling property as well as water resistance and weather resistance. The used paints are similar to those of the bottom part. For the top side, epoxy and polyurethane-based products are mainly used considering anticorrosion and aesthetics.

c. Paints for tanks

Tanks include ballast tank, ballast tank for crude oil and seawater and cargo tank, and each of them requires an appropriate coating system. The applications of phenolic for chemical carriers, epoxy or inorganic zinc dust paint for oil refining products carriers, and tar-free epoxy for various seawater tanks are increasing.

d. Paints for deck

The paints for deck are similar to those for the top side. Inorganic zinc silicate, chlorinated rubber, vinyl and epoxy paints are mainly used. Furthermore, paints mixed with sands or special plastics are also used to prevent slip.

e. Paints for cargo hold

Oil paints are sufficient for dry cargo hold, but coal tar epoxy paints are used for cargo holds for minerals and coals. For container ships, epoxy paints are generally used[5, 30].

2.1.4 Ship coating system

Ship coatings can be largely divided into new ship coating and repair ship coating. By work process, they can be divided into ground and onboard works. For new ship building, the ground work consists of the process from machining to hull assembly on the yard or tack welding of blocks. Furthermore, depending on the coated product in the ground work, the painting work is divided into block painting and fitting painting. In the ground work, primer to mid coating is mainly performed, excluding the top coating. Fig. 2.1 shows the process flow of ship coating.

Heavy duty coating or high performance coating is a coating method for protecting large structures including bridges, offshore structures, power generation equipment, various plants, ships and containers, or other steel structures in a severe corrosive environment from corrosion. It is an anticorrosion coating system that can endure severe corrosive environment for a long time. Heavy duty coating for ships cannot provide excellent adhesion, anticorrosion and environmental resistance with one single layer. Hence, multi-layer coating combination is required as shown in Fig. 2.2. First, after surface pretreatment, a zinc primer is applied for temporary anticorrosion of the steel until the painting from the tie coat to top coat is completed. The thickness of the primer is very thin, 15 ~ 30 ㎛. Then, the primer and intermediate coats, which are most important layers that give anticorrosion performance to the coating system are applied with epoxy or zinc rich paint. Finally, a thick top coat is applied using a polyurethane paint or glass flake paint for aesthetics, gloss and weather resistance.

The ship building cost is rising sharply currently due to high oil prices and international material prices. In particular, the price increase of paints and emulsification products, which are the major application products of petrochemical industry is the largest cause of the rising cost in all industries.

Therefore, heavy duty coating can be an economical option to improve the anticorrosive performance[5, 30].

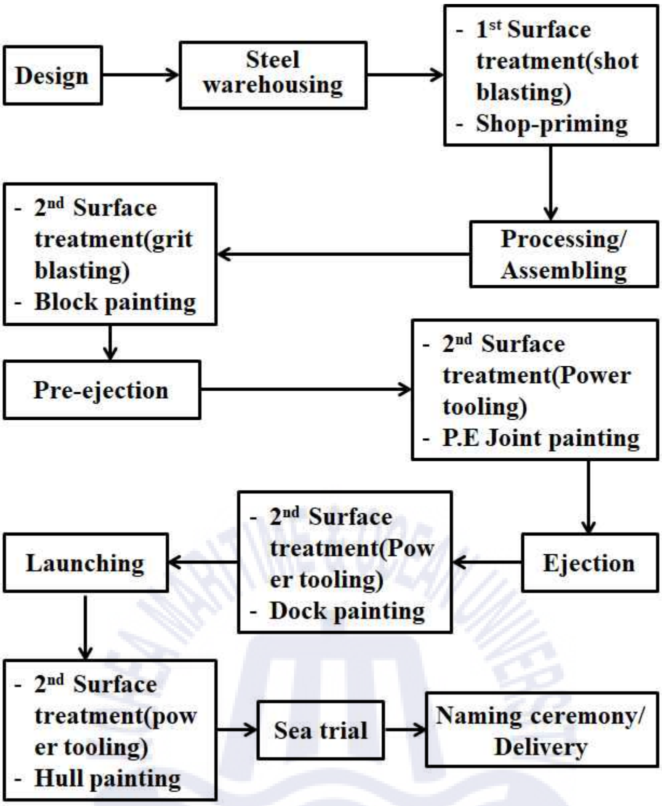

Fig. 2.1 Process flow of ship coating

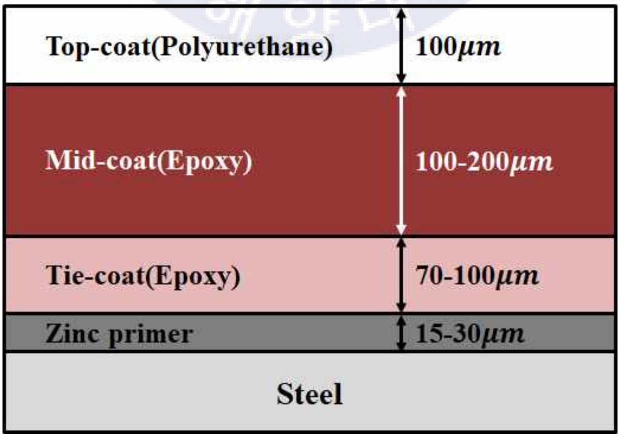

Fig. 2.2 System of anticorrosion coating for ship

2.2 Characteristics of laser cleaning process

2.2.1 Parameters of laser cleaning process

The laser cleaning process has parameters that need to be controlled. Fig. 2.3 shows the parameters of laser cleaning process. Major process parameters include laser wavelength, laser pulse, laser energy density, and material characteristics.

(1) Laser wavelength

Laser is an electromagnetic wave just like the wave used for general light, broadcast, television and smartphone. Electromagnetic waves are combination of electric and magnetic fields that can be propagated through the space. As shown in Fig. 2.4, the electric field intensity of waves can be represented as a sinusoidal curve, which is a function of time, and the electric field intensity E vibrates with a period of T between −E and +E.

When a laser beam is irradiated to material surface, the reflectivity(R), which is the amount of reflected laser energy, is greatly dependent on the wavelength. As shown in Fig. 2.5, in the case of metals, the shorter the wavelength, the lower the reflectivity becomes, resulting in more effective beam absorption. However, insulators such as ceramic have a large absorbency in the infrared(IR) region with long wavelengths.

For the laser cleaning process, the selection of a laser wavelength according to the type of pollutants and metal substrate is crucial. In general, laser with a short ultraviolet(UV) wavelength is effective for cleaning and removal of organic pollutants from the surface of metals. Near infrared lasers such as Nd:YAG and fiber laser remove pollutants by a high temperature of the surface which has the evaporation effect of pollutants[8, 38 ~ 40].

(2) Laser pulse

The laser outputs phenomena are divided into continuous wave(CW) oscillation and pulse oscillation according to the output and time wave forms as shown in Fig. 2.6. Continuous laser has a constant output as long as excitation is continued, and is indicated as power(W). The pulse laser is to output the energy accumulated in the laser at once, and is indicated as peak power(W), pulse width(s) and pulse energy(J). When this pulse is irradiated repeatedly, the pulse frequency(Hz) and average power(W) may be also used. The relationships of the pulse laser parameters are expressed as Eq. (2-1) and (2-2). Fig. 2.7 shows the laser processing regime according to the interaction time and power density. The laser cleaning process in this experiment requires short interaction time and high power density. Therefore, using pulse laser, which shows a high peak power in a short pulse irradiation time, is effective for the laser cleaning process. The peak power of laser in laser cleaning is a critical factor for heat transfer to the coating material. When the peak power of laser is increased, pollutants can be removed more easily, thus reducing the interaction time between laser heat source and metal substrate. As a result, the thermal effect on the metal substrate can be reduced[8, 38~39].

$$Pulse\,energy(J) = Peak\,power(W) \times Pulse\,width(s) \qquad (2\text{-}1)$$

$$Average\,power(W) = Pulse\,energy(J) \times Repetition\,rate(Hz) \qquad (2\text{-}2)$$

The energy per laser pulse does not have a significant effect on the laser processing. The actual incident energy on the surface is determined by the laser pulse width, frequency and laser spot size. The laser pulse width means the beam irradiation time from pulse laser. As shown in Fig. 2.8, when using a long pulse laser of microsecond level, thermal diffusion is caused by the relatively long irradiation time, which has thermal effect on the metal substrate under the pollution layer. Furthermore, in this case, ablation occurs over the machining part due to plastic strain or stress, causing a limit in precision machining. To prevent this, laser cleaning can be performed using a laser with a very short pulse width below nanosecond and a high peak power using Q-switching to instantly evaporate and remove pollutants on the surface. Consequently, precision machining is possible with minimal thermal diffusion to the surroundings of the processing material[41 ~ 48]. Fig. 2.9 shows the Q-switching oscillation mechanism. When a laser medium is excited, the density of the upper level becomes high. As the residence time increases in this excited state, light is emitted by natural emission. This emitted light is amplified further by induced emission, and when this amplification rate becomes greater than the loss of the resonator, it oscillates as shown in Fig. 2.9 (a). When the laser medium is continuously excited by inserting a Q-switch in the resonator as shown in Fig. 2.9 (b), a higher inversion distribution density can be obtained with no laser oscillation. In other words, the Q value of resonator [ω, (light energy accumulated in the resonator)/(loss in the resonator per unit time)] is increased from a low state to a high state, laser oscillation starts rapidly as shown in Fig. 2.9 (c). As a result, the energy accumulated as an inverse distribution is released as a laser pulse with a giant peak power. This is called Q-switching oscillation[49].

(3) Laser intensity and laser energy density

The TEM_{00} mode, which is the basic mode of laser beam is very important because it is used in most laser processes. The laser intensity of this mode shows a Gaussian distribution along the circumference from the center of the surface on which the beam is irradiated as shown in Fig. 2.10. The distribution of laser intensity, I(r), is given by Eq. (2-3), where r is the diameter of laser beam, w_0 is the beam radius at the focus (the distance where the power intensity becomes $1/e^2$ of the center), and I_0 is the maximum laser intensity at the beam center. That is, the farther from the focus, the lower the laser beam intensity becomes. When a laser beam with a Gaussian distribution is used for laser cleaning, there is no thermal effect on the material at the edges due to the low energy intensity. Therefore, the overlap of laser beams is essential for precise laser cleaning.

$$I(r) = I_0 \exp\left[-\left(\frac{r}{w_0}\right)^2\right] \qquad (2\text{-}3)$$

One parameter that is widely used in the laser cleaning process is the laser energy density, which is defined as the incident pulse energy per unit area, and the unit is J/cm^2. The laser beam size can vary by the focal length of the lens, and this can have a significant effect on the laser energy density. The longer the focal length, the larger the beam size becomes, resulting in a lower energy density. Therefore, the beam size can be easily controlled by adjusting the focal length to optimize focusing of the laser beam on the material. The selection and control of an appropriate energy density according to the metal substrate and pollutant type is a critical factor for successful cleaning process[8, 38, 40, 50].

(4) Material characteristics

When a laser beam is irradiated on the material, the incident beam is divided into three parts as shown in Fig. 2.11, and some of the beam is reflected from the material surface, and some of the beam is transmitted, and the remaining beam is absorbed. When losses due to some scattering are ignored, the incident laser beam(E_I) is the sum of there reflected beam(E_R), absorbed beam(E_A), and transmitted beam(E_T), as shown in Eq. (2-4). When the material is a metal, most beams are reflected and some are absorbed because the laser beams cannot transmitted into the metals. The absorption of laser beam occurs on the material surface. The collision with the phonons of metal grids and free electrons is changed into heat within 10^{-13}sec, which increases the temperature on the metal surface. The depth of the surface layer to which heat is conducted, is greatly affected by the thermal diffusivity(D) and laser pulse width(τ_P) as expressed in Eq. (2-5). Furthermore, there are differences by the wavelength of laser beam and the metal. The relationship between the wavelength of the laser beam and absorption rate according to the metal has been explained above.

$$E_I = E_R + E_A + E_T \tag{2-4}$$

$$L_T = \sqrt{D \cdot \tau_P} \tag{2-5}$$

Furthermore, when the wavelength of the laser beam is constant, the reflectivity of metal decreases with the decreasing electric conductivity of the metal, thus increasing the absorption rate of the laser beam. Since the electric conductivity of metals decreases at lower temperatures, the absorption rate of the laser beam increases with the rising temperature. In addition, the surface state of material also has a significant effect. If the surface of the metal is well polished and maintains flat, the incident beam on the surface is absorbed and reflected once. However, if there are irregularities on the surface, multiple absorptions and multiple reflections occur and the absorption rate of the laser beam increases[8, 40, 50].

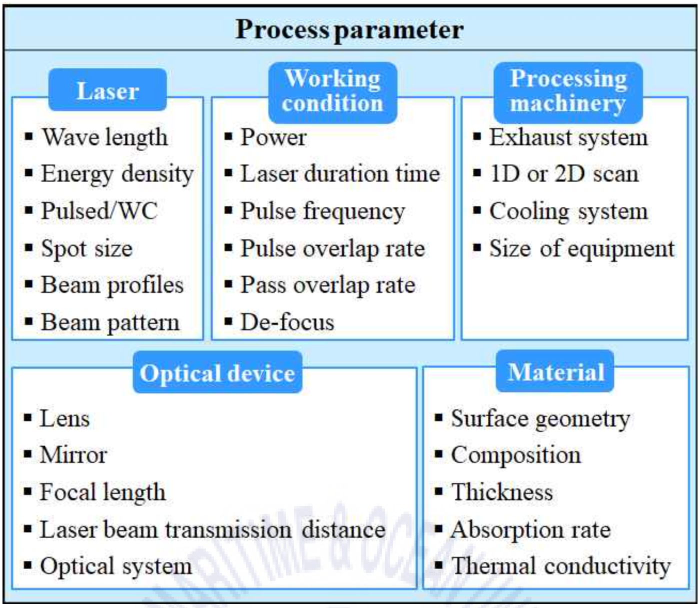

Fig. 2.3 Process parameters of laser cleaning

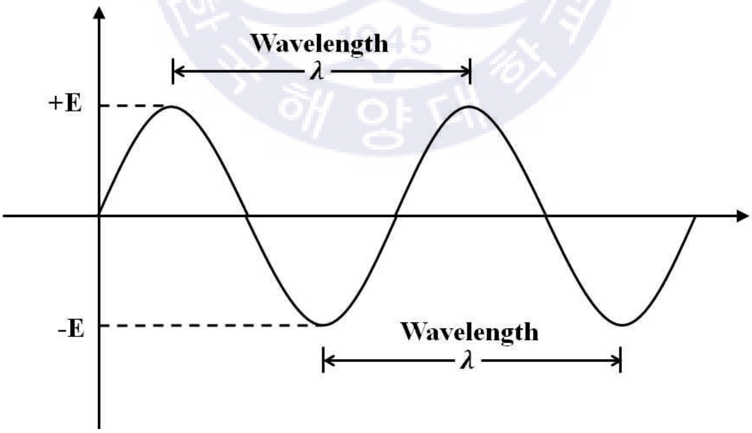

Fig. 2.4 Laser wavelength

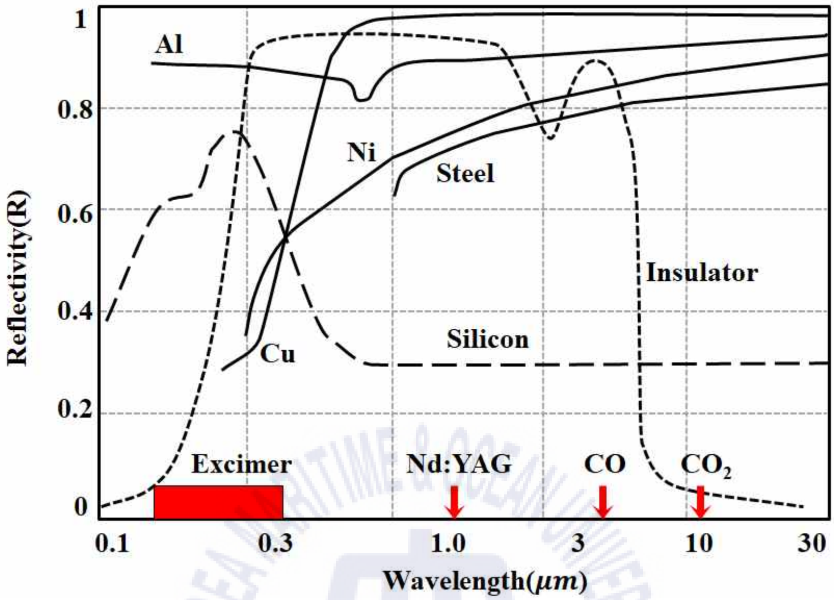

Fig. 2.5 Surface reflectivity of materials as a function of the wavelength

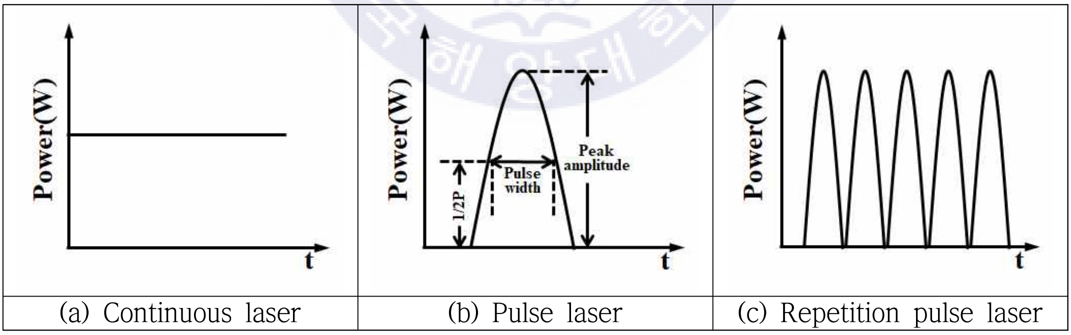

Fig. 2.6 Laser beam types

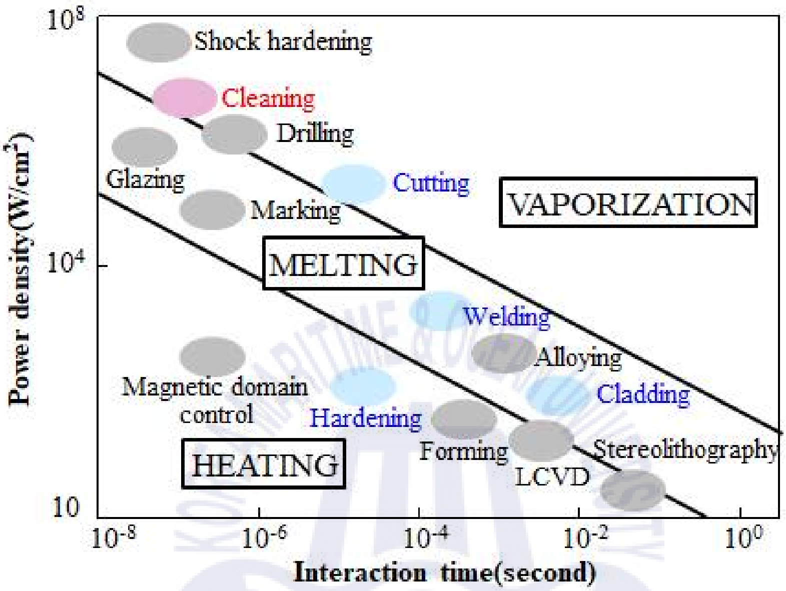

Fig. 2.7 Laser material processing regime

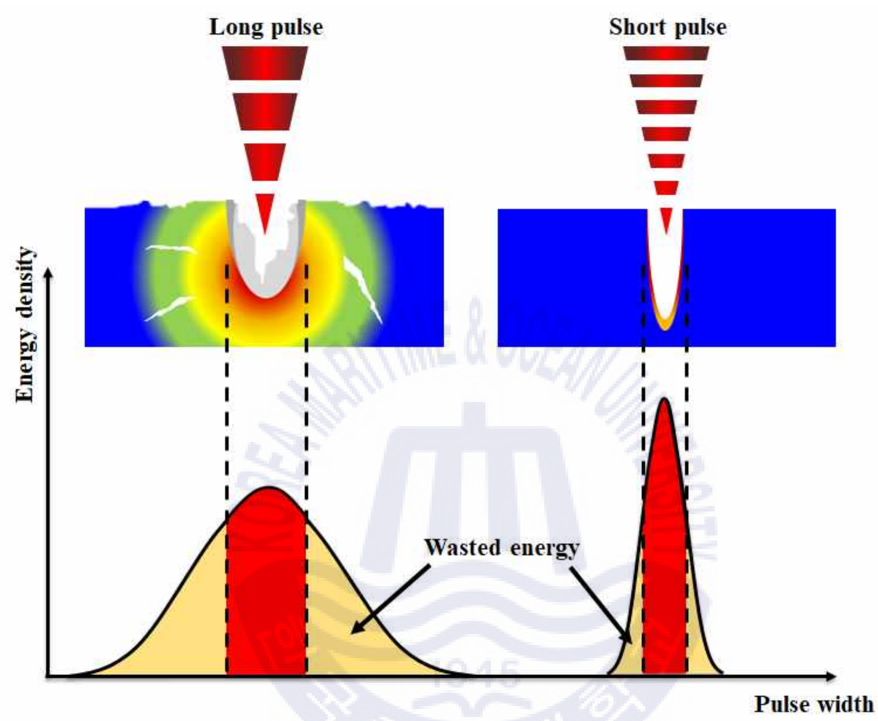

Fig. 2.8 A schematic representation of different processing phenomena between a long laser pulse and short laser pulse(Mi-rae Lim, 2016)

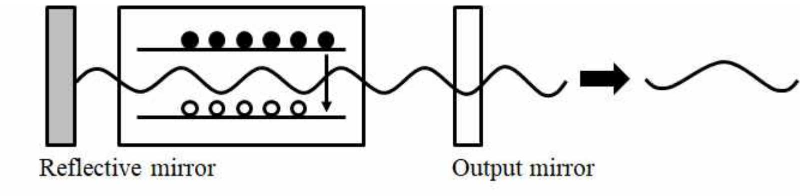

(a) Non Q-switch

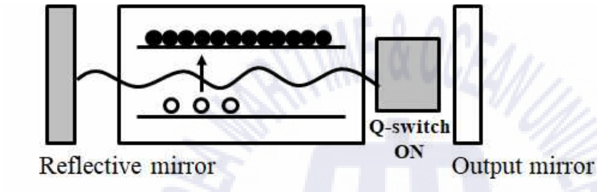

(b) Q-switch ON(low Q-state)

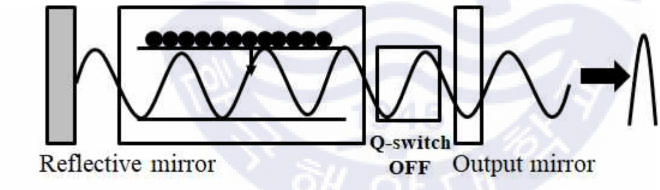

(c) Q-switch OFF(high Q-state)

Fig. 2.9 Mechanism of Q-switching oscillation

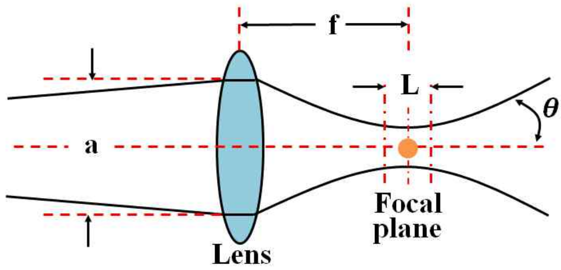

(a) Laser beam is first expanded, and then focused by a lens

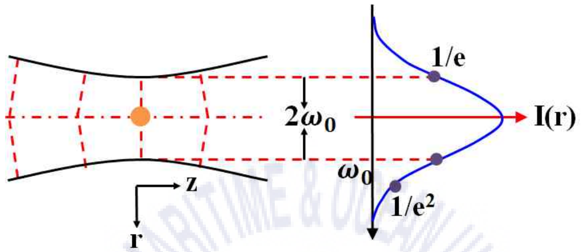

(b) Intensity distribution and formation of Gaussian shape laser beam near the focal plane

Fig. 2.10 Principal of Gaussian beam formation

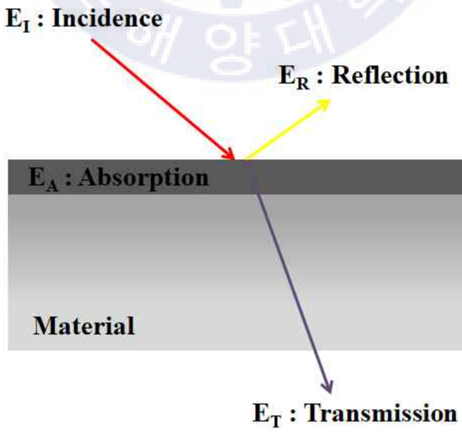

Fig. 2.11 Separation of incident laser beam to material

2.2.2 Laser cleaning mechanism

Laser cleaning technology selectively removes contaminants on the surface by evaporation without damaging the base metal by irradiating laser beam, a eco-friendly energy source, to contaminants. Only contaminants can be selectively removed by the differences in evaporation point and thermal conductivity between the metal substrate and pollutants, and the thermal effect on the metal substrate can be also reduced. The result of laser cleaning varies greatly depending on the laser process parameters such as laser wavelength, pulse width and energy density and material parameters such as the physical and chemical properties and surface condition of material. This laser cleaning mechanism can be explained largely by thermal process, quantum process and mechanical process.

(1) Thermal process

The mechanism of thermal process is that the material to be removed absorbs a laser beam and is heated, evaporated and removed. A schematic of this mechanism is shown in Fig. 2.12. This thermal process is dominant when the energy of the laser beam is low and the pulse width is long, such as the waves in the IR region. The pollutant removal from the surface by thermal process occurs when the laser beam absorption rate of the surface pollutant is higher than that of the metal substrate. In other words, if the evaporation temperature of the pollutant is lower than the melting temperature of the metal substrate, the pollutants are selectively removed without damaging the metal substrate. The laser beam irradiated to a laser cleaned surface which the pollutants on the surface have been removed is mostly reflected due to the high reflectivity of the metal substrate[8 ~ 9, 38 ~ 39, 51].

(2) Quantum process

Laser has a unique wavelength according to the laser medium and the photons comprising it have a different energy depending on the wavelength. Pollutants are forming various bonds such as covalent bonds, ionic bonds and hydrogen bonds. Therefore, the high energy of the laser photon can destroy the chemical bonds of pollutants, thus removing them. Most of the binding energy can be broken by the impact of photons in the UV region. Therefore, organic pollutant particles absorb UV waves very effectively and are removed by being decomposed to micro particles. This fine particle removal process by photodecomposition is called quantum process. The UV laser cleaning by quantum process is used for precise processing because it performs very limited reaction on the surface and the laser beam size is very small. Furthermore, the interaction time with material is also very short in the level of femto seconds(fsec) and pico seconds(psec), generating almost no heat, thus making it effective for processing material sensitive to heat[8 ~ 9, 38 ~ 39, 51].

(3) Mechanical process

The mechanical effect of laser cleaning is realized in the conditions of short pulse width(less than 20 nsec) and high laser intensity($10^7 \sim 10^{10}$ W/cm^2), and is explained by the photon pressure, thermoelastic pressure and ablation pressure. The photon pressure removes pollutants when high power CO_2 laser is irradiated. However, the photon pressure cannot provide the physical pressure required to remove solid pollutants such as oxide and paint attached closely to the surface. The thermoelastic pressure is known to be a laser cleaning mechanism to remove small particles on solid surface. When a pulse laser with a short pulse width and a high intensity is irradiated to the surface, the surface particles absorb the laser energy, and this causes an instantaneous thermal expansion. Laser cleaning is performed when the thermoelastic pressure caused by thermal expansion is larger than the adhesion between the particle and metal substrate. Fig. 2.13 shows the laser ablation mechanism. When a strong pulse laser is irradiated to the material surface, an evaporation phenomenon occurs instantly on the surface pollution layer. As a result, the pollutants are quickly evaporated, which generates plasma. If the pulse laser is irradiated continuously, the temperature of the plasma rises quickly. This plasma generates a strong shock wave and removes the pollutants by decomposing them to fine particles. In addition, the shock waves progress to the inside of the metal substrate after removing the pollution layer and strengthens the mechanical properties of the metal. When the shock waves enter the inside of the metal, it induces tensile strain first, and when the shock waves disappear, a compressive strain is generated. Since this shock wave is larger than that of shot peening which is used in many industrial sites, a larger and deeper compressive stress can be created. The deeper the compressive stress, the better the mechanical properties of the metal become[8 ~ 9, 38 ~ 39, 51)].

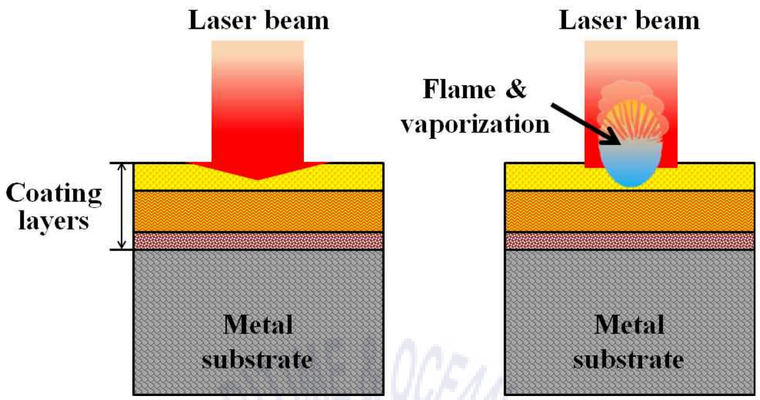

Fig. 2.12 Illustration of the laser thermal decomposition(Mongelli, 2005)

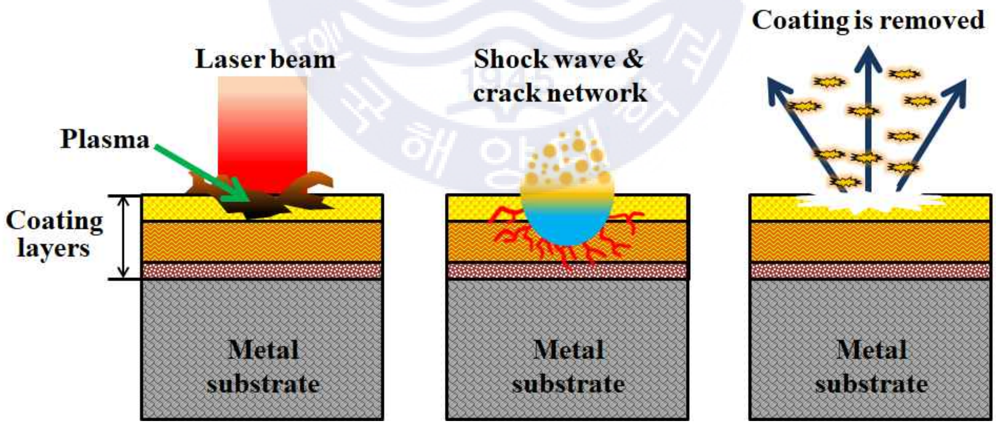

Fig. 2.13 Illustration of the laser ablation mechanism(Mongelli, 2005)

Chapter 3 Experiment Method

3.1 Experimental materials and equipment

3.1.1 Experimental materials

The material used in this study is SS400 painted with epoxy and shop primer paints, which is universally used in ships. SS400 is widely used in ships because of excellent processability and economics. Fig. 3.1 and 3.2 show the cross section and surface photographs of the specimens. The paint layer thickness is 200 ㎛ for epoxy and 15 ㎛ for shop primer. There is an oxide layer with a thickness of approximately 11 ㎛ on the surface of the base metal, which is a light rust in a new ship. The epoxy and shop primer painted surfaces have a significant difference in roughness. As it can be seen with the naked eye, the shop primer painted surface is much rougher. Hence, the differences in surface roughness changes after laser cleaning were examined.

Table 3.1 outlines the XRF analysis results of the painted steel surfaces. In the case of epoxy, Si, Mg, Al and Ba were detected as major components. In the case of shop primer, the contents of Si, Mg and Zn were detected. In particular, the Si, Mg, Al and Zn elements comprising the paints play the role of preventing or reducing metal corrosion under the paint layer because they have excellent corrosion resistance and sacrificial anode properties.

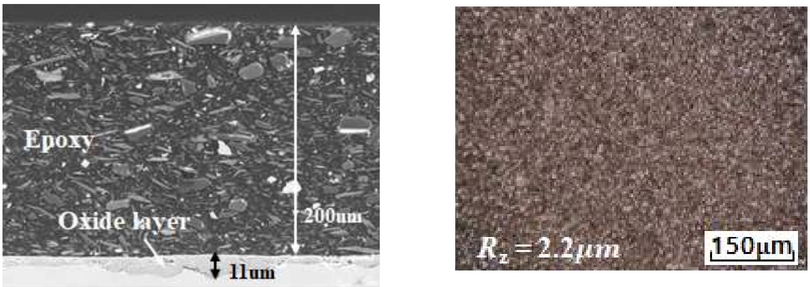

(a) Cross-section (b) Surface

Fig. 3.1 Cross-Section and surface of epoxy painted specimens

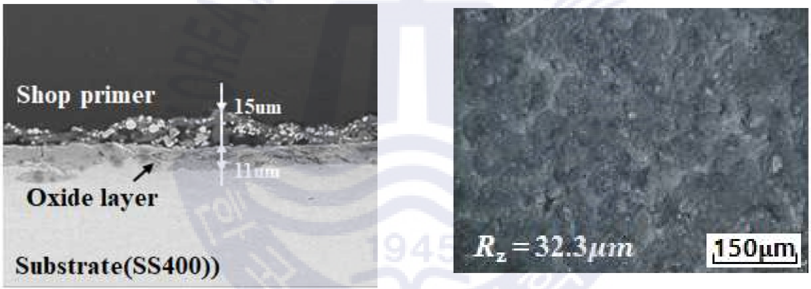

(a) Cross-section (b) Surface

Fig. 3.2 Cross-Section and surface of shop primer painted specimens

Table 3.1 XRF analysis results of specimens

Material \ Element(%)	Si	Mg	Al	Ca	Zn	P	Mn	Ba	S	Cl	Fe
Epoxy	23.1	19.1	11.3	0.9	-	-	-	11.1	1.3	0.7	32.0
Shop primer	12.9	7.6	0.6	0.7	13.6	3.5	0.3	-	-	-	60.4

3.1.2 Experimental equipment

The laser cleaning equipment used in this study is a low power Q-switching fiber laser with an average power(P_{ave}) of 100 W. Table 3.2 lists the specifications of the laser cleaning equipment. Fig. 3.3 shows a setup of the cleaning equipment and a schematic of the inside of the optical head.

The laser used in this experiment has a wavelength of 1070±5 nm and oscillates with a short pulse duration time of 100 ns and a high peak power(P_p). The laser beam with a diameter of 98 ㎛ sent from the resonator to the optical head is irradiated to the specimen through the 2D scanner and F-theta lens, during which the laser irradiation position and focal length are controlled to be constant. The power density of laser shows a Gaussian distribution.

This is a fundamental study to apply laser cleaning to the painting process in the shipbuilding and marine industry, and the mobility and portability of the laser cleaning equipment are critical. If the average power of laser increases from 100 W to 200 W or higher, the cooling system of the laser cleaning equipment must be changed from air cooling to water cooling, which increases the volume of the equipment and greatly affects mobility and portability. Therefore, to improve field applicability, we used laser cleaning equipment with an average power of 100 W, which can be relatively lightweight in this experiment.

Table 3.2 Specification of laser cleaning equipment

Laser type	Q-switching fiber laser
Maker	IMT
Wave length	1070±5 nm
Average laser power	100 W
Pulse duration time	100 ns
Focal spot diameter	98 ㎛
Working distance	254 mm
Cooling type	Air cooling

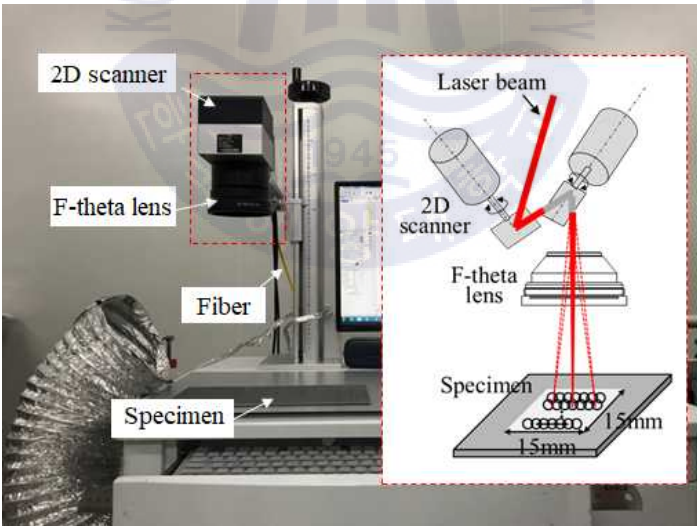

Fig. 3.3 Setup of experimental equipment in laser cleaning

3.2 Experimental and analysis method

3.2.1 Experimental method

Experiments were largely divided into the cleaning of epoxy and shop primer paints by applying the same laser cleaning process parameters to different materials. The laser cleaning characteristics and efficiency were compared according to material properties, the number of laser scans(N_s), pulse overlap rate(R_{po}), pass overlap rate(R_{pao}) and energy density(D_e) among the various process parameters of laser cleaning,

The laser beam transmitted through fiber scans a range of 15 mm × 15 mm of the fixed specimen. The number of laser scans was increased until the paint and oxide layer were fully removed. In this study, one scan was defined as one time cleaning of an area 15 mm × 15 mm by multiple irradiation of laser beam through pulse overlap and pass overlap. Therefore, the number of scans was different by the process parameters and material characteristics. Fig. 3.4 shows the laser cleaning experimental method. Due to the Gaussian beam that shows the highest energy intensity at the center, if the laser beams are not sufficiently overlapped, precise cleaning is impossible because there are parts that do not receive the effect of the laser heat source. Therefore, in this study, cleaning experiments were performed at different overlap rates of laser beam. The pulse overlap rate is defined as the ratio of the overlaps of two consecutive pulses. The pass overlap rate is defined as the ratio of overlaps of two up and down passes in the laser irradiation direction.

For two materials, the removal of the paint and oxide layer and the characteristics of the laser cleaned area were observed while changing the number of scans and the pulse overlap rate. Based on the results obtained from this, the laser cleaning characteristics were evaluated while changing the pass overlap rate and energy density. In particular, the change of pulse overlap rate and energy density generates differences in the scan speed. Since the scan speed affects the cleaning time for the same laser scan area, the optimum condition was selected through the laser cleaning efficiency calculated as the removal rate per cleaning time for each process parameter. Finally, the mechanical and microstructure characteristics of the cleaned area were analyzed by observing the hardness and microstructure of the specimen that was laser cleaned at the optimum condition.

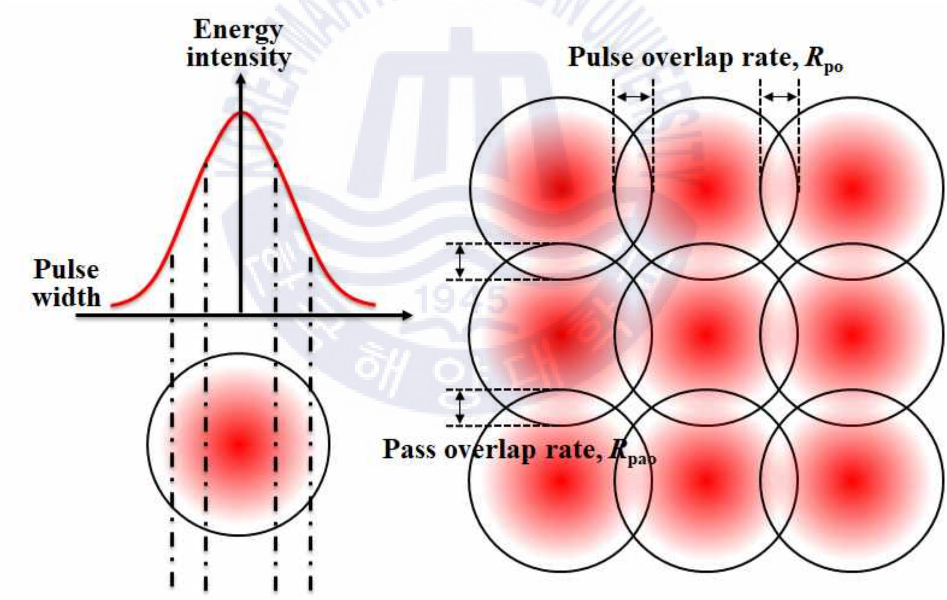

Fig. 3.4 Schematic of laser cleaning experimental method

3.2.2 Analysis method

(1) Sampling of the specimen

To observe the surface morphologies of the laser cleaned specimens and analyze the cross sections, the surface photographs were taken and the specimens were cut using a grinder. To obtain stable cleaned area, 13 mm × 13 mm size specimens were sampled. Fig. 3.5 shows the sampling positions of the specimens.

(2) Analysis of the laser cleaned surface

The surface of the cleaned area was observed at ×500 magnification using a digital microscope HiROX RH-2000 and the 3D images of the surface were captured. In addition, the surface roughness was measured using a surface roughness tester Mitutoyo SV-3200 to analyze the changes in surface roughness according to the laser cleaning process parameters. The surface roughness of the laser cleaned area according to the pulse overlap rate was measured in the laser irradiation direction, and the surface roughness of the laser cleaned area according to the pass overlap rate was measured in the perpendicular direction to the laser irradiation direction. The roughness measurement range was 6 mm and the average roughness was calculated. Fig. 3.6 shows the surface roughness measurement positions according to pulse overlap rate and pass overlap rate.

Furthermore, to check whether there are residues of the paint and oxide layer, spot and mapping analyses were performed for the laser cleaned surface using EDS(energy-dispersive x-ray spectroscopy) and the components were analyzed using XRD(x-ray diffraction).

(3) Cross section analysis of the cleaned area

The cross section of the cleaned area was observed using scanning electron microscopy(SEM). To examine the removal amount and conditions of the paint and oxide layer according to the process parameters, the thicknesses of the paint and oxide layer of the cleaned surface were measured.

(4) Vickers hardness test

To analyze the mechanical characteristics of the laser cleaned area, the hardness was measured in the depth direction from the surface using a micro Vickers hardness tester. Fig. 3.7 shows the hardness measurement positions on the surface of the laser cleaned area. Hardness was measured by 5 points in the transverse direction of the cleaned surface and the average was calculated. In addition, hardness was measured in 50 ㎛ in longitudinal direction from the surface. The load was set at 980.7 mN(Hv 0.1) and a duration time of 10 sec was given.

(5) Etching of the specimen and observation of microstructure

The laser cleaned specimen was polished and then etched using an solution (2 % Nital). After that, the microstructure was observed using optical microscopy(OM) and SEM.

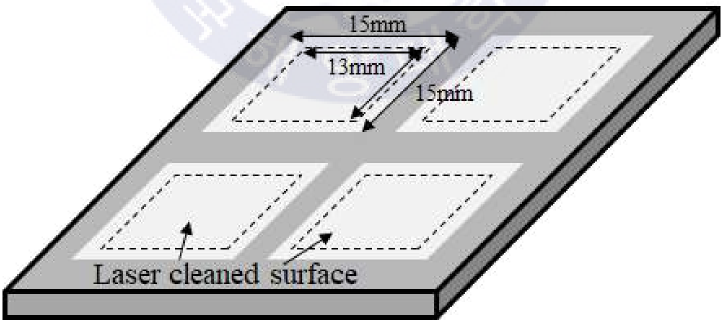

Fig. 3.5 Position of sampling for observing surface and cross section

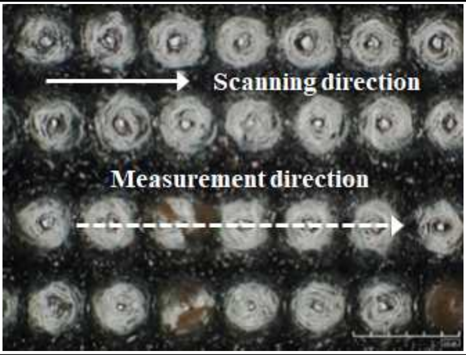

(a) Pass overlap rate

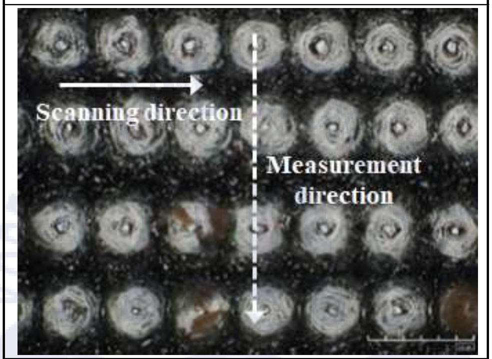

(b) Pulse overlap rate

Fig. 3.6 Measurement position for surface roughness by parameters

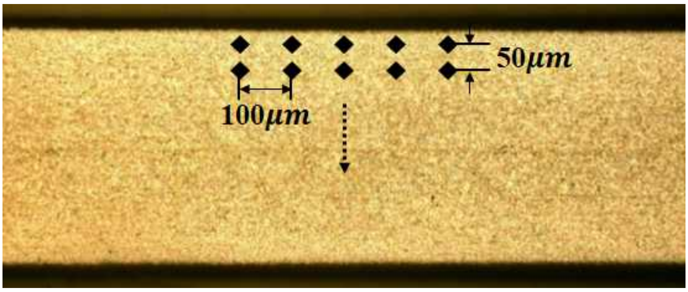

Fig. 3.7 Measurement position for hardness test

Chapter 4 Results and Discussion

4.1 Laser cleaning characteristics of epoxy painted steel

4.1.1 The effect of the number of scans and pulse overlap rate

(1) Effect of the number of scans and pulse overlap rate on the cleaned area

The 200 ㎛ thick epoxy paint and oxide layer cannot be fully removed by one laser scan; hence laser scans must be repeated several times. The number of scans affects not only the removal of the paint and oxide layer, but also the surface roughness and the damage of the base metal. Furthermore, the pulse overlap rate is a indicator of how much overlapped the pulse laser beams irradiated to the specimen are, and is directly associated with the removal efficiency of the paint. A high pulse overlap rate means that the pulse laser beams are overlapped in many parts. It also increases the heat input per unit area, thus affecting the number of scans required to remove the epoxy paint and oxide layer. Therefore, to analyze the effects of the number of scans and pulse overlap rate on the epoxy paint removal, cleaning was performed with an energy density of 7.9 J/cm^2 and a pass overlap rate of 0 % while changing the pulse overlap rate to 20 %, 50 % and 70 %. The number of scans was increased in regular intervals until the epoxy paint and oxide layer were fully removed for each condition.

Fig. 4.1 ~ 4.3 show the surface and cross section of the laser cleaned specimen at each pulse overlap rate condition. At the 20 % pulse overlap rate condition, the epoxy paint was mostly removed as the number of scans increased. However, a small amount of residue remained on the surface of the specimen that was scanned 45 times. The oxide layer also remained in every condition as shown in the cross section photographs. When the pulse overlap rate was changed 50 %, the epoxy paint remained a little at 11 scans and mostly removed at 14 scans. However, the oxide layer was not removed even at 23 scans, the maximum number of scans, as in the previous 20 % condition. To examine the laser cleaning result of 70 % pulse overlap rate, and the epoxy paint was fully removed at 7 scans. In this condition, even the oxide layer was removed at 13 or higher scans.

Consequently, when the epoxy paint and oxide layer removal conditions were examined according to the pulse overlap rate, as the pulse overlap rate increased, the number of scans required for removing the epoxy paint decreased. Furthermore, at 70 % pulse overlap rate, the oxide layer could be removed, but at lower pulse overlap rates, the oxide layer could not be fully removed. This is because, in the low pulse overlap rate condition in the laser cleaning with a thermal process mechanism, laser energy above the threshold for oxide layer removal was not irradiated to the specimen. The amount of laser energy irradiated to the specimen per unit area according to the pulse overlap rate can be compared through the number of pulses in a spot(NOP). This can be calculated using Eq. (4.1). NOP is defined by the number of pulses irradiated to the one spot of the laser beam. Fig. 4.4 shows a schematic of NOP. As a result of calculating the NOP for each overlap rate, the number of pulses is 1 when the overlap rate is 20 %, 2 when it is 50 %, and 3 when it is 70 %. This confirms that the amount of laser energy irradiated to the specimen is changed by different pulse overlap rates in the same laser energy density. Therefore, as the pulse overlap rate increases the amount of laser energy irradiated to the specimen per unit area increases, making it easier to remove the epoxy paint and oxide layer[9].

$$NOP = \frac{d}{v} f \qquad (4.1)$$

Note : v is the scan speed(mm/s), d is the beam diameter(mm), and f is the pulse frequency(Hz).

To observe the roughness of the laser cleaned surface according to the number of scans and pulse overlap rate, the roughness was measured and the results are shown in Fig. 4.5. Before laser cleaning, the surface roughness of the base metal and epoxy paint layer are R_z = 3.8 ㎛ and R_z = 2.2 ㎛, respectively. The change in the surface roughness according to the number of scans shows similar tendency in every overlap rate. Representative based on the 3D profile of the specimen cleaned in the 70 % pulse overlap rate as shown in Fig. 4.6, it could be seen that when laser is irradiated to a smooth paint layer before laser cleaning, the epoxy paint is evaporated by laser ablation, thus increasing the surface irregularity and roughness, resulting in high surface roughness. In the condition of 7 scans, most of the paint was removed, the smooth surface of the base metal was revealed, and the lowest roughness value was observed. However, after the paint was removed and laser was irradiated, the damage of the base metal worsened and the surface roughness gradually increased. As shown in Fig. 4.7, the surface roughness according to the pulse overlap rate decreased as the overlap rate increased, which made gentle curves between pulses formed by the laser beam. In other words, the epoxy paint and oxide layer could be easily removed while minimizing the damage of the base metal by controlling the number of scans at a relatively high pulse overlap rate.

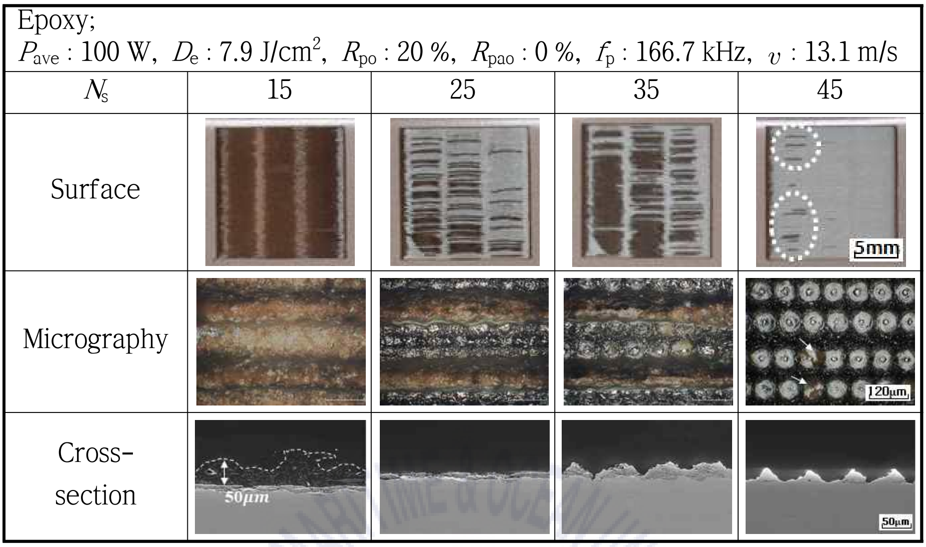

Fig. 4.1 Surface and cross-section of laser cleaned epoxy surface in R_{po} = 20 %, R_{pao} = 0 %

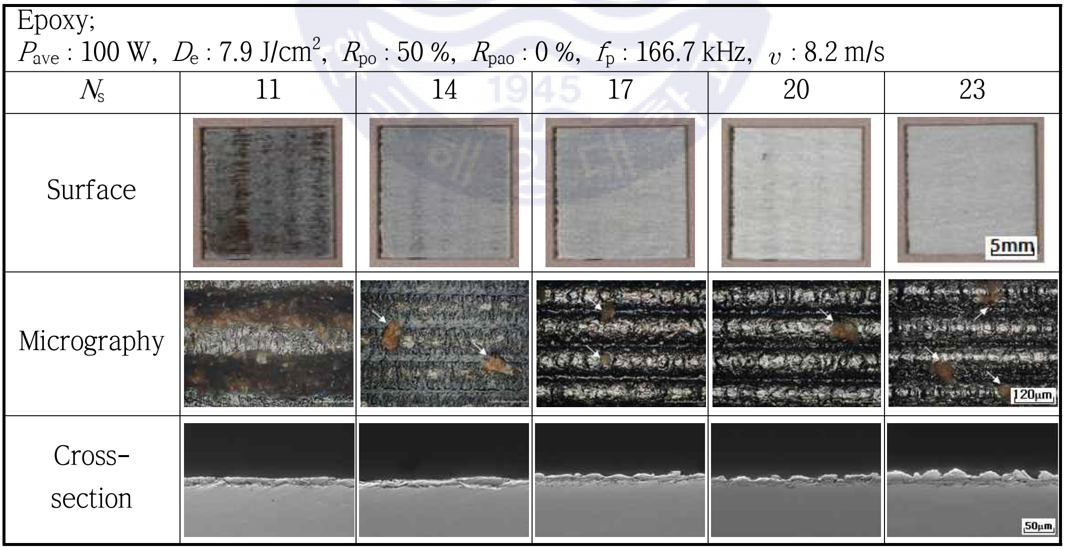

Fig. 4.2 Surface and cross-section of laser cleaned epoxy surface in R_{po} = 50 %, R_{pao} = 0 %

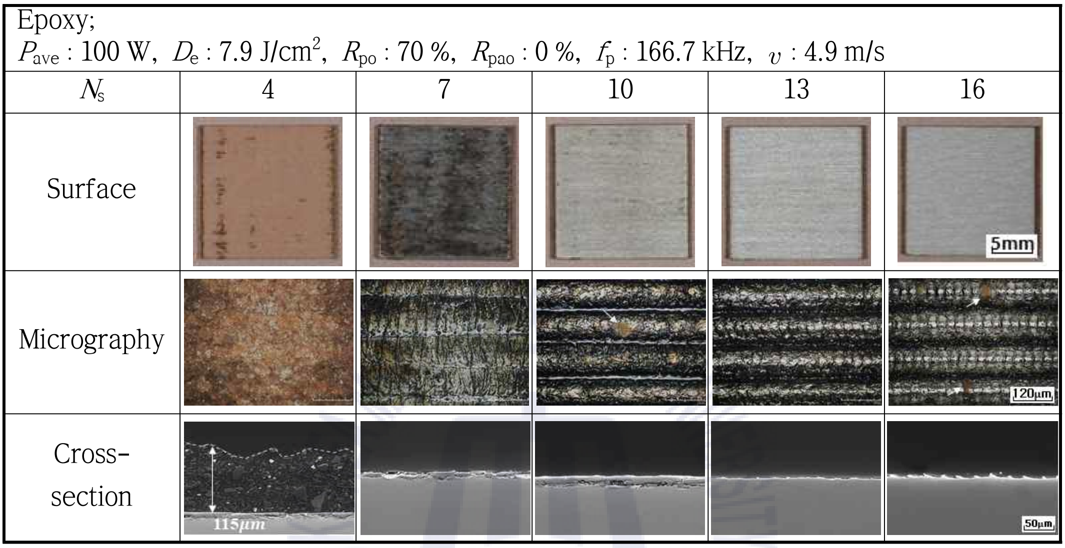

Fig. 4.3 Surface and cross-section of laser cleaned epoxy surface in R_{po} = 70 %, R_{pao} = 0 %

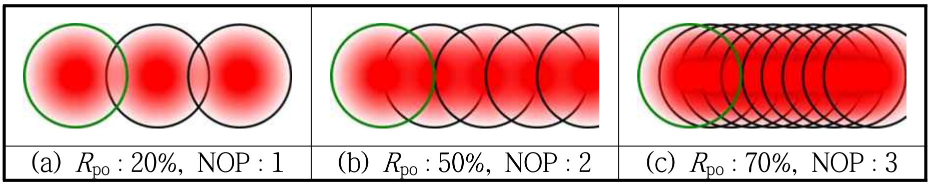

Fig. 4.4 NOP variation with pulse overlap rate

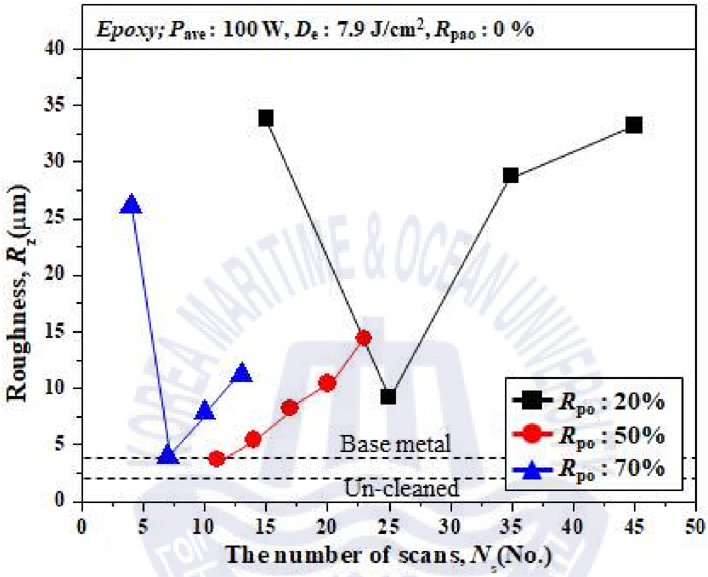

Fig. 4.5 Roughness variation of laser cleaned surface with the number of scans and pulse overlap rate in R_{pao} = 0 %

Epoxy; P_{ave} : 100 W, D_e : 7.9 J/cm^2, R_{po} : 70 %, R_{pao} : 0 %, f_p : 166.7 kHz, v : 4.9 m/s			
N_s	un-cleaned	4	7
3D profile	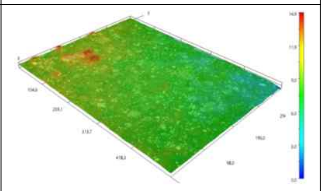	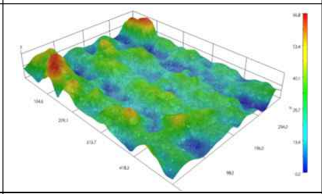	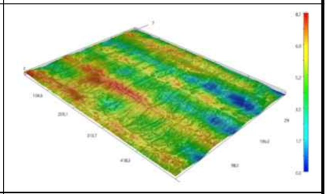
N_s	10	13	
3D profile	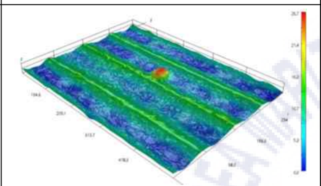	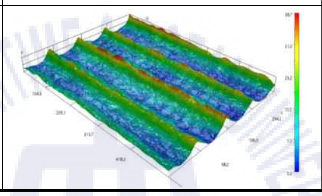	

Fig. 4.6 3D-profile of laser cleaned surface with the number of scans in R_{po} = 70%

Epoxy; P_{ave} : 100 W, D_e : 7.9 J/cm^2, R_{pao} : 0 %			
$R_{po}(N_s)$	20 %(45)	50 %(23)	70 %(13)
3D profile	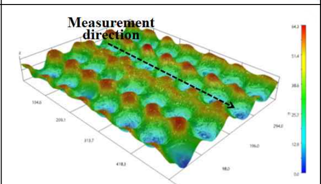	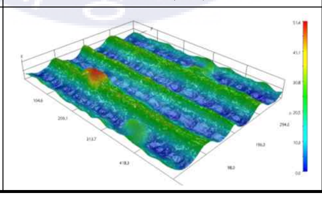	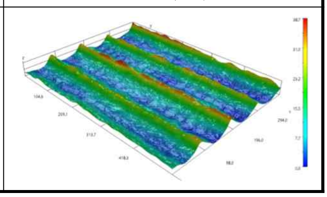

Fig. 4.7 3D-profile of laser cleaned surface with pulse overlap rate in R_{pao} = 0%

(2) Analysis of components before and after laser cleaning

EDS spot analysis was performed for the laser cleaned surface to determine the existence of residues of epoxy paint and oxide layer at each overlap rate for laser cleaning, and the results are shown in Fig. 4.8 ~ 4.10. Before the laser cleaning, the result of the EDS spot analysis detected Mg, Al and Si, which are the component elements of epoxy paint. When the pulse overlap rate was 20 %, S and Ba were detected at 15 and 35 scans, which confirmed the remaining epoxy paint on the surface. When the number of scans increased to 45, most of the paint was removed and only O and Fe were detected with no components of paint, which confirmed the remaining oxide layer on the surface. At the 50 % pulse overlap rate condition, Mg and Si were detected, which are the components of paint in 11 scans. At 14 and 23 scans, the components of the epoxy paint were not detected, and the proportions of O and Fe, the components of oxide layer, were high. At 70 % pulse overlap rate, the paint components were fully removed in 10 scans, and only Fe was detected in 13 scans, which confirmed the fully removal of the epoxy paint and oxide layer. In other words, the previous analysis result using the surface and cross section photographs of the laser cleaned area agreed with the result of the EDS spot analysis.

Epoxy;
P_{ave} : 100 W, D_{e} : 7.9 J/cm^2, R_{po} : 20 %, R_{pao} : 0 %, f_{p} : 166.7 kHz, v : 13.1 m/s

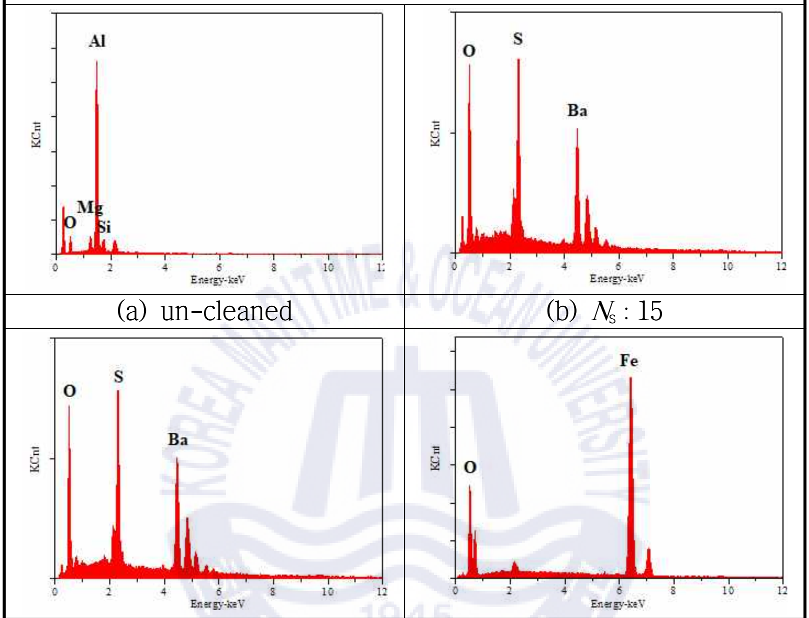

(a) un-cleaned (b) N_{s} : 15

(c) N_{s} : 35 (d) N_{s} : 45

No.	Elements content(At%)						
	O	Mg	Al	Si	S	Ba	Fe
(a)	17.4	4.9	66.8	8.2	0.3	0.2	1.8
(b)	48.1	0.4	1.4	0.6	23.6	24.9	0.7
(c)	48.1	0.2	0.5	0.6	23.9	25.8	0.3
(d)	28.9	0.3	0.5	0.5	0.3	0.1	68.9

Fig. 4.8 EDS spot analysis results on laser cleaned epoxy surface in R_{po} = 20 %, R_{pao} = 0 %

Epoxy;
P_{ave} : 100 W, D_e : 7.9 J/cm^2, R_{po} : 50 %, R_{pao} : 0 %, f_p : 166.7 kHz,
v : 8.2 m/s

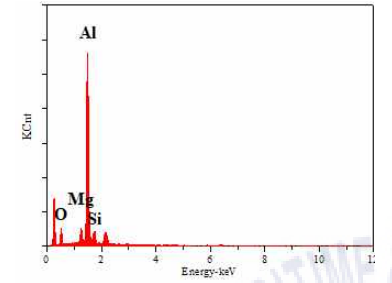

(a) un-cleaned

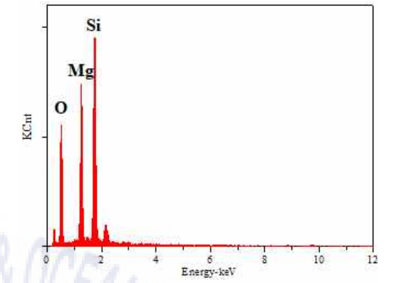

(b) N_s : 11

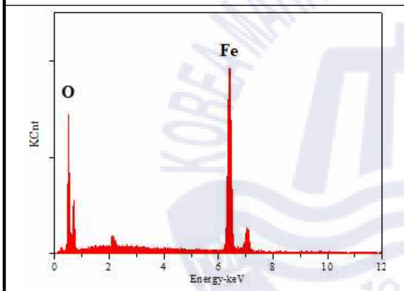

(c) N_s : 14

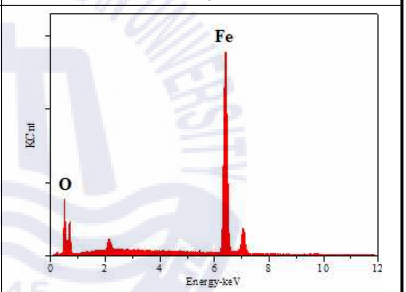

(d) N_s : 23

No.	Elements content(At%)						
	O	Mg	Al	Si	S	Ba	Fe
(a)	17.4	4.9	66.8	8.2	0.3	0.2	1.8
(b)	45.9	19.8	0.6	33.7	0.0	0.0	0.1
(c)	36.9	0.3	0.4	0.3	0.2	0.2	61.0
(d)	18.9	0.3	0.4	0.4	0.3	0.2	79.0

Fig. 4.9 EDS spot analysis results on laser cleaned epoxy surface in R_{po} = 50 %, R_{pao} = 0 %

Epoxy;
P_{ave} : 100 W, D_e : 7.9 J/cm^2, R_{po} : 70 %, R_{pao} : 0 %, f_p : 166.7 kHz,
v : 4.9 m/s

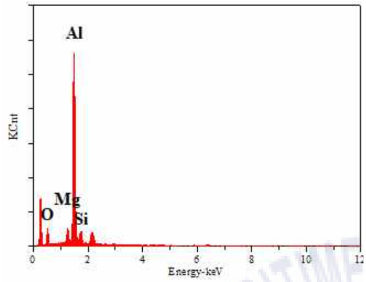

(a) un-cleaned

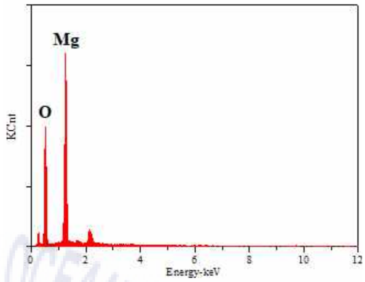

(b) N_s : 4

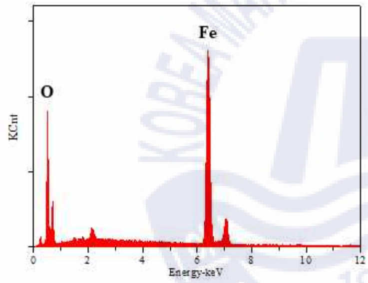

(c) N_s : 10

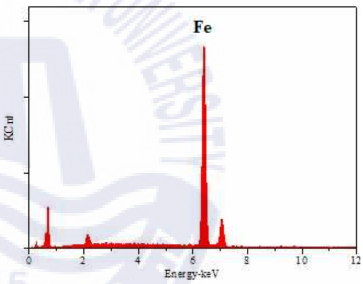

(d) N_s : 13

No.	Elements content(At%)						
	O	Mg	Al	Si	S	Ba	Fe
(a)	17.4	4.9	66.8	8.2	0.3	0.2	1.8
(b)	55.0	42.2	0.4	1.0	0.6	0.0	0.35
(c)	36.0	0.1	0.7	0.5	0.4	0.1	61.6
(d)	1.1	0.2	0.2	0.3	0.4	0.2	96.8

Fig. 4.10 EDS spot analysis results on laser cleaned epoxy surface in R_{po} = 70 %, R_{pao} = 0 %

4.1.2 The effect of the pass overlap rate

(1) Comparison of the removal characteristics of the epoxy paint and oxide layer

The previous experiment results verified that the increase of NOP, that is, the increase of heat input per unit area facilitated the removal of the epoxy paint and oxide layer. Among the laser cleaning process parameters, the pass overlap rate can be also controlled to generate a significant effect on the heat input per unit area. The pass overlap rate represents the overlap parts between subsequent passes. If the pass overlap rate increases, the number of laser passes per unit area increases, which in turn increases the heat input. Therefore, to analyze the laser cleaning characteristics according to the pass overlap rate, experiments were conducted while changing the pass overlap rate from 0 % to 20 % and 50 % at the pulse overlap rates of 20 %, 50 % and 70 %. The energy density was fixed to 7.9 J/cm^2 as in previous experiments. The epoxy paint and oxide layer removal conditions were compared and analyzed through the surface and cross section of the laser cleaned area and EDS mapping analysis at each condition.

Fig. 4.11 shows the surface micrography and SEM images of the cross section of the laser cleaned area according to the pass overlap rate at 20 % pulse overlap rate. In every pass overlap rate condition, the thickness of the paint layer decreased with the rising number of scans. The 200 ㎛ thick epoxy paint layer was fully removed in 45, 18 and 12 scans at the pass overlap rate of 0 %, 20 % and 50 %, respectively. The surface micrography shows that when the pass overlap rate was 0 %, even when the number of scans was increased, a small amount of epoxy paint particles remained on the cleaned surface. They were fully removed when the pass overlap rate was increased to 20 % and 50 %. This was presumed to be due to the laser beam having Gaussian distribution. A laser beam with a Gaussian distribution has a higher energy density at the center and the energy density decreases toward the edges of the beam. Therefore, if the overlaps of laser beams are insufficient during cleaning, areas that do not receive the thermal effect of laser beams generated, making precise laser cleaning impossible. Consequently, more than 20 % overlaps were necessary when cleaning is performed using laser beam having Gaussian distribution. In the case of the oxide layer, the removal conditions were examined using EDS mapping analysis of the laser cleaned surface due to vague boundary with the base metal. Fig. 4.12 shows the result of the mapping analysis for the specimen before and after laser cleaning at the maximum number of scans with pass overlap rate. Mg and Si were detected, which are major components of the epoxy paint, in the specimen before laser cleaning. Because there was a thin oxide layer of approximately 11 ㎛ thickness below the epoxy paint layer, a high proportion of O and a low proportion of Fe were detected. Furthermore, only Fe was detected as a component of the base metal. At the conditions of 0 % pass overlap rate and 45 scans, 20 % and 24 scans, and 50 % and 18 scans, the components of the epoxy paint were fully removed, but the oxide layer on the surface was not removed.

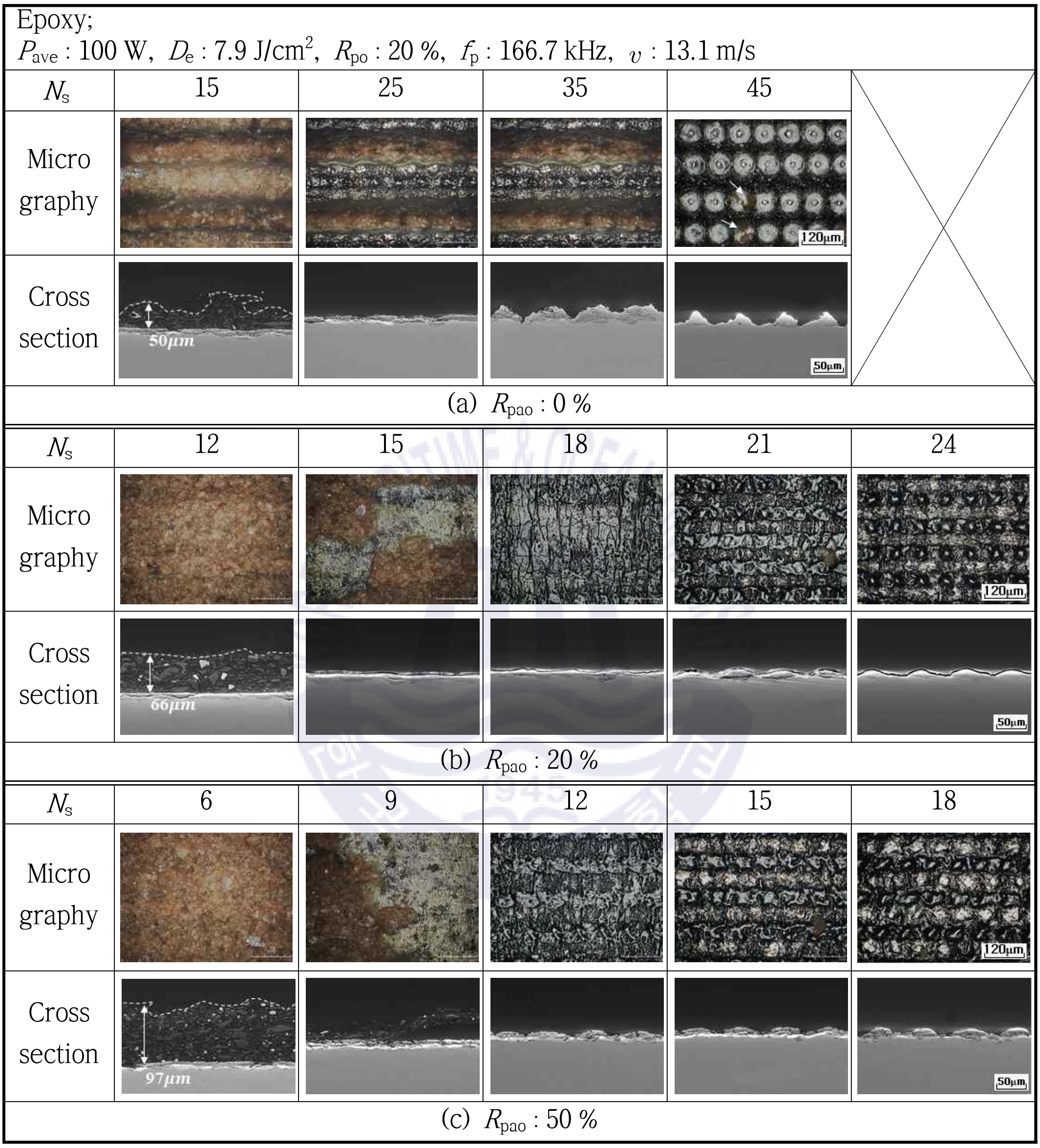

Fig. 4.11 Micrography and cross-section of laser cleaned epoxy surface with pass overlap rate in R_{po} = 20 %

Epoxy; P_{ave} : 100 W, D_e : 7.9 J/cm^2, R_{po} : 20 %, f_p : 166.7 kHz, v : 13.1 m/s				
$R_{pao}(N_s)$	un-cleaned	0 %(45)	20 %(24)	50 %(18)
SEM images	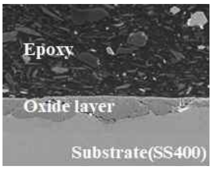		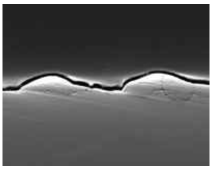	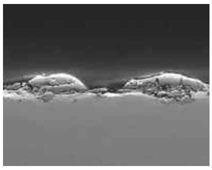
O	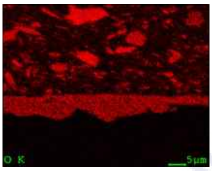	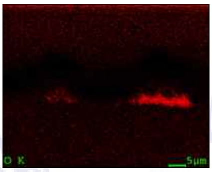	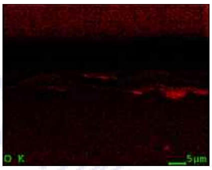	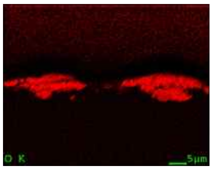
Mg	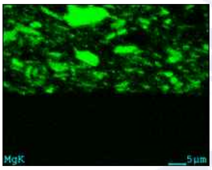			
Si	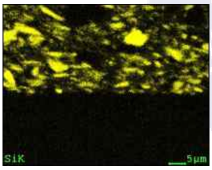	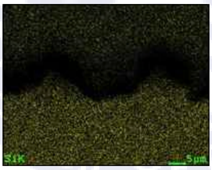		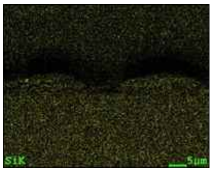
Fe	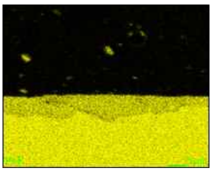	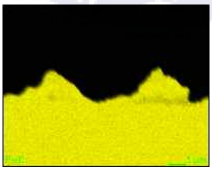	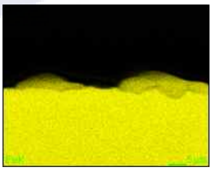	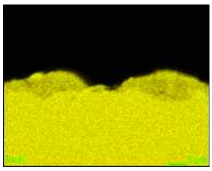

Fig. 4.12 EDS mapping analysis results on cross-section of laser cleaned epoxy surface with pass overlap rate in R_{po} = 20 %

At the 20 % pulse overlap rate, the oxide layer was not removed even when the pass overlap rate and the number of scans were increased. Hence, a higher heat input than the above conditions was required to remove the oxide layer. Therefore, laser cleaning experiments were performed while changing the pass overlap rate at 50 % pulse overlap rate, and the results are shown in Fig. 4.13. The epoxy paint was fully removed in 14, 11 and 8 scans at 0 %, 20 % and 50 % pass overlap rate, respectively. The oxide layer was not removed at 0 % and 20 % pass overlap rates, but when the pass overlap rate was raised to 50 %, it was fully removed at 14 scans. In other words, at 50 % pulse overlap rate, the oxide layer could be removed by increasing the heat input through the control of the pass overlap rate.

The removal characteristics of the epoxy paint and oxide layer according to the pass overlap rate could be clearly observed through the laser cleaning experiment results at 70 % pulse overlap rate in Fig. 4.14. At the pass overlap rates of 0 %, 20 % and 50 %, the epoxy paint was removed in 7, 7 and 5 scans, respectively, and the oxide layer was also removed in 13, 13 and 8 scans, respectively. The EDS mapping analysis result of the specimen cleaned at the representative condition of 50 % pass overlap rate is shown in Fig. 4.15. As shown in this figure, the components of epoxy paint and oxide layer were detected in 2 scans, but all the components of the epoxy paint were removed and a oxide layer remained in 5 scans. When the number of scans was increased to 8, both the epoxy paint and oxide layer were removed. The above experiment results verified that as the pass overlap rate increased, the number of scans required to remove the epoxy paint and oxide layer decreased. This means the removal amount of the epoxy paint and oxide layer per laser scan increases. When the removal amount of one laser scan at each pass overlap rate was calculated, it was 16.23 ㎛ at 0 % and 20 % pass overlap rates, but it increased to 26.38 ㎛ at 70 % pass overlap rate 70 %.

Consequently, more precise laser cleaning was possible as the pass overlap rate increased. Better removal characteristics of the epoxy paint and oxide layer could be derived by changing the amount of thermal energy irradiated to the material during laser cleaning by controlling the pass overlap rate as well as the pulse overlap rate.

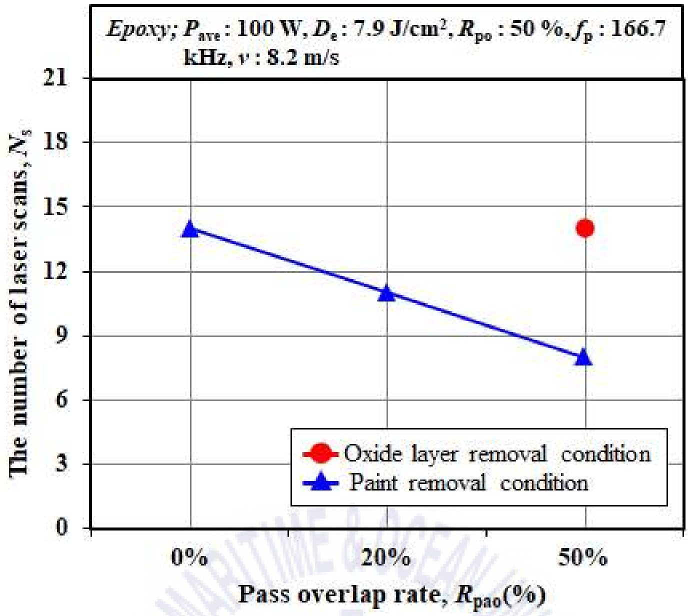

Fig. 4.13 Epoxy paint and oxide layer removal condition with pass overlap rate in R_{po} = 50 %

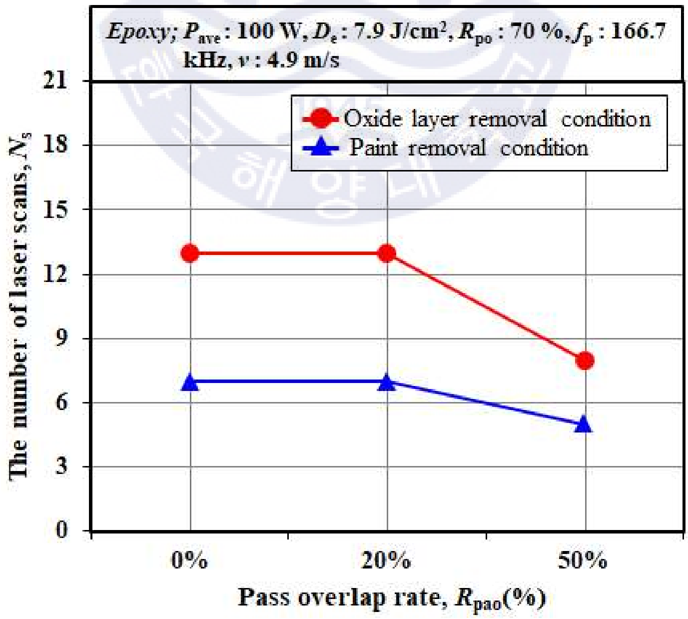

Fig. 4.14 Epoxy paint and oxide layer removal condition with pass overlap rate in R_{po} = 70 %

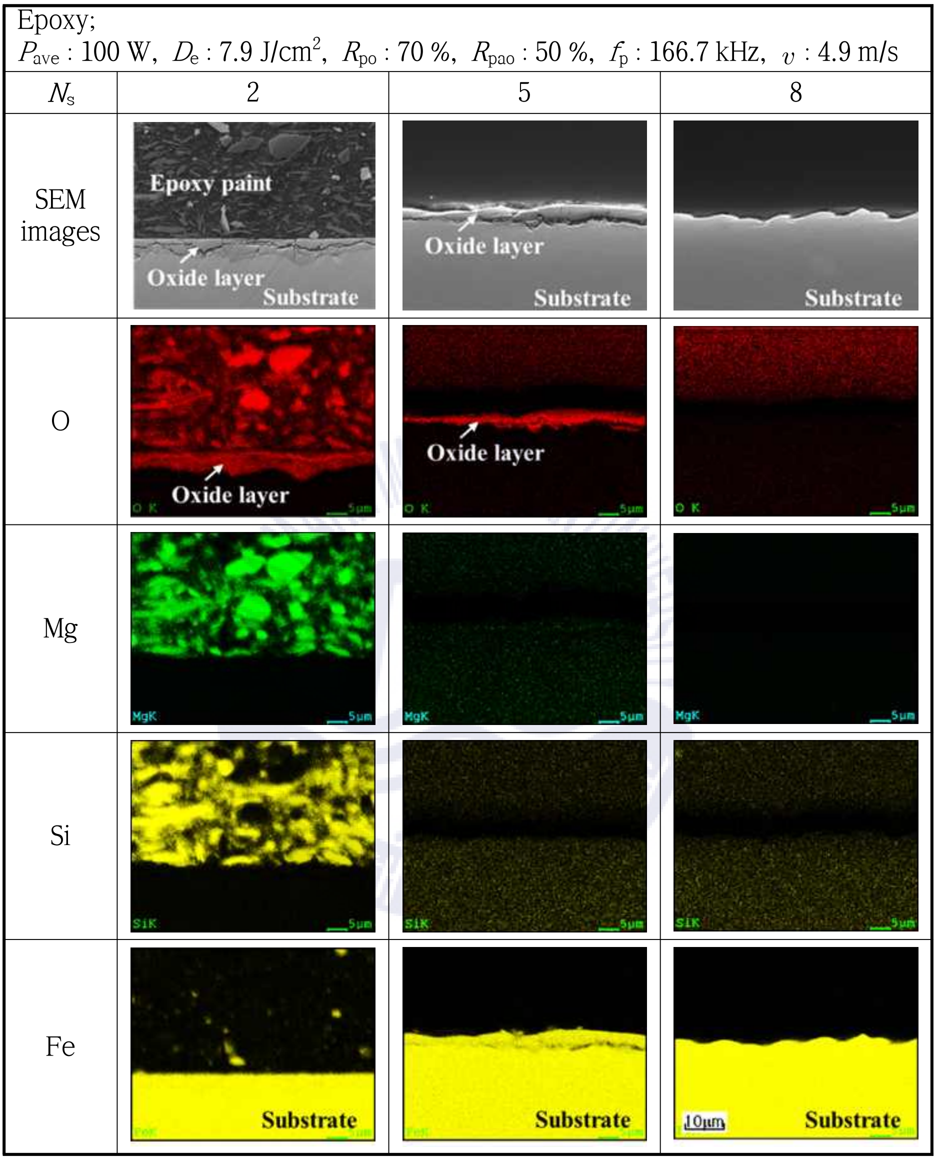

Fig. 4.15 EDS mapping analysis results on cross-section of laser cleaned epoxy surface with the number of scans in R_{po} = 70 % and R_{pao} = 50 %

(2) Comparison of the roughness of the laser cleaned surface

When analyzing the laser cleaning characteristics, the existence of the base metal damage is as important as the removal efficiency according to the process parameters. Depending on the laser cleaning applied area, a surface roughness higher than a specific value may be formed for the adhesiveness of paint and coating. However, laser cleaning is applied to remove undesired layers while minimizing the base metal damage in principle. In this section, at the representative pulse overlap rate of 70 %, the extent of the base metal damage according to the pass overlap rate was analyzed through the laser cleaned surface roughness and 3D profiles.

Fig. 4.16 shows the roughness of the laser cleaned surface according to the pass overlap rate and the number of scans. The variation of the roughness according to the number of scans was similar to the above analysis result. Fig. 4.17 shows the 3D profiles of the oxide layer removal condition at each pass overlap rate. The curves between passes formed perpendicular to the laser irradiation direction gradually decreased with the rising pass overlap rate and the cleaned surface geometry became smooth. Furthermore, at high overlap condition of laser beams, the surface layers were all removed with a small number of scans. Therefore, we obtained the laser cleaning result of a shortened interaction time between the base metal and laser beam and minimized the damage of the base metal.

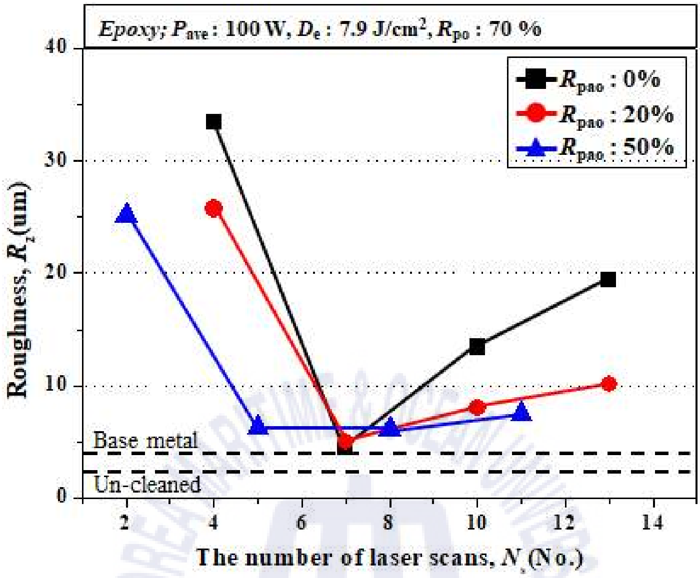

Fig. 4.16 Roughness variation of laser cleaned surface with pass overlap rate in R_{po} = 70 %

Epoxy; P_{ave} : 100 W, D_e : 7.9 J/cm^2, R_{po} : 70 %, f_p : 166.7 kHz, v : 4.9 m/s			
$R_{pao}(N_s)$	0 %(13)	20 %(13)	50 %(8)
3D profile	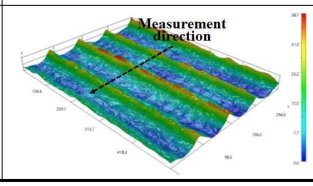	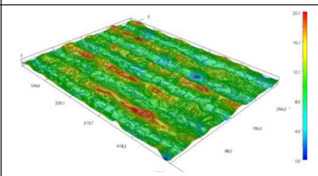	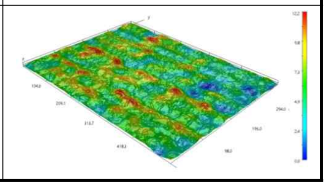

Fig. 4.17 3D-profile of laser cleaned surface with pass overlap rate in R_{po} = 70%

4.1.3 The effect of the energy density

(1) Removal characteristics of the epoxy paint and oxide layer according to the increasing heat input

The results of the previous experiments using major process parameters of laser cleaning according to pulse and pass overlap rates showed that the oxide layer was not removed at 20 % pulse overlap rate even if the number of scans and pass overlap rate were increased. Therefore, the laser cleaning experiment according to the energy density was performed while changing the energy density to 7.9 J/cm^2, 10.5 J/cm^2 and 13.2 J/cm^2 for every condition of 0 %, 20 % and 50 % pass overlap rates when the pulse overlap rate was 50 % and 70 %. The energy density is defined as the incident laser pulse energy per unit area and is a major process parameter that can control the heat input irradiated to the material during cleaning. Therefore, the energy density is an essential parameter that must be examined through an analysis of the laser cleaning characteristics because it can affect the paint removal efficiency and surface discoloration.

a. 50 % pulse overlap rate condition

Laser cleaning experiments according to energy density were performed at the pass overlap rates of 0 %, 20 % and 50 %. First, the epoxy paint and oxide layer removal conditions at 0 % pass overlap rate are shown in Fig. 4.18. At the energy density of 7.9 J/cm^2, the epoxy paint was removed in 14 scans, but the oxide layer was not removed even when the number of scans was increased. This tendency was also observed in the energy density conditions of 10.5 J/cm^2 and 13.2 J/cm^2. At these conditions, the epoxy paint was removed in 9 and 7 scans, respectively, but the oxide layer was not removed. To determine the epoxy paint and oxide layer removal conditions, XRD component analysis was performed on the laser cleaned surface and the results are shown in Fig. 4.19. The component analysis result for the specimen before laser cleaning detected pyrophyllite, barite and magnesite, which are the components of epoxy paint. The components of epoxy paint were fully removed in 14, 12 and 10 scans at the energy density of 7.9 J/cm^2, 10.5 J/cm^2 and 13.2 J/cm^2, respectively. After the epoxy paint was removed, magnetite, a component of oxide layer below the paint, and Fe, a component of the base metal, were detected. However, at the pulse overlap rate of 50 % and the pass overlap rate of 0 %, a peak of the oxide layer was detected even in 23, 15 and 13 scans in each energy density. This verified that the oxide layer is not fully removed in low heat input condition.

Fig. 4.20 and 4.21 show the epoxy paint and oxide layer removal conditions according to the energy density at the pass overlap rates of 20 % and 50 %. At the pass overlap rate of 20 %, the epoxy paint was fully removed in 11 and 9 scans at the energy density of 7.9 J/cm^2 and 10.5 J/cm^2, respectively, but the oxide layer remained on the base metal. However, when the energy density was 13.2 J/cm^2, both the epoxy paint and oxide layer could be removed at 13 scans. At 50 % pass overlap rate, the paint and oxide layer were fully removed at every condition. As the energy density increased from 7.9 J/cm^2 to 13.2 J/cm^2, the number of scans required for oxide layer removal decreased from 14 to 8. Therefore, it was found that in higher energy density condition, not only the removal of oxide layer was easier, but also the laser cleaning was completed with a smaller number of scans.

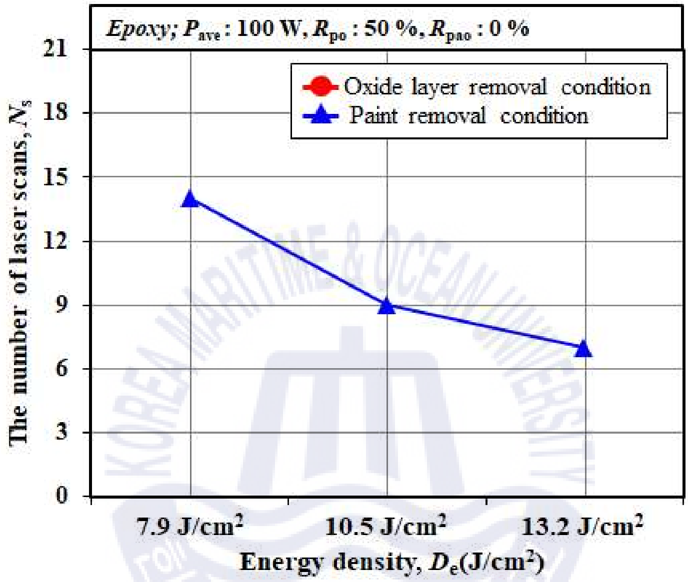

Fig. 4.18 Epoxy paint and oxide layer removal condition with energy density in R_{po} = 50 % and R_{pao} = 0 %

Epoxy;
P_{ave} : 100 W, R_{po} : 50 %, R_{pao} : 0 %

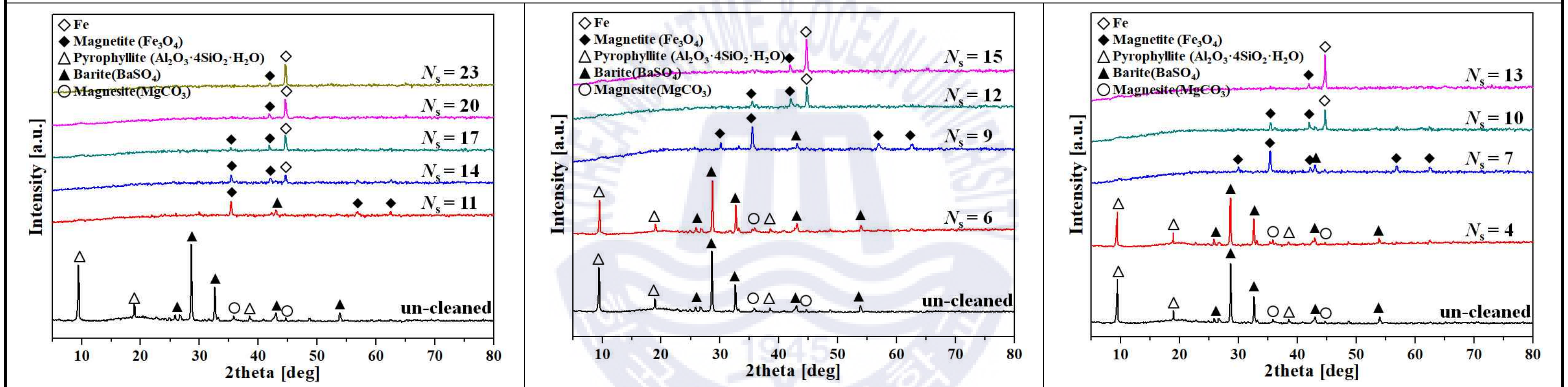

(a) D_e : 7.9 J/cm^2 | (b) D_e : 10.5 J/cm^2 | (c) D_e : 13.2 J/cm^2

Fig. 4.19 XRD results of laser cleaned epoxy surface with energy density in R_{po} = 50 %, R_{pao} = 0 %

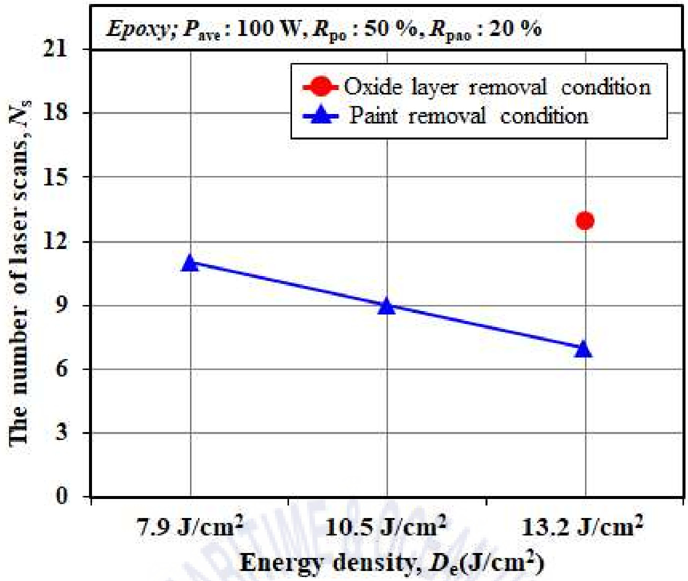

Fig. 4.20 Epoxy paint and oxide layer removal condition with energy density in R_{po} = 50 % and R_{pao} = 20 %

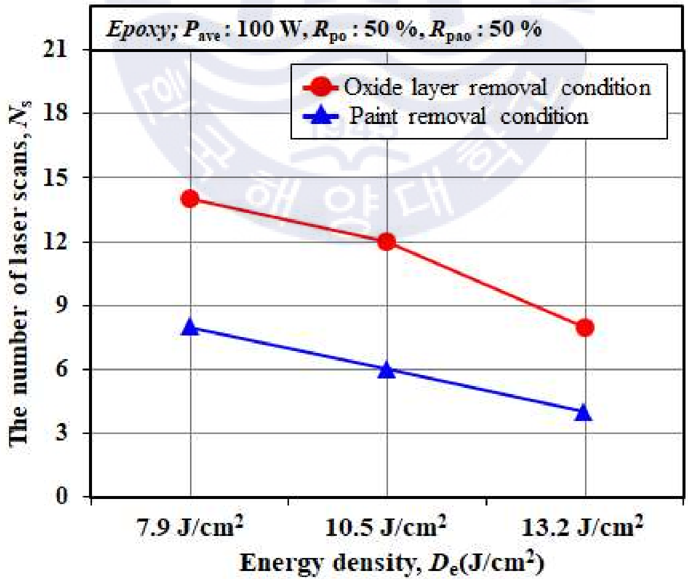

Fig. 4.21 Epoxy paint and oxide layer removal condition with energy density in R_{po} = 50 % and R_{pao} = 50 %

b. 70 % pulse overlap rate condition

In the laser cleaning process of the epoxy paint and oxide layer which accompanies thermal process, laser energy higher than the evaporation point must be irradiated to remove them. At 50 % pulse overlap rate, the oxide layer was not removed in the conditions of lower pass overlap rate and energy density. In this section, experiments were conducted to examine the effects of the change of the energy density on laser cleaning at 70 % pulse overlap rate where the cleaning characteristics according to the pulse overlap rate were excellent.

The results of the laser cleaning experiment according to the pass overlap rate and energy density are shown in Fig. 4.22 ~ 4.24. The epoxy paint and oxide layer could be removed in every condition. As the pass overlap rate and energy density increased, the number of scans required to remove the epoxy paint and oxide layer decreased gradually. When the pass overlap rate was 0 %, the oxide layer was fully removed at the energy density of 7.9 J/cm^2, 10.5 J/cm^2 and 13.2 J/cm^2 in 13, 13 and 9 scans, respectively. Furthermore, at 20 % pass overlap rate, the oxide layer was fully removed in 13, 11 and 5 scans at 7.9 J/cm^2, 10.5 J/cm^2 and 13.2 J/cm^2. At the maximum pass overlap rate condition of 50 % in this study, as the energy density increased, the oxide layer was fully removed in 8, 6 and 4 scans. This can be also confirmed in the XRD component analysis in Fig. 4.25. The components of the epoxy paint were removed in 5, 4 and 2 scans at the energy density of 7.9 J/cm^2, 10.5 J/cm^2 and 13.2 J/cm^2. Furthermore, the components of the oxide layer were also fully removed in 8, 6 and 4 scans, respectively. After the removal of oxide layer, only the peak of Fe, a component of the base metal, was detected.

The above experiment results show that the laser cleaning removal effect was greatly affected by the heat input. The removal mechanism of the epoxy paint and oxide layer through laser cleaning starts after the absorption of laser energy for the coating layer exceeds the laser ablation threshold of coated material. The removal characteristics of the epoxy paint and oxide layer according to the energy density during laser cleaning can be explained by Eq. (4.2), the Beer-Lambert absorption law. When the material absorption coefficient(α) and the threshold energy density for paint removal to occur (F_T) are fixed, the thickness of the removed paint(d) becomes proportional to the laser energy density(F). In other words, when the energy density increases, the thickness of the removed paint is increased as well. However, in the laser cleaning process, not only the energy density, but also various laser cleaning process parameters such as the laser beam overlap rate affect the heat input. As a result, at the maximum heat input conditions of 70 % pulse overlap rate, 50 % pass overlap rate, and 13.2 J/cm^2 energy density, the 200 ㎛ thick epoxy paint and 11 ㎛ thick oxide layer were all removed with the lowest number of scans[8, 52 ~ 57].

$$d = [\ln(F/F_T)]/\alpha \tag{4.2}$$

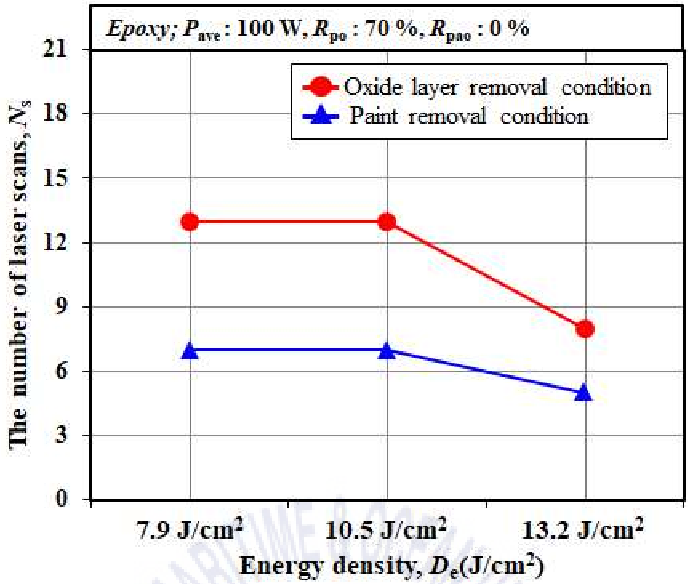

Fig. 4.22 Epoxy paint and oxide layer removal condition with energy density in R_{po} = 70 % and R_{pao} = 0 %

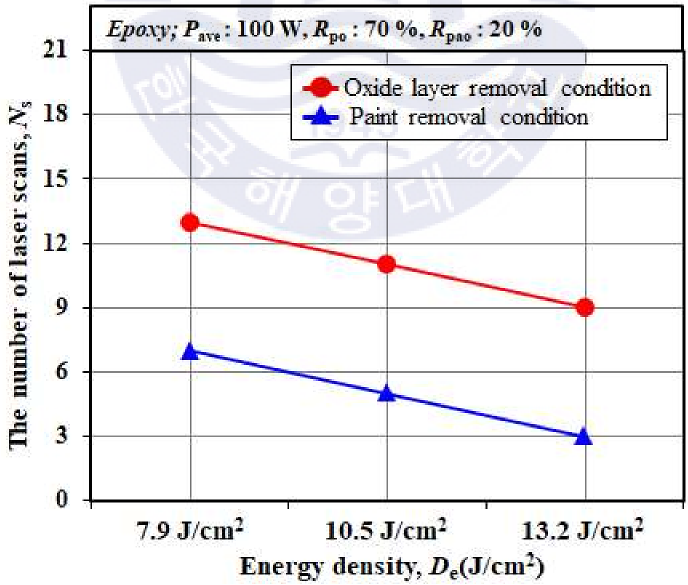

Fig. 4.23 Epoxy paint and oxide layer removal condition with energy density in R_{po} = 70 % and R_{pao} = 20 %

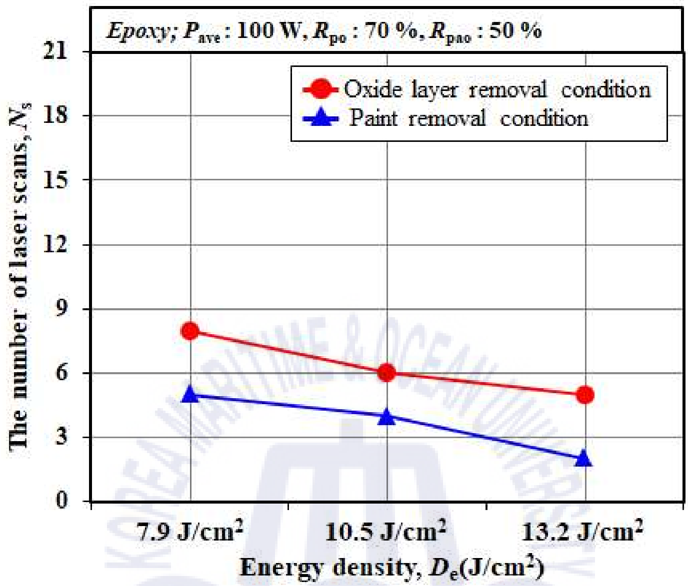

Fig. 4.24 Epoxy paint and oxide layer removal condition with energy density in R_{po} = 70 % and R_{pao} = 50 %

Epoxy;
P_{ave} : 100 W, R_{po} : 70 %, R_{pao} : 50 %

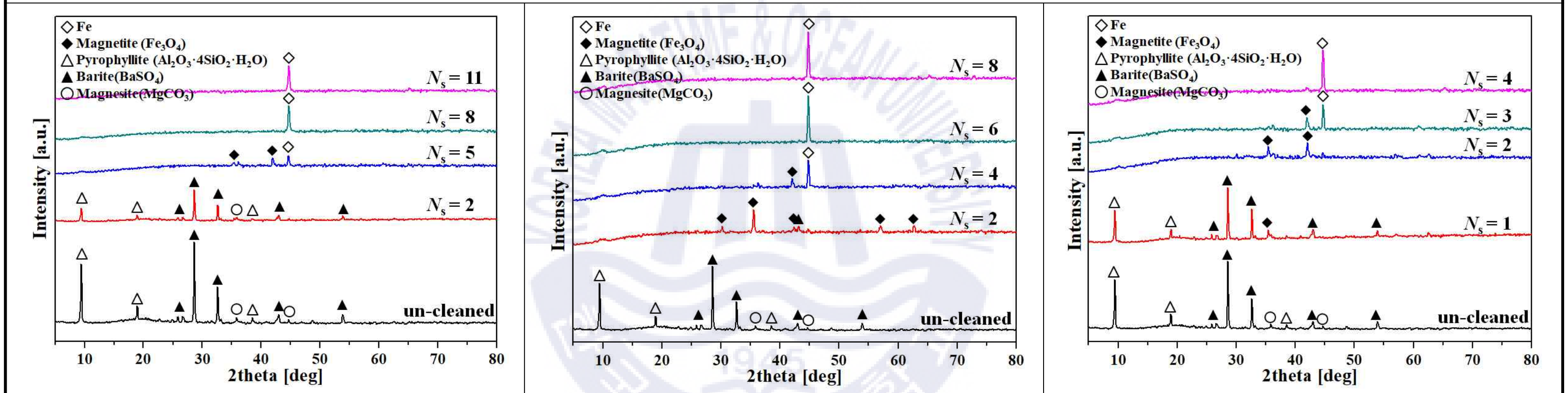

(a) D_e : 7.9 J/cm^2 (b) D_e : 10.5 J/cm^2 (c) D_e : 13.2 J/cm^2

Fig. 4.25 XRD results of laser cleaned epoxy surface with energy density in R_{po} = 70 %, R_{pao} = 50 %

(2) Analysis of the laser cleaned surface

The roughness and images of the laser cleaned surface were observed to compare and analyze the damage of the base metal and discoloration according to energy density and laser beam overlap rate. The roughness analysis of the cleaned surface was performed at the pulse overlap rate of 70 % and the pass overlap rate 50 %.

Fig. 4.26 shows the roughness analysis result of the laser cleaned surface according to the energy density at the pulse overlap rate of 70 % and the pass overlap rate of 50 %. The surface roughness variation according to the energy density was not clear. After the epoxy paint was removed, the roughness decreased to lower than 15 ㎛ at every condition. Consequently, at low energy density and laser beam overlap rate, the damage of the base metal may be caused because multiple scans are required to remove the surface layer. Therefore, excellent cleaning result with minimal damage of the base metal could be derived by selectively removing the epoxy paint and oxide layer while performing laser cleaning at relatively high heat input.

Fig. 4.27 shows the photograph of the laser cleaned surface. It can be seen that at the relatively low energy density of 7.9 J/cm^2, the cleanliness of the surface increases at higher numbers of scans. However, in the high energy density conditions, the peak power also increased, and the discoloration of the surface became worse as excessive laser energy was irradiated to the specimens. However, the discoloration of the surface would not cause a serious problem because the surface is repainted after laser cleaning, unless changes in mechanical properties and microstructure of the cleaned surface are caused by thermal effect.

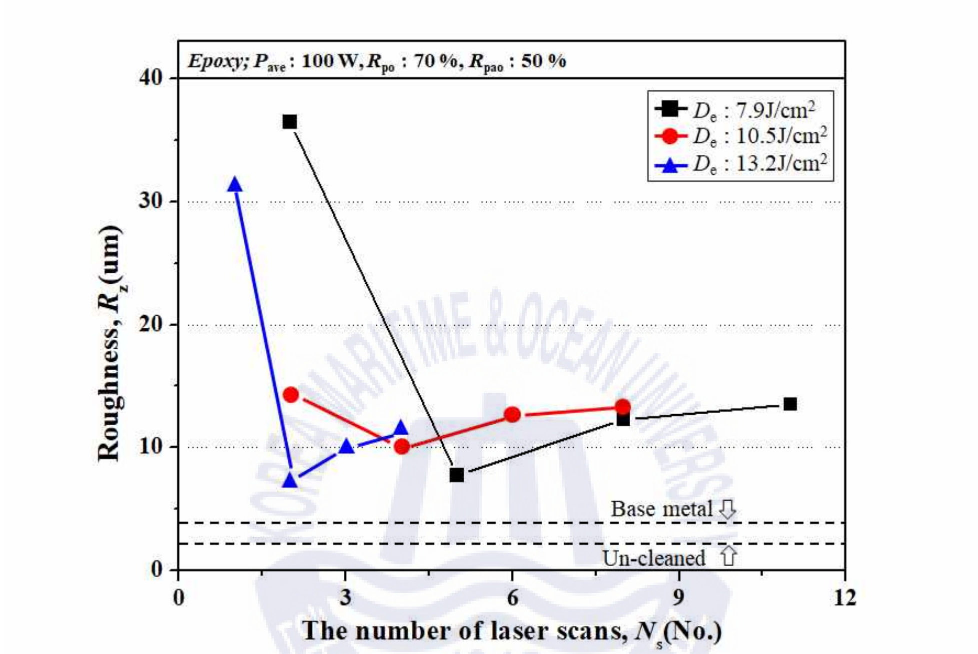

Fig. 4.26 Roughness variation of laser cleaned epoxy surface with energy density in R_{po} = 70 %, R_{pao} = 50 %

Epoxy; P_{ave} : 100 W, R_{po} : 70 %, R_{pao} : 50 %				
D_e \ N_s	2	5	8	11
7.9 J/cm^2 (P_p : 6 kW)				
D_e \ N_s	2	4	6	8
10.5 J/cm^2 (P_p : 8 kW)				
D_e \ N_s	1	2	3	4
13.2 J/cm^2 (P_p : 10 kW)		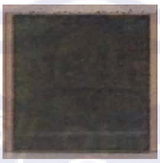		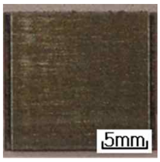

Fig. 4.27 Photos of laser cleaned surface with energy density

4.2 Laser cleaning characteristics of shop primer painted steel

4.2.1 The effect of the laser beam overlap rate

Shop primer plays a temporary anticorrosion role in the storage of steels and unlike epoxy paint, it is painted very thin with a thickness of 15 ~ 30 ㎛. Therefore, to analyze the laser cleaning characteristics of the thin shop primer and oxide layer, cleaning experiments were performed while changing the pulse and pass overlap rates, which are major process parameters of laser cleaning, in the same way as the cleaning experiment for epoxy paint. The laser beam overlap rates such as pulse and pass overlap rate greatly affect the scan speed during laser cleaning. Therefore, the effects of the laser beam overlap rates during laser cleaning on the scan speed were compared and analyzed.

(1) Comparison of cleaning characteristics according to the pulse overlap rate

a. Analysis of the laser cleaned surface

The laser cleaning experiment was performed while changing the pulse overlap rate to 20 %, 50 % and 70 % at the fixed energy density of 7.9 J/cm^2 and the pass overlap rate of 0 %. The 15 ㎛ thick shop primer layer can be removed by one scan in most cases. Thus, one laser scan was performed to examine whether or not the paint is removed. After that, the removal of the oxide layer was verified while increasing the number of scans at regular intervals.

Fig. 4.28 ~ 4.30 show the results of laser cleaning experiment performed in each condition. The photographs of the laser cleaned surface show that the grey shop primer was gradually removed and the surface cleanliness was improved with the rising number of scans. However, when the pulse overlap rate was 20 % and 50 %, it was observed that even when the number of scans increased to 20 and 15, the oxide layer on the base metal was not removed and only the surface roughness increased. When the pulse overlap rate became 70 %, the oxide layer was mostly removed at 9 scans and the surface geometry of the laser cleaned area was more smoother.

The above mentioned results of shop primer paint analysis demonstrated that the removal of the oxide layer was easy at a relatively high pulse overlap rate. This can be explained by Eq. (4.3) which is the calculation equation of the pulse overlap rate. Because the laser beam diameter(d) and the pulse frequency(f) are fixed parameters, the pulse overlap rate(R) is inversely proportional to the scan speed(v). In other words, at a low pulse overlap rate, the scan speed is fast; at a high pulse overlap rate, the scan speed is slow. When the scan speed decreases from 13.1 m/s to 4.9 m/s as the pulse overlap rate increases from 20 % to 70 % during laser cleaning, the incident laser energy per unit area increases sharply. Hence, at a high overlap condition of 70 %, the evaporation and decomposition of the paint and oxide layer becomes active, facilitating the removal of the oxide layer.

$$R(\%) = \left[1 - \left(\frac{v}{d \times f}\right)\right] \times 100 \qquad (4.3)$$

Note : R is the pulse overlap rate(%), v is the scan speed(mm/s), d is the laser beam diameter(mm), and f is the pulse frequency(Hz).

Fig. 4.31 shows the variation in surface roughness according to the pulse overlap rate and the number of scans. The shop primer specimen has high surface roughness values of the base metal and paint layer before laser cleaning. However, when some of the non-uniform paint and the irregularities of the surface are removed by laser cleaning, the surface roughness becomes somewhat smoother, resulting in a decrease of the roughness after laser cleaning. Furthermore, the micrography of the laser cleaned surface shows that there is no trace of laser irradiation on the surface of every specimen at a low number of scans, but as the number of scans increased, the laser energy reacted with the specimen and the traces of pulse laser became distinct. Consequently, the surface roughness increased as the number of scans increased at each overlap rate. In particular, at the pulse overlap rate of 20 %, the roughness of the laser cleaned surface increased to the roughness of the base metal after 17 laser scans. When the laser was irradiated further, the roughness of the laser cleaned surface increased higher than the roughness of the base metal due to the damage of the base metal. Furthermore, when the pulse overlap rate increased from 20 % to 70 %, the laser beam overlaps became evident. Hence, in the 70 % pulse overlap rate condition, the surface curve formed by the laser beam became smoother and the surface roughness became the lowest and this was confirmed to be the condition where the damage of the base metal becomes the smallest.

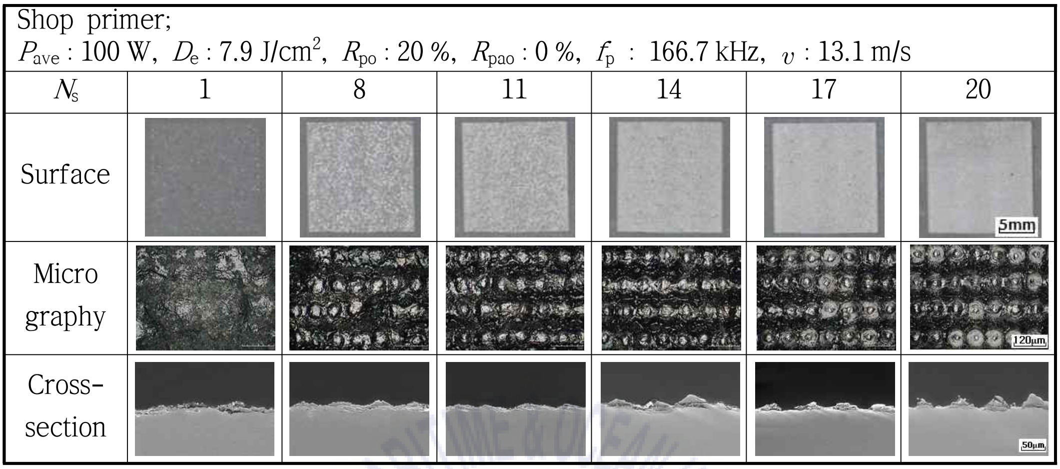

Fig. 4.28 Surface and cross-section of laser cleaned shop primer surface in R_{po} = 20 %, R_{pao} = 0 %

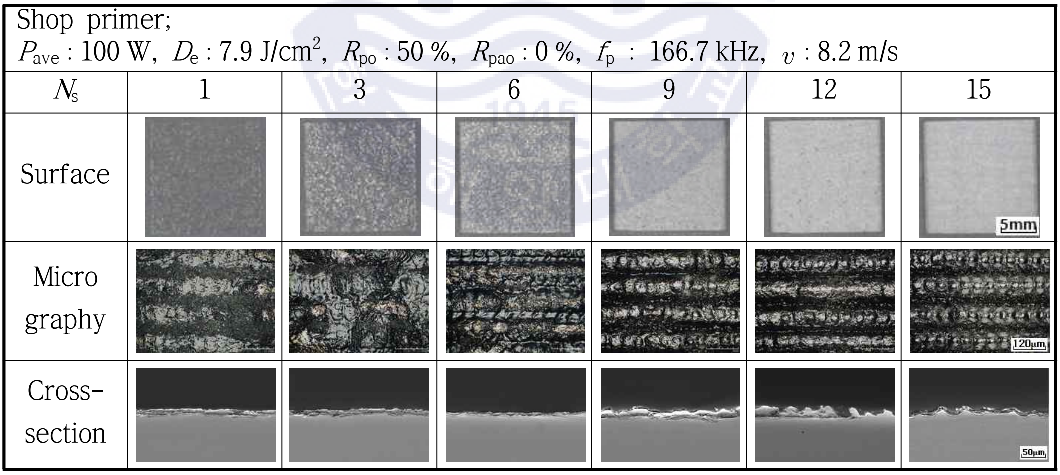

Fig. 4.29 Surface and cross-section of laser cleaned shop primer surface in R_{po} = 50 %, R_{pao} = 0 %

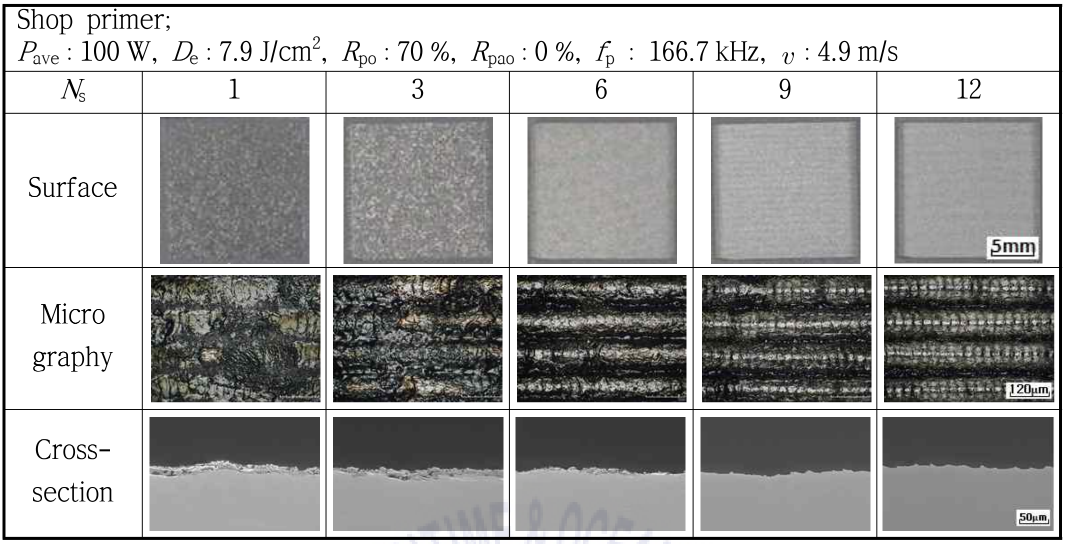

Fig. 4.30 Surface and cross-section of laser cleaned shop primer surface in R_{po} = 70 %, R_{pao} = 0 %

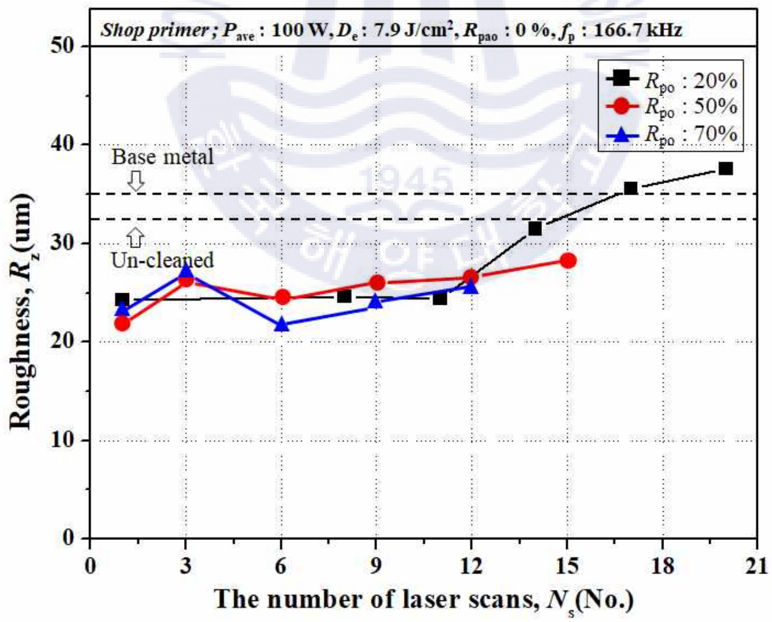

Fig. 4.31 Roughness variation of laser cleaned shop primer surface with pulse overlap rate in R_{pao} = 0 %

b. Component analysis of laser cleaned area

In the case of shop primer, it is difficult to clearly distinguish the paint and oxide layer because the paint layer is very thin. Thus, EDS analysis was performed to clearly determine whether the components remaining on the surface are a paint or an oxide layer. Fig. 4.32 shows the results of EDS mapping analysis of the specimen before laser cleaning, and Fig. 4.33 ~ 4.35 show the results of EDS spot analysis of the laser cleaned surface according to the pulse overlap rate.

The component analysis result for the specimen before laser cleaning detected Mg, Al, Si, P, Ca and Zn, the components of the shop primer paint. Below the shop primer, O and Fe, components of the oxide layer, were detected. As the component of the base metal, the Fe content was the highest. In the 20 % pulse overlap rate condition, Al, Si and Ca, the components of shop primer paint, were detected when the number of scans was 1. When the number of scans increased to 8 and 20, the contents of the elements of the paint decreased sharply, and the contents of O and Fe were the highest. This tendency can be also observed in the 50 % pulse overlap rate condition. The components of the paint remained at 1 scan, and were fully removed in 3 scans. However, the components of the oxide layer were not removed and continuously detected even at 15 scans. Thus, in the 20 % and 50 % conditions of the pulse overlap rate, most of the components of the shop primer print were mostly removed, but the oxide layer still remained on the surface. When the pulse overlap rate increased to 70 %, zinc was detected, which is a major component of the shop primer at one scan, but after 3 scans, the components of the paint were fully removed. Furthermore, when the number of scans increased further to 9, the O content decreased and only the Fe component was detected. Therefore, it was confirmed that in the 70 % pulse overlap rate condition, not only the paint, but also the oxide layer can be removed.

As a result of the component analysis, the removal conditions of the paint and oxide layer could be clearly determined. The shop primer was removed in 8, 3 and 3 scans at the pulse overlap rates of 20 %, 50 % and 70 %, respectively. In addition, in the 70 % pulse overlap rate condition, the oxide layer on the surface could be fully removed as well. Therefore, at a relatively low scan speed, the shop primer paint and oxide layer could be removed by a small number of scans by increasing the heat input.

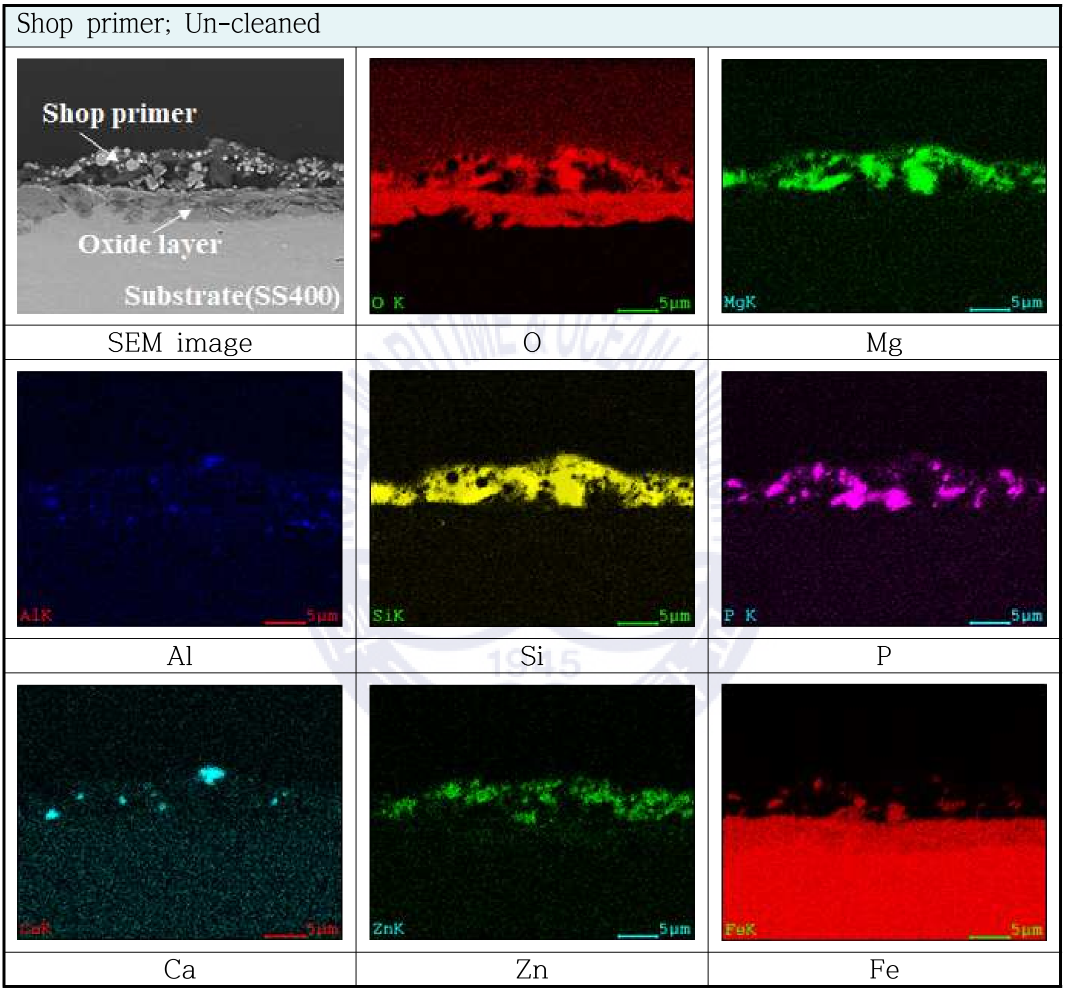

Fig. 4.32 EDS mapping analysis results on cross-section of un-cleaned shop primer specimen

Shop primer;
P_{ave} : 100 W, D_e : 7.9 J/cm^2, R_{po} : 20 %, R_{pao} : 0 %, f_p : 166.7 kHz, v : 13.1 m/s

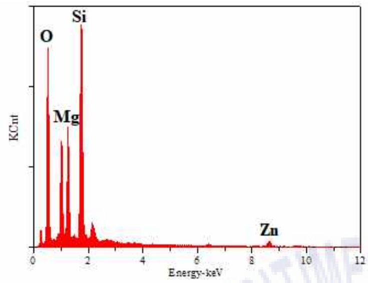

(a) un-cleaned

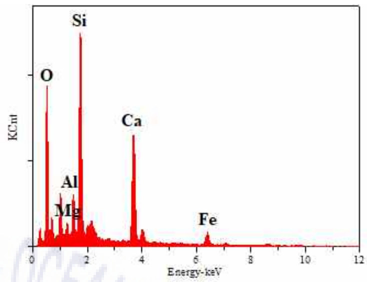

(b) N_s : 1

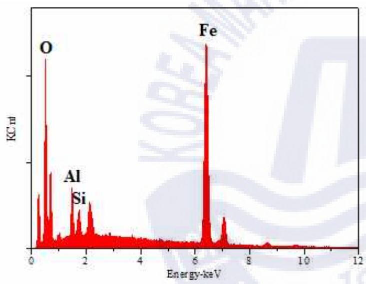

(c) N_s : 8

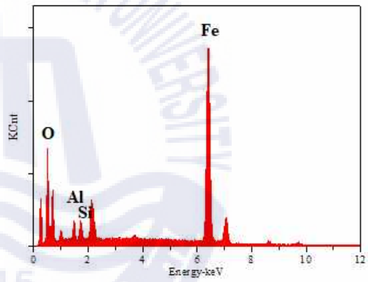

(d) N_s : 20

No.	Elements content(At%)							
	O	Mg	Al	Si	P	Ca	Zn	Fe
(a)	46.8	14.1	0.3	29.5	0.1	0.1	8.0	1.2
(b)	49.8	1.4	4.0	20.8	1.2	16.1	2.3	4.5
(c)	23.9	0.2	4.9	2.5	0.2	0.3	3.1	64.9
(d)	15.8	0.7	2.7	2.7	0.5	0.6	3.1	74.0

Fig. 4.33 EDS spot analysis results on laser cleaned shop primer surface in R_{po} = 20 %, R_{pao} = 0 %

Shop primer;
P_{ave} : 100 W, D_e : 7.9 J/cm^2, R_{po} : 50 %, R_{pao} : 0 %, f_p : 166.7 kHz, v : 8.2 m/s

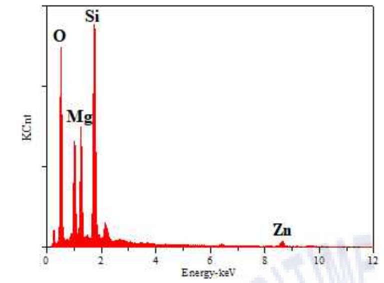

(a) un-cleaned

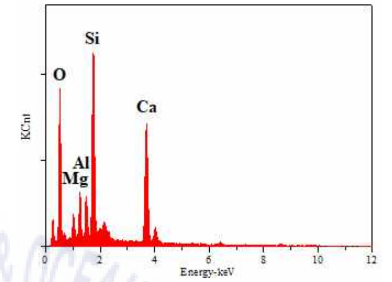

(b) N_s : 1

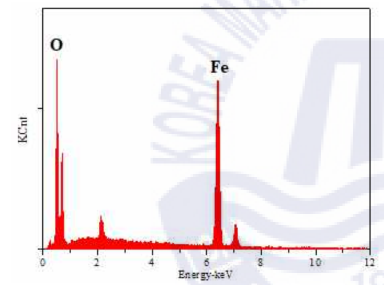

(c) N_s : 3

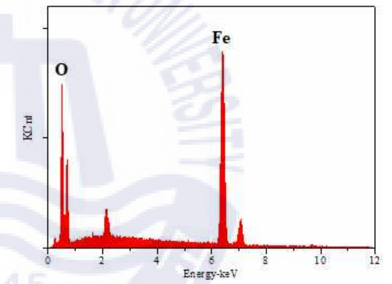

(d) N_s : 15

No.	Elements content(At%)							
	O	Mg	Al	Si	P	Ca	Zn	Fe
(a)	46.8	14.1	0.3	29.5	0.1	0.1	8.0	1.2
(b)	51.9	4.4	3.7	19.1	0.8	16.8	2.0	1.3
(c)	33.2	0.0	0.2	0.2	0.1	0.1	0.5	65.8
(d)	28.0	0.2	0.2	0.3	0.3	0.2	1.1	69.7

Fig. 4.34 EDS spot analysis results on laser cleaned shop primer surface in R_{po} = 50 %, R_{pao} = 0 %

Shop primer;
P_{ave} : 100 W, D_e : 7.9 J/cm^2, R_{po} : 70 %, R_{pao} : 0 %, f_p : 166.7 kHz, v : 4.9 m/s

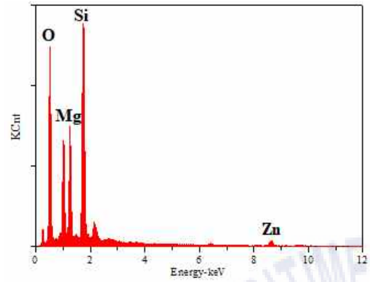

(a) un-cleaned

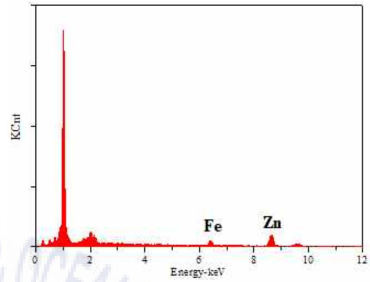

(b) N_s : 1

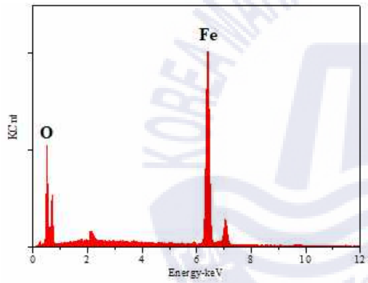

(c) N_s : 3

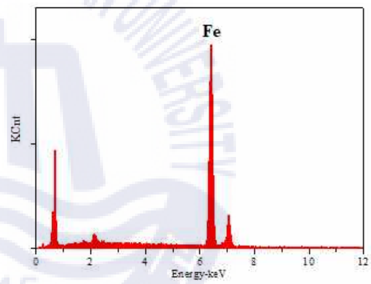

(d) N_s : 9

No.	Elements content(At%)							
	O	Mg	Al	Si	P	Ca	Zn	Fe
(a)	46.8	14.1	0.3	29.5	0.1	0.1	8.0	1.2
(b)	5.6	3.8	0.2	3.0	8.5	0.0	69.0	9.9
(c)	35.0	0.7	0.6	0.6	0.4	0.3	0.4	62.1
(d)	2.8	0.1	0.6	1.0	0.4	0.3	0.4	93.6

Fig. 4.35 EDS spot analysis results on laser cleaned shop primer surface in R_{po} = 70 %, R_{pao} = 0 %

(2) Comparison of cleaning characteristics according to the pass overlap rate

As mentioned above, when the energy density was constant, the scan speed changed when the pulse overlap rate was changed. By contrast, the pass overlap rate is a process parameter that affects the scan time, rather than the scan speed. When laser cleaning experiments are performed according to the pass overlap rate, the scan speed is determined by the pulse overlap rate, and the pass overlap rate determines the number of passes required to scan the entire area of 15 mm × 15 mm. Cleaning experiments were performed while changing the pulse overlap rate at 20 % and 50 % pass overlap rates, and the cleaning effects and the characteristics of the laser leaned area were analyzed in comparison with the 0 % pass overlap rate condition in the previous experiment.

Fig. 4.36 shows the paint and oxide layer removal conditions when the pulse overlap rate was changed to 20 %, 50 % and 70 % with the pass overlap rate fixed to 20 %, and Fig. 4.37 shows the surface roughness value. In the 20 % pulse overlap rate condition, the paint could be removed at 9 scans, but the oxide layer was not removed. When the pulse overlap rate increased to 50 % and 70 %, the paint was fully removed at one scan, and the oxide layer was removed at 18 and 9 scans, respectively. When the surface roughness values are examined, the laser cleaned surface was the roughest at the pulse overlap rate of 20 %, but at the pulse overlap rates of 50 % and 70 %, the surface roughness was lower than that of the specimen before laser cleaning as the non-uniform oxide layer on the base metal surface was removed.

This tendency can be also observed at the pass overlap rate of 50 % as shown in Fig. 4.38. The paint was fully removed at 7, 1 and 1 scans in each condition. The oxide layer was not removed at the pulse overlap rate of 20 % but when the pulse overlap rate increased to 50 % and 70 %, it was removed in 11 and 7 scans, respectively. The roughness of the laser cleaned surface in

Fig. 4.39 also showed a tendency to increase as the number of scans increased and to decrease as the pulse overlap rate increased.

To examine the laser cleaning characteristics according to the pass overlap rate, in the same pulse overlap rate condition, as the pass overlap rate increased, the oxide layer could be removed with a smaller number of scans. This is because as the number of laser passes to san the same area increases, and this increases the time that the laser beam stays on the material. As a result, the boiling point of the oxide layer is reached within a shorter time by the heat accumulation in the material, enabling the removal of the oxide layer with a fewer number of scans. Furthermore, when the pass overlap rate increases from 0 % to 50 %, the roughness of the laser cleaned surface stays similar or slightly increases in every overlap rate condition, thus reducing the damage of the base metal.

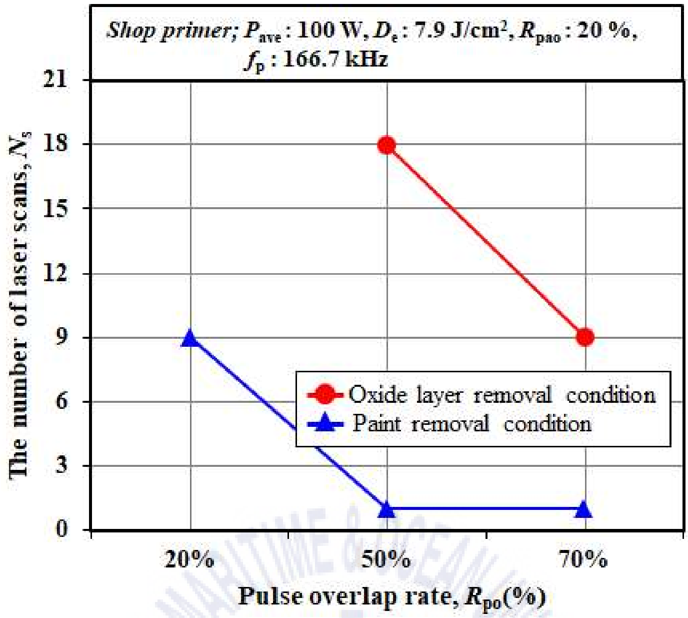

Fig. 4.36 Shop primer paint and oxide layer removal condition with pulse overlap rate in R_{pao} = 20 %

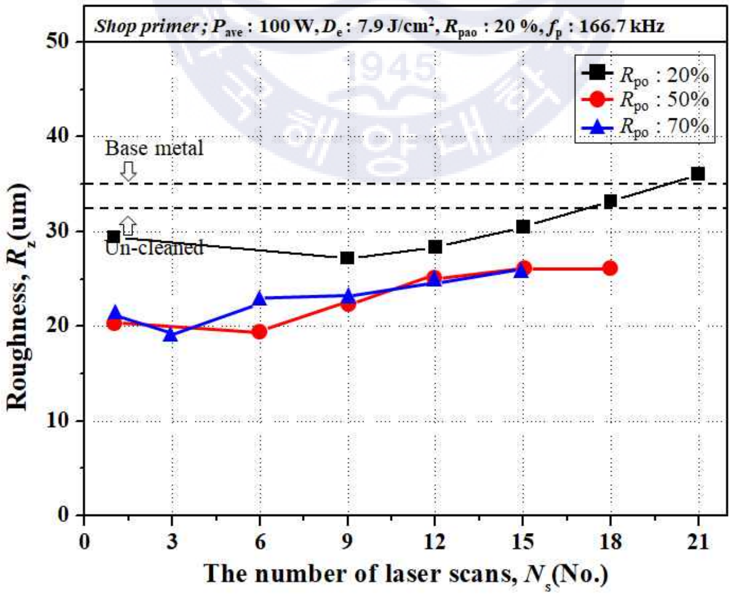

Fig. 4.37 Roughness variation of laser cleaned shop primer surface with pulse overlap rate in R_{pao} = 20 %

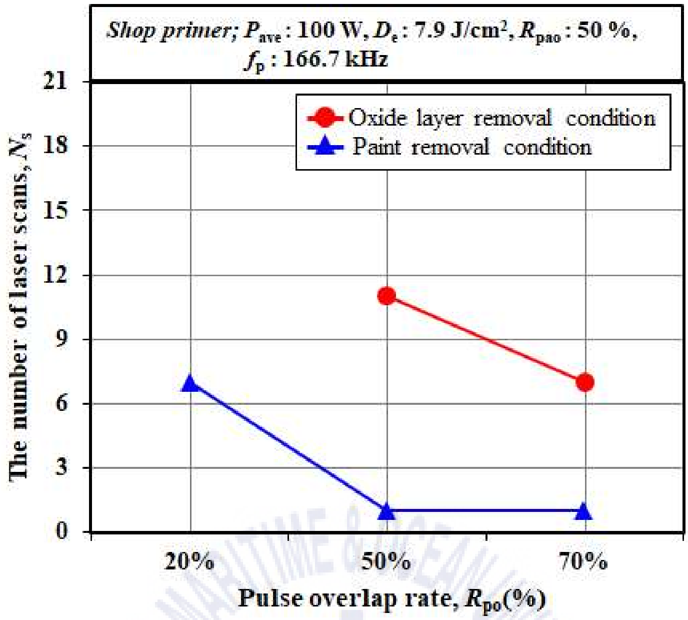

Fig. 4.38 Shop primer paint and oxide layer removal condition with pulse overlap rate in R_{pao} = 50 %

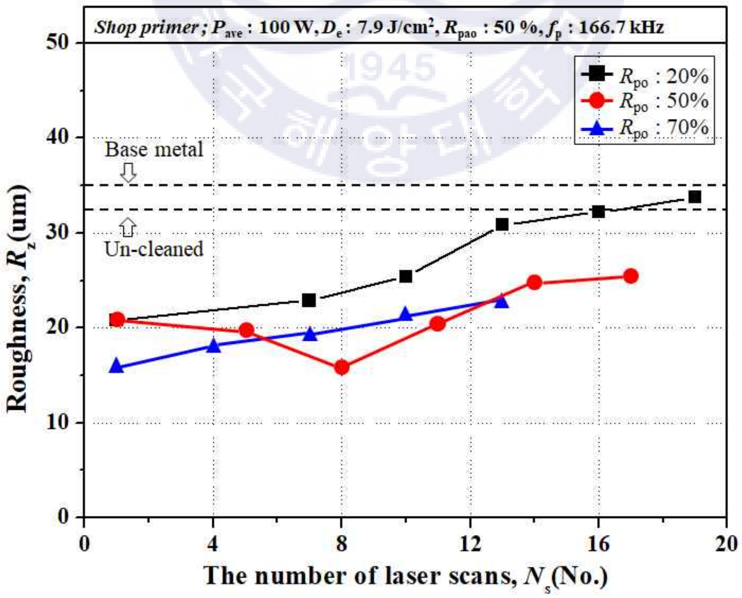

Fig. 4.39 Roughness variation of laser cleaned shop primer surface with pulse overlap rate in R_{pao} = 50 %

4.2.2 The effect of the energy density

(1) Comparison of removal characteristics of the paint and oxide layer

When the laser cleaning characteristics according to the laser beam overlap rate were compared and analyzed, it was found that the pulse overlap rate of 70 % represented the best laser cleaning characteristics. Therefore, during the cleaning experiment according to the energy density, the energy density was changed to 7.9 J/cm^2, 10.5 J/cm^2 and 13.2 J/cm^2 at the pass overlap rates of 0 %, 20 % and 50 % with the pulse overlap rate fixed at 70 %. As a result, the scan speed in each condition changed to 4.9 m/s, 3.7 m/s and 2.9 m/s, respectively. XRD component analysis was performed to clearly determine the removal of the paint and oxide layer, and the cross section of the laser cleaned area was also observed.

Fig. 4.40 shows the results of the laser cleaning experiment according to the energy density at the pass overlap rate of 0 %. The XRD component analysis for the specimen before laser cleaning detected magnetite, pyrophyllite and zinc, which is a major component of shop primer. In each condition, the components of the shop primer paint were all removed as the number of scans increased, and magnetite was detected, which is a component of the oxide layer below the paint layer. When laser was further irradiated and the oxide layer was removed, only Fe was detected, which is a component of the base metal. The components of paint were fully removed in 3 scans at the energy densities of 7.9 J/cm^2, 10.5 J/cm^2 and 13.2 J/cm^2. The oxide layer is considered to have been removed at 9, 6 and 7 scans in each condition. Fig. 4.41 shows the result of laser cleaning experiment at the pass overlap rate of 20 %. In every condition, the shop primer paint was removed at 1 scan. The oxide layer removal conditions were 9, 7 and 5 scans at the energy densities of 7.9 J/cm^2, 10.5 J/cm^2 and 13.2 J/cm^2, respectively. When the pass overlap rate increased from 0 % to 20 %, the paint removal effect according to the energy density increased, but the oxide layer removal effects were similar. However, when the pass overlap rate increased to 50 %, the oxide layer removal effect according to the energy density increased significantly. Fig. 4.42 confirms that the oxide layer removal condition greatly decreased to 7, 4 and 3 scans at the energy densities of 7.9 J/cm^2, 10.5 J/cm^2 and 13.2 J/cm^2, respectively. Because the shop primer paint layer is thin with a thickness of 15 ㎛, it was fully removed at 1 scan when a laser energy higher than the threshold for paint removal was irradiated.

Through the above experiment, it was found that the removal amount of the paint and oxide layer increased with the rising energy density. This can be explained by a change of scan speed according to the pulse energy, peak power and pulse frequency, which are changed by the energy density, and the scan speed according to the pulse frequency. The energy density is a pulse energy that is incident on one spot of the laser beam and is calculated by Eq. (4.4). When the laser beam area(A) is constant, the pulse energy(E_p) increases as the energy density(D_e) increases. Furthermore, the relationship between pulse energy and peak power(P_p) is defined by Eq. (4.5). In this experiment, the pulse duration time(t) is constant at 100 ns, which suggests that the two parameters are proportional to each other. Therefore, when the energy density increases, the heat input to the material increases because the pulse energy and peak power become higher.

$$D_e = E_p / A \; (J/cm^2) \qquad (4.4)$$

$$E_p = t \times P_p \; (J) \qquad (4.5)$$

Eq. (4.6) shows that when the average power(P_a) is constant at 100 W, the energy density increases, and when the peak power increases, the pulse duty ratio(D) decreases. The pulse duty ratio represents the ratio of the laser on time per pulse and is given by Eq. (4.7). When the pulse duty ratio decreases, the pulse cycle(T) increases and the pulse frequency(f) decreases by Eq. (4.8). It can be seen from Eq. (4.9), which is a rearrangement of Eq. (4.1), that the pulse frequency and scan speed(v) are mutually proportional. In other words, as the energy density increases the pulse frequency decreases. As a result, the scan speed is slow, and the incident laser energy per unit area during laser cleaning increases.

$$P_a = P_P / D \ \text{(W)} \tag{4.6}$$

$$D = t/T \ (\%) \tag{4.7}$$

$$f = 1/T \ \text{(Hz)} \tag{4.8}$$

$$f = NOP \times \frac{v}{d} \ \text{(Hz)} \tag{4.9}$$

Consequently, as the energy density decreases, the pulse energy, peak power and pulse frequency, which are laser cleaning parameters, are changed. In particular, a change in the pulse frequency leads to a change in the scan speed. Since the above mentioned process parameters greatly affect the heat input during laser cleaning, there are significant differences in removal characteristics of the paint and oxide layers according to the energy density.

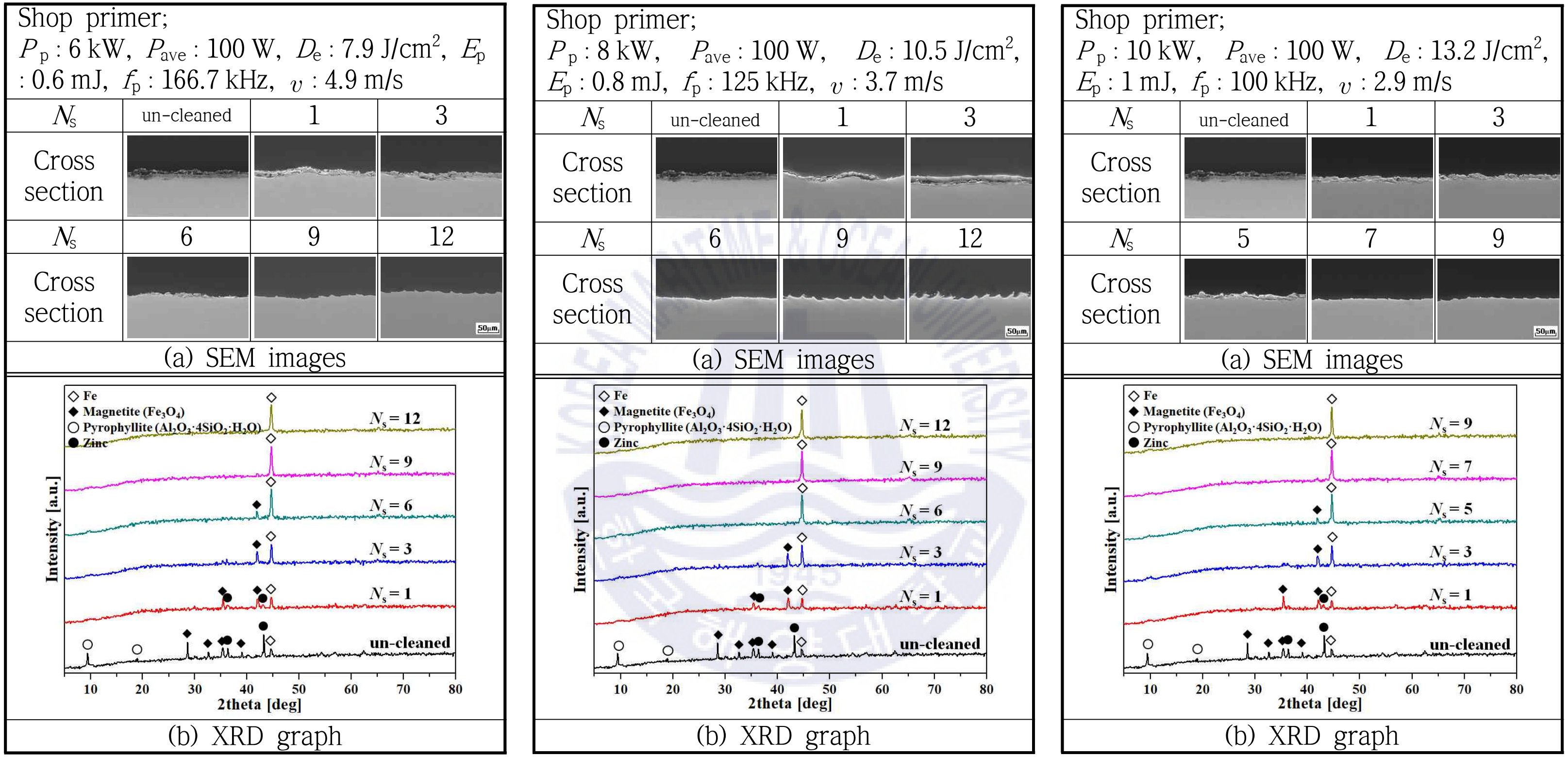

(A) D_e : 7.9 J/cm^2 (B) D_e : 10.5 J/cm^2 (C) D_e : 13.2 J/cm^2

Fig. 4.40 Cross-section and XRD results of laser cleaned shop primer surface with energy density in R_{po} = 70 %, R_{pao} = 0 %

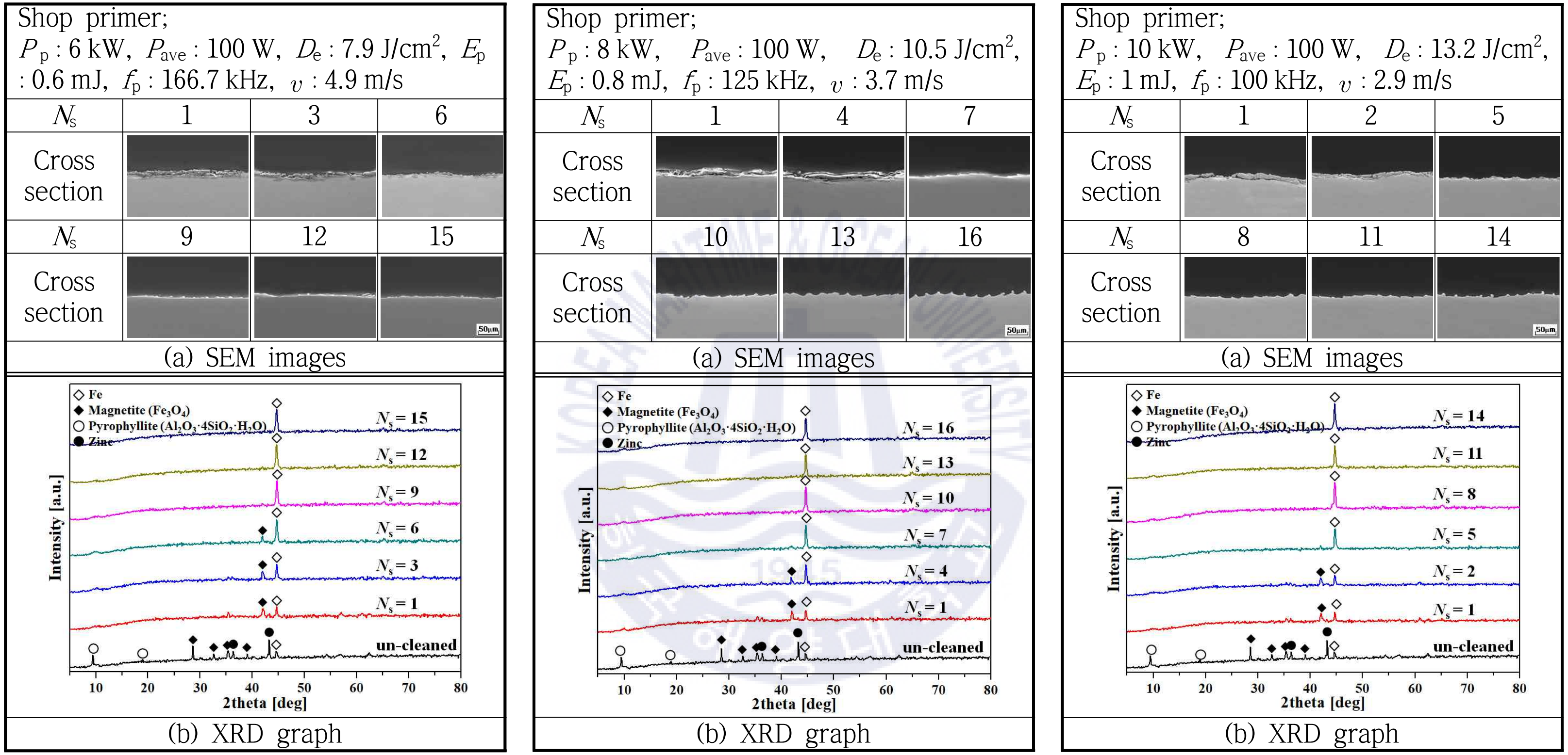

(A) D_e : 7.9 J/cm^2 (B) D_e : 10.5 J/cm^2 (C) D_e : 13.2 J/cm^2

Fig. 4.41 Cross-section and XRD results of laser cleaned shop primer surface with energy density in R_{po} = 70 %, R_{pao} = 20 %

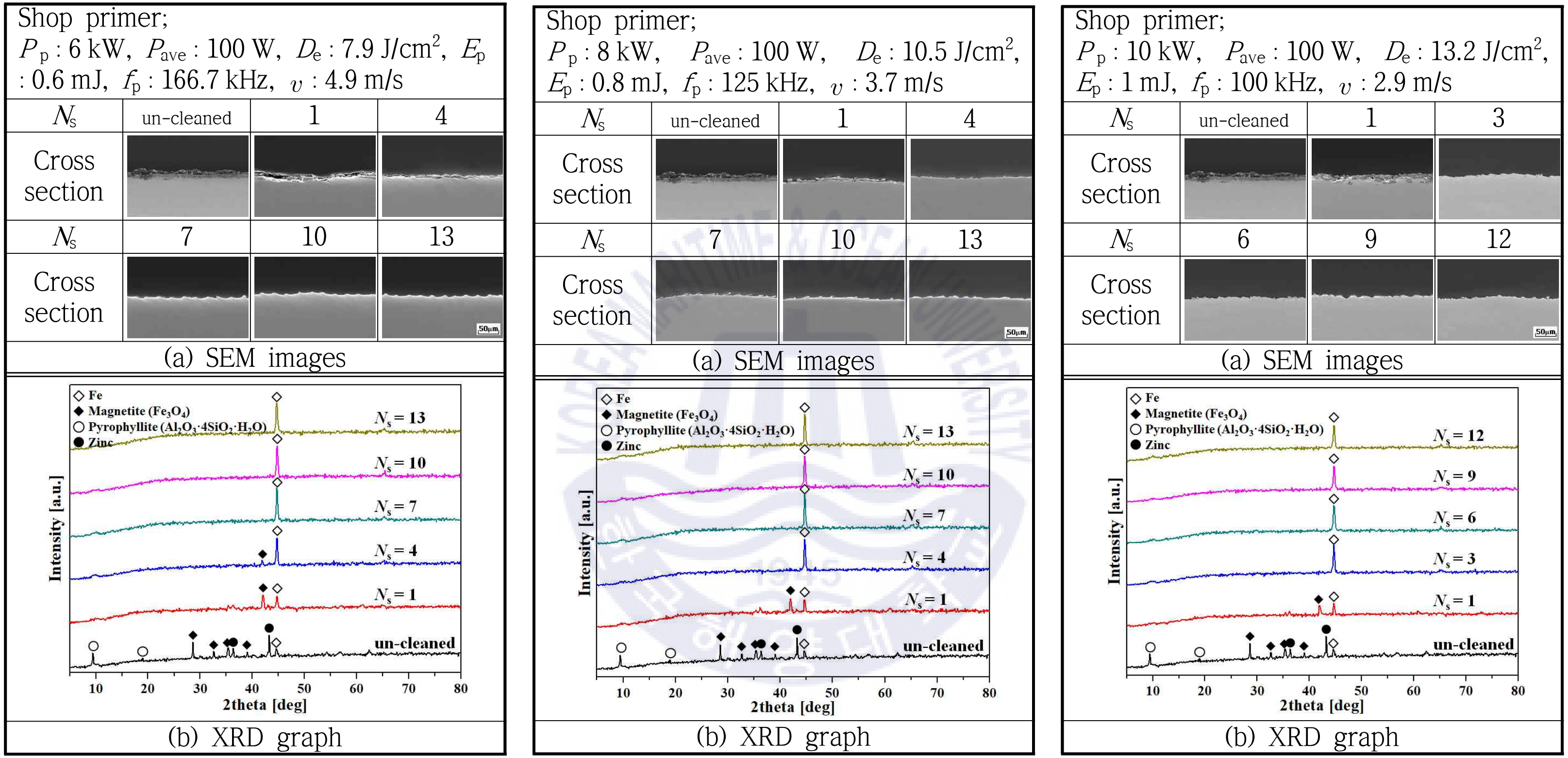

(A) D_e : 7.9 J/cm^2 (B) D_e : 10.5 J/cm^2 (C) D_e : 13.2 J/cm^2

Fig. 4.42 Cross-section and XRD results of laser cleaned shop primer surface with energy density in R_{po} = 70 %, R_{pao} = 50 %

(2) Analysis of the laser cleaned surface

Increasing the energy density during laser cleaning increases the removal amount of the paint and oxide layer. However, the increase of peak power and pulse energy and the decrease of scan speed can cause a thermal effect on the base metal. This thermal effect is expected to further deepened as the laser beam overlap rate rises. Therefore, to analyze the damage of the base metal and the discoloration of the laser cleaned surface due to the change in the heat input, the variation of the laser cleaned surface and roughness at the pulse overlap rate of 70 % and at the pass overlap rates of 20 % and 50 % were observed.

The variation tendency of surface roughness according to the energy density appeared somewhat differently depending on the laser beam overlap rate. Fig. 4.43 shows the surface micrography and 3D profile of the laser cleaned area according to the energy density and the number of scans at the pass overlap rate of 20 %, which is relatively low laser beam overlap rate. When the number of scans was 1 at each energy density, the shop primer paint and impurities on the surface were removed and the surface became the smoothest. Furthermore, the laser energy irradiated to the specimen is mostly consumed to remove the shop primer paint, and hence almost no trace of laser irradiation appears on the laser cleaned surface. However, when the number of scans increases, the trace of pulse laser becomes gradually distinct and curves are formed on the surface. Consequently, as shown in Fig. 4.44, the surface roughness increases with the rising number of scans, and this tendency becomes intensified as the energy density increases. In particular, when the energy density is 10.5 J/cm^2 or 13.2 J/cm^2, the surface roughness after laser cleaning in the 10, 11 scans, respectively becomes higher than the surface roughness before laser cleaning. Therefore, this could cause a severe damage of the base metal.

However, somewhat different tendencies were observed at the relatively high pass overlap rate of 50 %. When the geometry of the laser cleaned surface in Fig. 4.45 was examined, the curves of the surface became smooth as the pass overlap rate increased and the surface geometry did not change significantly even after the number of scans increased. Fig. 4.46 shows the surface roughness and the roughness did not change much even when the number of scans and energy density were increased. It was confirmed that surface roughness was approximately 10 ~ 16.2 ㎛ in every condition.

The micrography of the laser cleaned surface shows that as the heat input to the specimen increased, the discoloration of the laser cleaned surface worsened. This indicates that the laser cleaning mechanism of the paint and oxide layer is accompanied by thermal process. Therefore, if degradation of mechanical properties and damage of the base metal are not caused by the thermal effect, excellent removal effect can be obtained in the laser cleaning condition of high heat input. Therefore, discoloration of the surface does not need to be considered a serious issue in terms of laser cleaning efficiency.

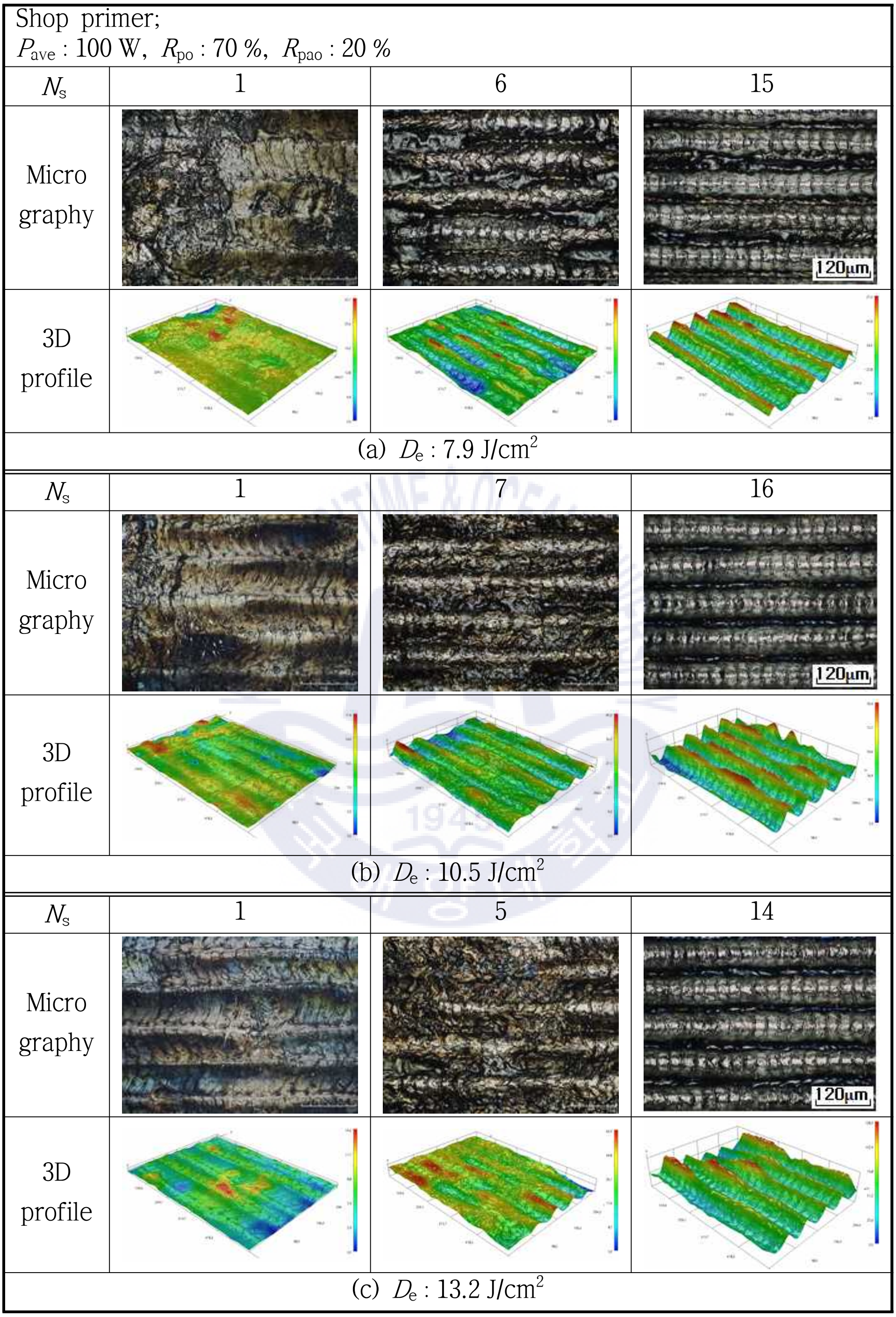

Fig. 4.43 Surface analysis results of laser cleaned shop primer surface with energy density in R_{po} = 70 %, R_{pao} = 20 %

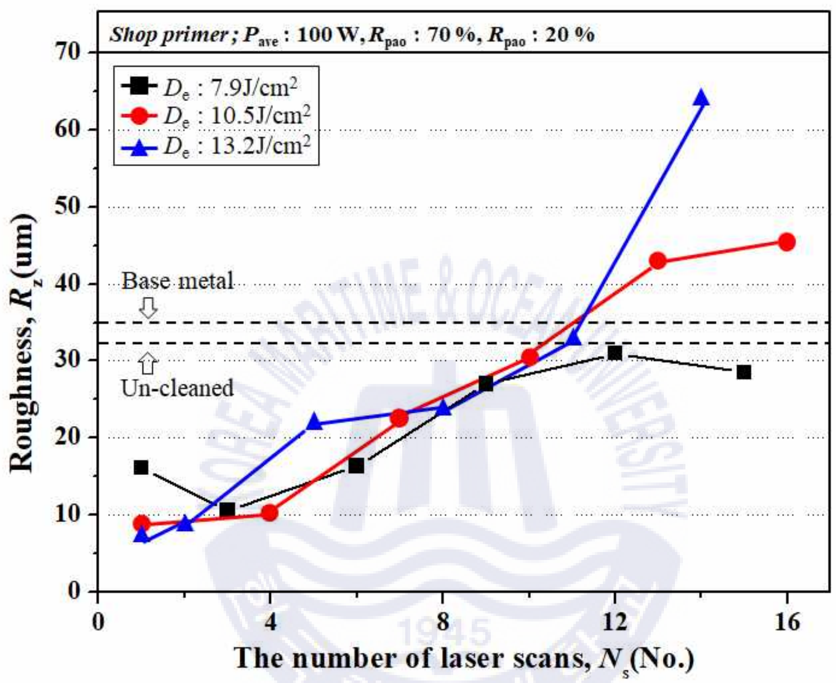

Fig. 4.44 Roughness variation of laser cleaned shop primer surface with energy density in R_{po} = 70 %, R_{pao} = 20 %

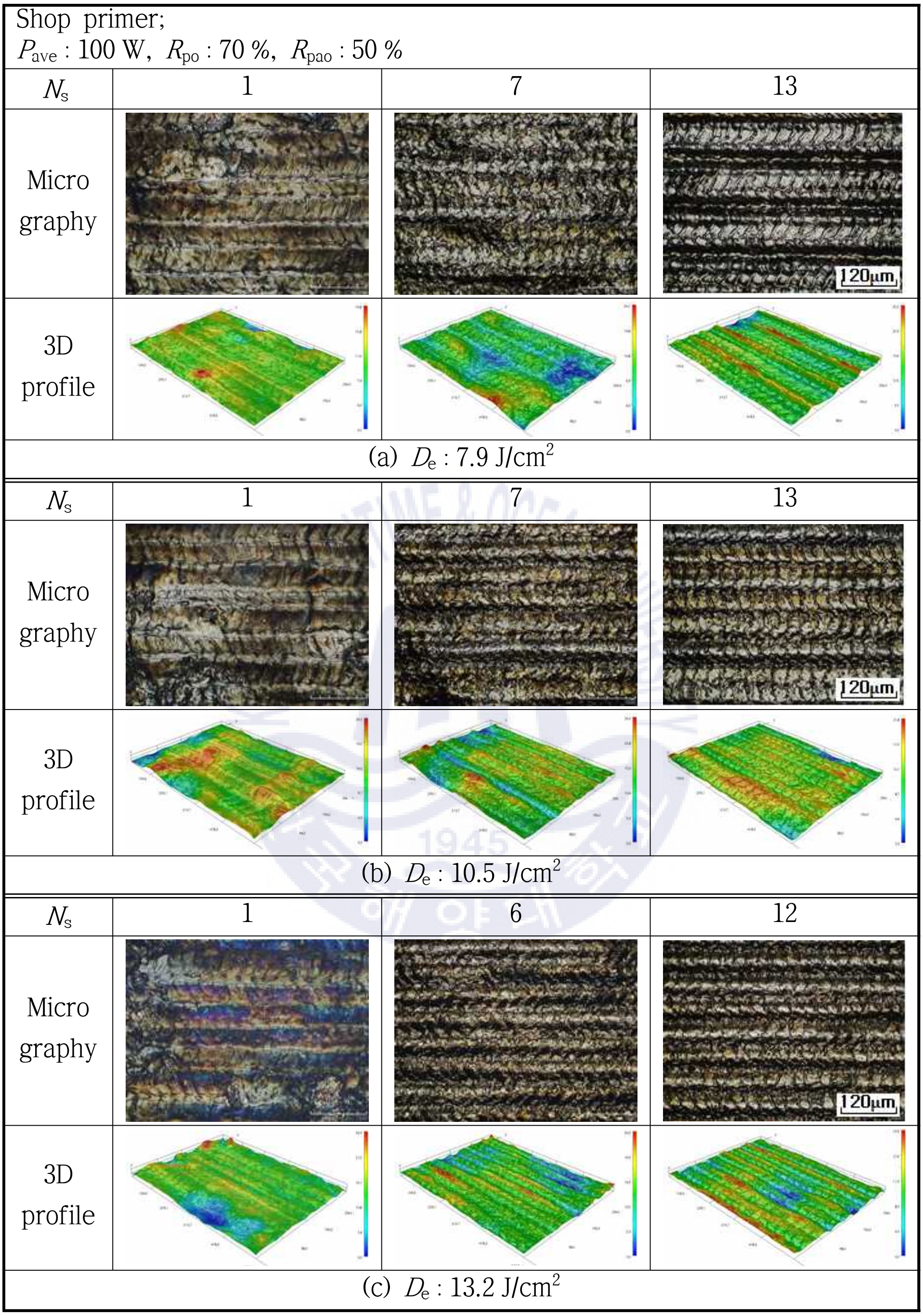

Fig. 4.45 Surface analysis results of laser cleaned shop primer surface with energy density in R_{po} = 70 %, R_{pao} = 50 %

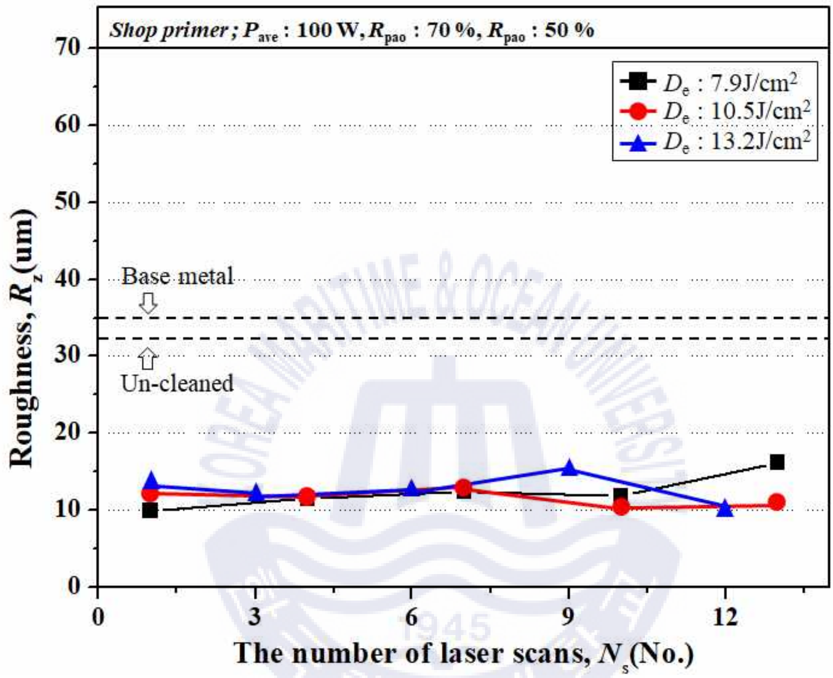

Fig. 4.46 Roughness variation of laser cleaned shop primer surface with energy density in R_{po} = 70 %, R_{pao} = 50 %

4.3 Comparison of laser cleaning characteristics by paint

4.3.1 Laser cleaning efficiency

Anticorrosion painting in shipbuilding and offshore industry is an essential process and paints are applied with various types and thicknesses depending on the area and application. However, rusts can be generated on the steel surface when the life span of paint expires, or paint is damaged by external shock or due to a corrosive environment such as seawater. To improve the quality of product, the paint and oxide layer of the steel surface are removed and the steel is repainted. Industrial sites try to promote the safety of workers, reduce environmental pollutions, and enhance the work efficiency than the existing surface pretreatment process by introducing laser cleaning to the paint removal process. To that end, the laser cleaning efficiency according to the process parameters obtained from the results of previous experiments was researched, and the optimum efficiency condition for laser cleaning were derived for each paint. The laser cleaning efficiency was calculated by the thickness of the paint and oxide layer removed when the laser beam scans an area of 15 mm × 15 mm once at each condition and the calculation equation is shown in Eq. (4.10).

$$\textit{Laser cleaning efficiency}[\mu m/s] = \textit{removal amount}(\mu m)/\textit{scan time}(s) \tag{4.10}$$

(1) Laser cleaning efficiency of epoxy paint

Table 4.1 shows the removal amount of epoxy paint and oxide layer and scan time at 1 scan. It was found through previous experiment results that the removal amount of the epoxy paint and oxide layer increased as the overlap rate and energy density of laser beam increased. This is because the amount of laser energy that reacts with the material, that is, the heat input to the material increased. However, as the laser beam overlap rate and energy density increase, the scan speed decreases, thus increasing the scan time. Therefore, in terms of work efficiency, the laser cleaning efficiency, which is calculated by the removal amount of the epoxy paint and oxide layer per unit time, needs to be compared and derived the optimum conditions.

Fig. 4.47 shows the laser cleaning efficiency of the epoxy paint and oxide layer according to the process parameters. When the laser cleaning efficiency according to the pulse overlap rate was examined, the cleaning efficiency was the highest at 70 %, followed by 20 % and 50 %. When the pulse overlap rate was 70 %, the scan speed was slow, but the cleaning efficiency was the highest due to the high removal amount. When the pulse overlap rate was 20 %, the cleaning efficiency was the second highest due to the shortest scan time relative to the paint removal amount. The results according to the energy density show that as the energy density increased to 13.2 J/cm^2, the conditions that can remove the oxide layer increased, and the laser cleaning efficiency also increased slightly in general. When the cleaning efficiency was compared by pass overlap rate, the cleaning efficiency was the highest at the pass overlap rate of 20 % where the scan time is relatively short. Consequently, the most efficient laser cleaning was possible at 70 % pulse overlap rate and 20 % pass overlap rate 20 % when the energy density was 13.2 J/cm^2.

Table 4.1 The removal amount of epoxy and oxide layer and scan time at 1 scan according to laser parameters

R_{pao}(%)	R_{po}(%)	The removal amount(㎛)			Scan time(s)		
		D_e : 7.9 J/cm^2	D_e : 10.5 J/cm^2	D_e : 13.2 J/cm^2	D_e : 7.9 J/cm^2	D_e : 10.5 J/cm^2	D_e : 13.2 J/cm^2
0	20	-	-	-	0.175	0.234	0.294
	50	-	-	-	0.280	0.376	0.469
	70	16.23	16.23	23.44	0.469	0.621	0.792
20	20	-	-	-	0.213	0.285	0.358
	50	-	-	16.23	0.341	0.458	0.570
	70	16.23	19.18	42.20	0.570	0.755	0.940
50	20	-	13.19	17.58	0.328	0.438	0.550
	50	15.07	17.58	26.38	0.523	0.704	0.876
	70	26.38	35.17	52.75	0.876	1.160	1.480

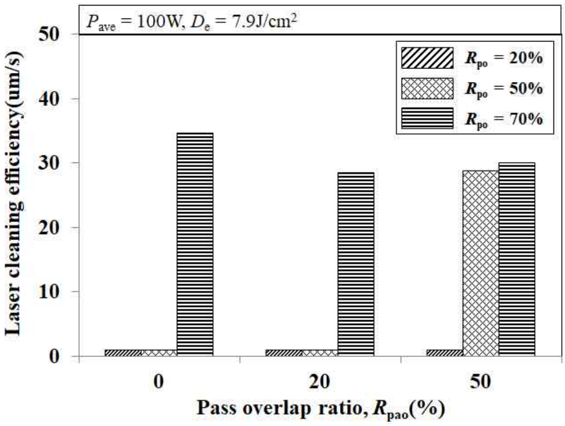

(a) D_e : 7.9 J/cm^2

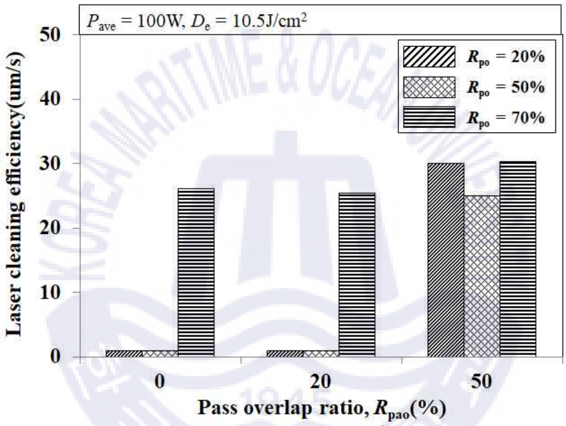

(b) D_e : 10.5 J/cm^2

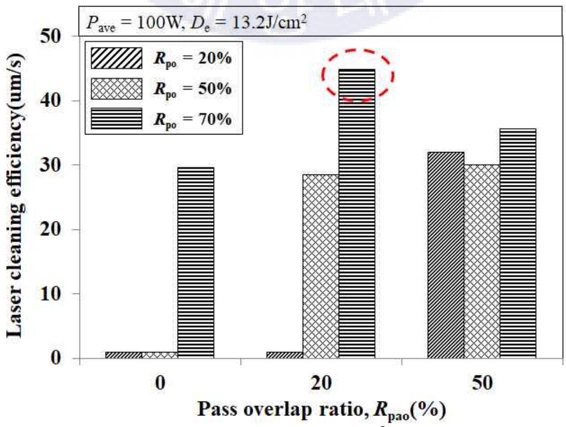

(c) D_e : 13.2 J/cm^2

Fig. 4.47 Laser cleaning efficiency of epoxy paint and oxide layer with process parameters and indication of optimum efficiency condition

(2) Laser cleaning efficiency of the shop primer paint

Table 4.2 shows the removal amount of shop primer and oxide layer and the scan time at one scan according to laser cleaning process parameters. In each condition, the removal amount was the highest at 8.67 ㎛ in the maximum heat input condition at an energy density of 13.2 J/cm^2, a pulse overlap rate of 70 % and a pass overlap rate of 50 %. However, the scan time was the longest at 1.48 s due to the slow scan speed in this condition. In the laser cleaning process of the paint and oxide layer, which have both thermal process and ablation mechanism, the selection of laser cleaning process parameters that can selectively remove only the paint and oxide layer without damaging the base metal within a short time is critical. Therefore, the laser cleaning efficiency was analyzed to select the laser cleaning condition where the removal amount relative to the scan time is the highest.

Fig. 4.48 shows the laser cleaning efficiency of the shop primer and oxide layer according to the process parameters. To examine the laser cleaning efficiency according to the energy density, it can be seen that at the energy density of 7.9 J/cm^2, it is relatively difficult to remove the oxide layer due to the low energy density. To compare the cleaning efficiency between the energy densities of 10.5 J/cm^2 and 13.2 J/cm^2, the cleaning efficiency was higher in most cases at the energy density of 10.5 J/cm^2 at which the scan time is relatively short. The laser cleaning efficiency according to the pulse overlap rate and pass overlap rate did not show any clear tendency due to the thin paint layer and the irregular oxide layer. Consequently, the removal amount per unit time was the highest at the pulse overlap rate of 70 % and the pass overlap rate of 0 % when the energy density was 10.5 J/cm^2.

As mentioned above, the laser cleaning efficiency of the 200 ㎛ thick epoxy paint layer and the 15 ㎛ thick shop primer paint layer show somewhat different tendencies. In the laser cleaning of the thick epoxy paint layer, the cleaning efficiency was the highest at an energy density of 13.2 J/cm^2, a pulse overlap rate of 70 %, and a pass overlap rate of 20 %, which is a high heat input condition. By contrast, the high heat input condition in the laser cleaning process of the thin shop primer paint layer can increase the removal amount, but the efficiency is low due to the slow scan speed. Therefore, it was found that the most efficient laser cleaning is possible in the condition of an energy density of 10.5 J/cm^2, a pulse overlap rate of 70 %, and a pass overlap rate of 0 % at which the shop primer and oxide layer can be selectively removed in the short interaction time between the material and laser. Consequently, thermal process was dominant in the laser cleaning of thick coating, whereas ablation was dominant in the laser cleaning of thin coating.

Table 4.2 The removal amount of shop primer and oxide layer and scan time at 1 scan according to laser parameters

R_{pao}(%)	R_{po}(%)	The removal amount(㎛)			Scan time(s)		
		D_e : 7.9 J/cm^2	D_e : 10.5 J/cm^2	D_e : 13.2 J/cm^2	D_e : 7.9 J/cm^2	D_e : 10.5 J/cm^2	D_e : 13.2 J/cm^2
0	20	-	-	-	0.175	0.234	0.294
	50	-	2.17	2.36	0.280	0.376	0.469
	70	2.17	4.33	3.71	0.469	0.621	0.792
20	20	-	1.44	1.73	0.213	0.285	0.358
	50	1.44	2.89	2.17	0.341	0.458	0.570
	70	2.89	3.71	3.25	0.570	0.755	0.940
50	20	-	2.60	2.17	0.328	0.438	0.550
	50	2.36	3.71	4.33	0.523	0.704	0.876
	70	3.71	6.50	8.67	0.876	1.160	1.480

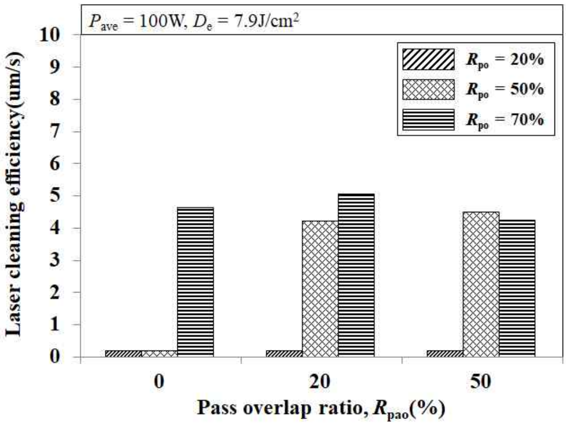

(a) D_e : 7.9 J/cm^2

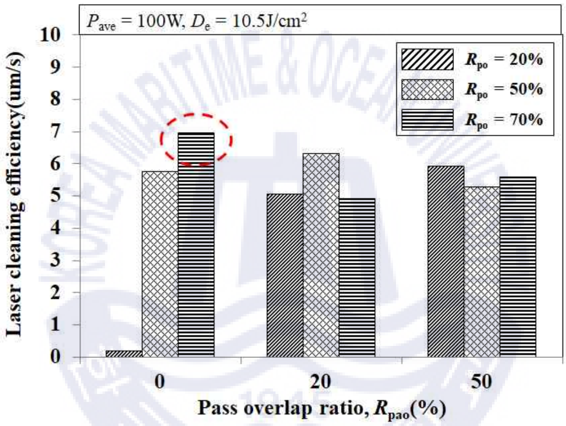

(b) D_e : 10.5 J/cm^2

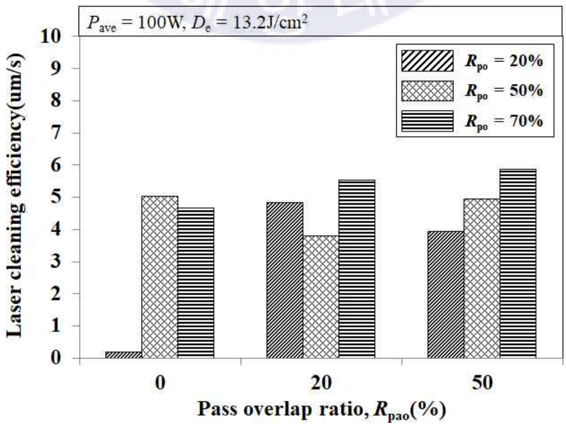

(c) D_e : 13.2 J/cm^2

Fig. 4.48 Laser cleaning efficiency of epoxy paint and oxide layer with process parameters and indication of optimum efficiency condition

4.3.2 Comparison of evaporation characteristics

In the laser cleaning process, the interaction between laser and material is affected by various parameters. The main parameters can be largely divided into laser parameters and material parameters. Among the material parameters, the laser cleaning characteristics according to the coating layer thickness were examined in the previous section. In this section, the laser cleaning results according to the evaporation point of each paint are compared.

To examine the average laser cleaning efficiency for each paint, it is 30.64 ㎛/s for epoxy paint and 5.10 ㎛/s for shop primer. This means that when the same laser energy is irradiated to the material, the removal amount of epoxy paint per unit time is larger than that of the shop primer. Table 4.3 lists the main components and properties of each paint. It can be seen that the boiling point of zinc dust, the main component of the shop primer, is approximately four times higher than that of the bisphenol epoxy A, the main component of the epoxy paint. Therefore, When the same laser energy is irradiated to the material during laser cleaning with ablation, the removal amount of the epoxy paint with a lower boiling point is larger than that of the shop primer paint. Consequently, among the material parameters, mechanical properties such as the boiling points and thermal conductivity of pollutant and base metal are expected to have a significant effect on the laser cleaning result.

Table 4.3 Main components and properties of paint

Property / Material	Main component	Melting point(℃)	Boiling point(℃)
Epoxy	bisphenol epoxy A	158	220
Shop primer	zinc dust	149	907

4.3.3 Mechanical and microstructure characteristics of laser cleaned area

Laser cleaning process can remove the pollutant layer while minimizing the damage of the base metal and thermal effect by using the Q-switching laser which oscillates with a short laser pulse and a high peak power. However, if the heat input of the material is increased excessively to increase the removal amount during laser cleaning, it can cause thermal effect on the laser cleaned area. Therefore, the mechanical and microstructure characteristics of the laser cleaned area were evaluated at the optimum efficiency and maximum heat input conditions.

(1) Hardness distribution of the laser cleaned area

To evaluate the mechanical properties by the heat input of epoxy and shop primer paints the hardness was measured in the longitudinal direction from the laser cleaned surface.

Fig. 4.49 shows the longitudinal hardness distribution of the laser cleaned epoxy painted surface at the optimum efficiency and maximum heat input conditions. The hardness was 139 ~ 168 Hv in the optimum condition and the hardness was 139 ~ 177 Hv in the maximum heat input condition, which is similar to the hardness of the substrate, 141 ~ 168 Hv. Therefore, laser cleaning results had no heat affected zone could be obtained from surface to 1 mm along the depth in both conditions.

Fig. 4.50 shows the hardness distribution of laser cleaned shop primer surface at the optimum efficiency and maximum heat input conditions. The hardness was 135 ~ 172 Hv in the optimum condition and the hardness in the maximum heat input condition was 136 ~ 171 Hv. Thus, the hardness did not show significant differences from the hardness of the base metal. Therefore, the mechanical properties of the laser cleaned area in the optimum efficiency and maximum heat input conditions were found to be similar to those of the base metal.

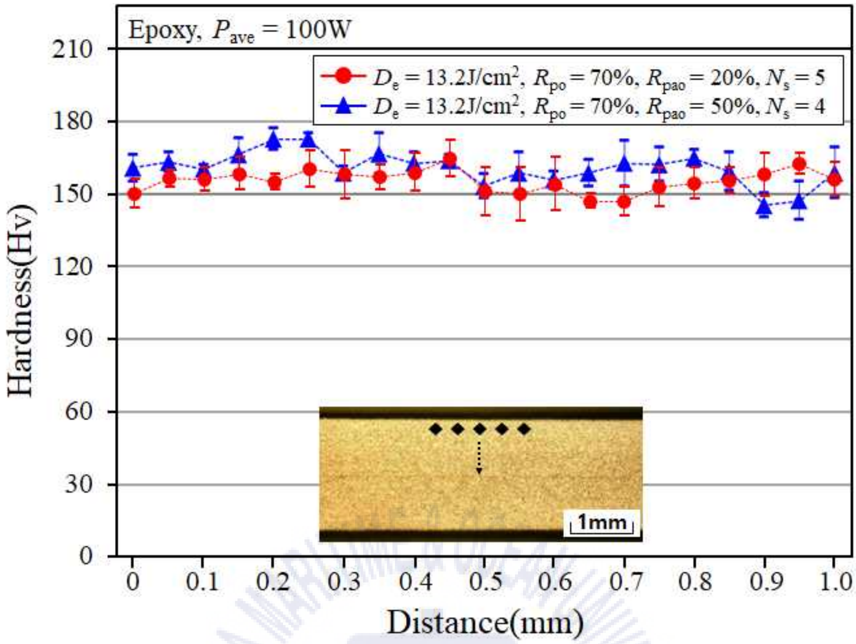

Fig. 4.49 Hardness distribution of laser cleaned epoxy surface

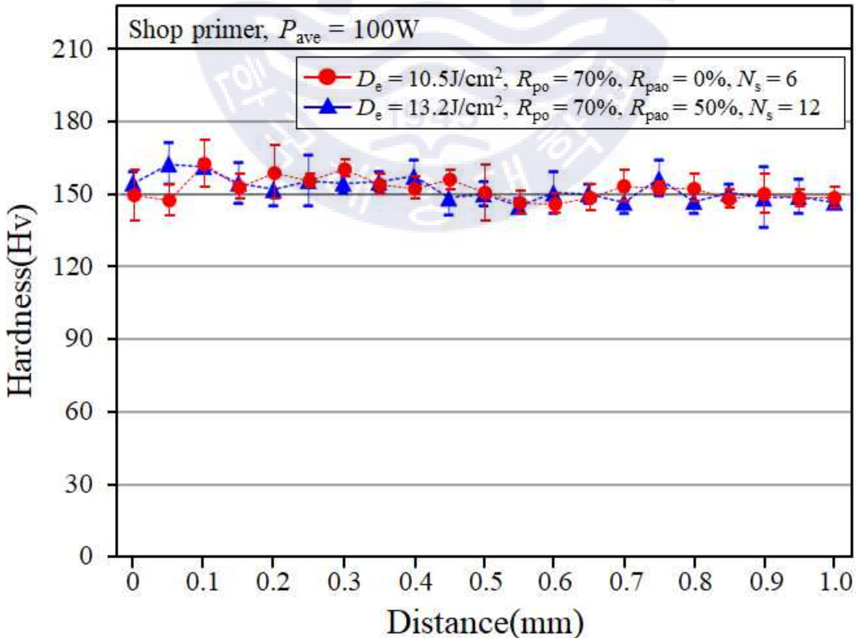

Fig. 4.50 Hardness distribution of laser cleaned shop primer surface

(2) Analysis of the microstructure

The microstructures of the laser cleaned surface in the optimum efficiency and maximum heat input conditions and the specimen before laser cleaning were compared using an optical microscope and SEM. After observing the microstructures with ×200 magnification[(A)~(C)] using an optical microscope, they were observed at ×1,500[(A-Ⅰ) ~ (C-Ⅰ)] and ×3,000 magnifications[(A-Ⅱ) ~(C-Ⅱ)] using SEM.

Fig. 4.51 shows the microstructure of the laser cleaned surface according to the heat input of the epoxy painted specimen. Zone A shows the microstructure of the specimen before laser cleaning. A non-uniform oxide layer with cracks and 200 ㎛ thick paint layer can be observed on the surface of the substrate. In zone B, the optimal condition, and zone C, the maximum heat input condition, the epoxy paint and oxide layer were fully removed. When compared with the substrate, no change in grain size was observed in either part.

Fig. 4.52 shows the microstructure of the laser cleaned surface according to the heat input of the shop primer painted specimen. When compared with the specimen before laser cleaning in zone A, the laser cleaned areas in zone B, C also showed similar microstructures along the depth from the surface as those of the substrate in the optimum efficiency and maximum heat input conditions. Furthermore, smooth surface geometry with no substrate damage could be obtained in both conditions.

When the mechanical and microstructure characteristics of the laser cleaned area were analyzed, a exellent cleaned area with no heat affected zone and melting zone could be obtained in the optimum efficiency and maximum heat input conditions. It is presumed that the damage of the substrate and thermal effect could be minimized as the paint and oxide layer with a lower boiling point than that of the substrate was selectively removed by evaporation.

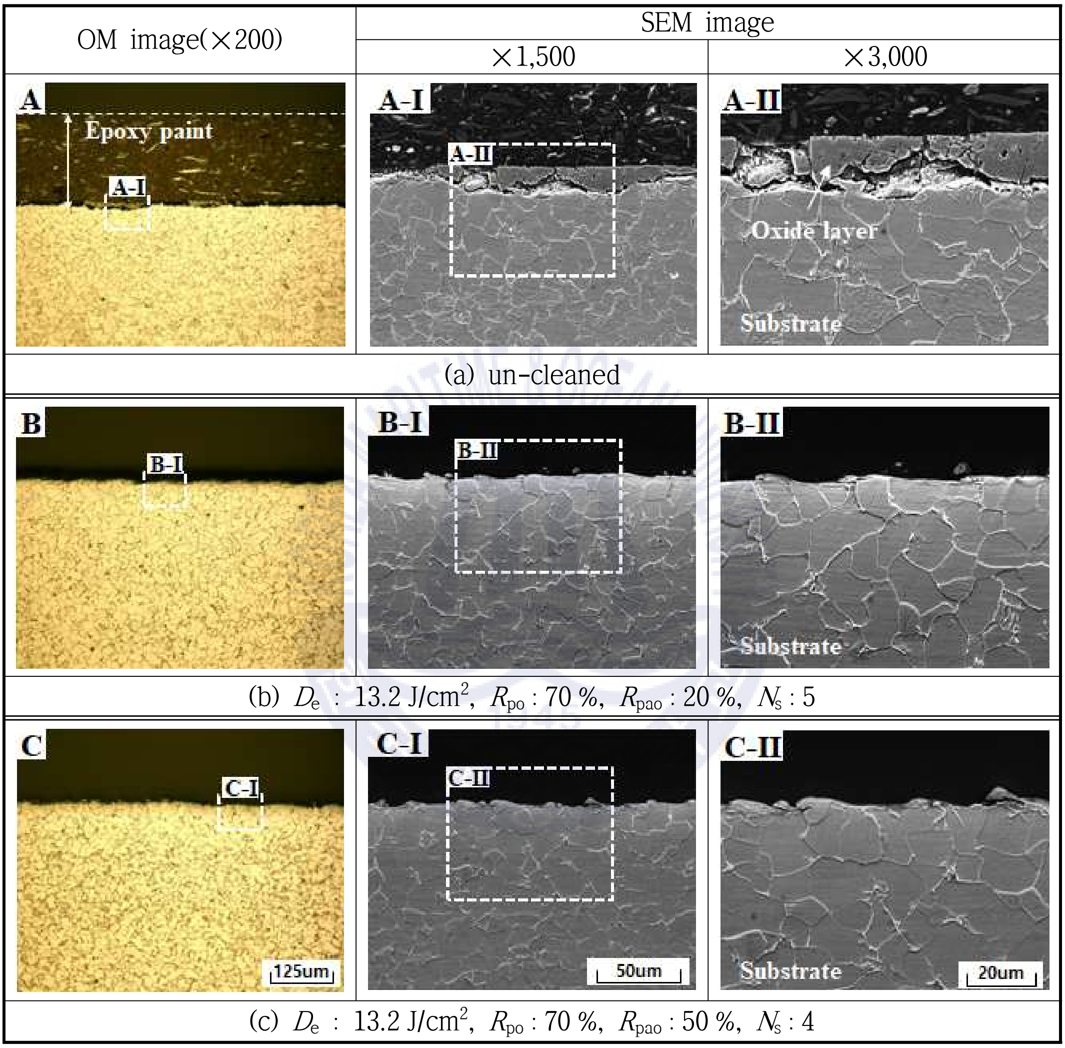

Fig. 4.51 Microstructure of laser cleaned epoxy surface

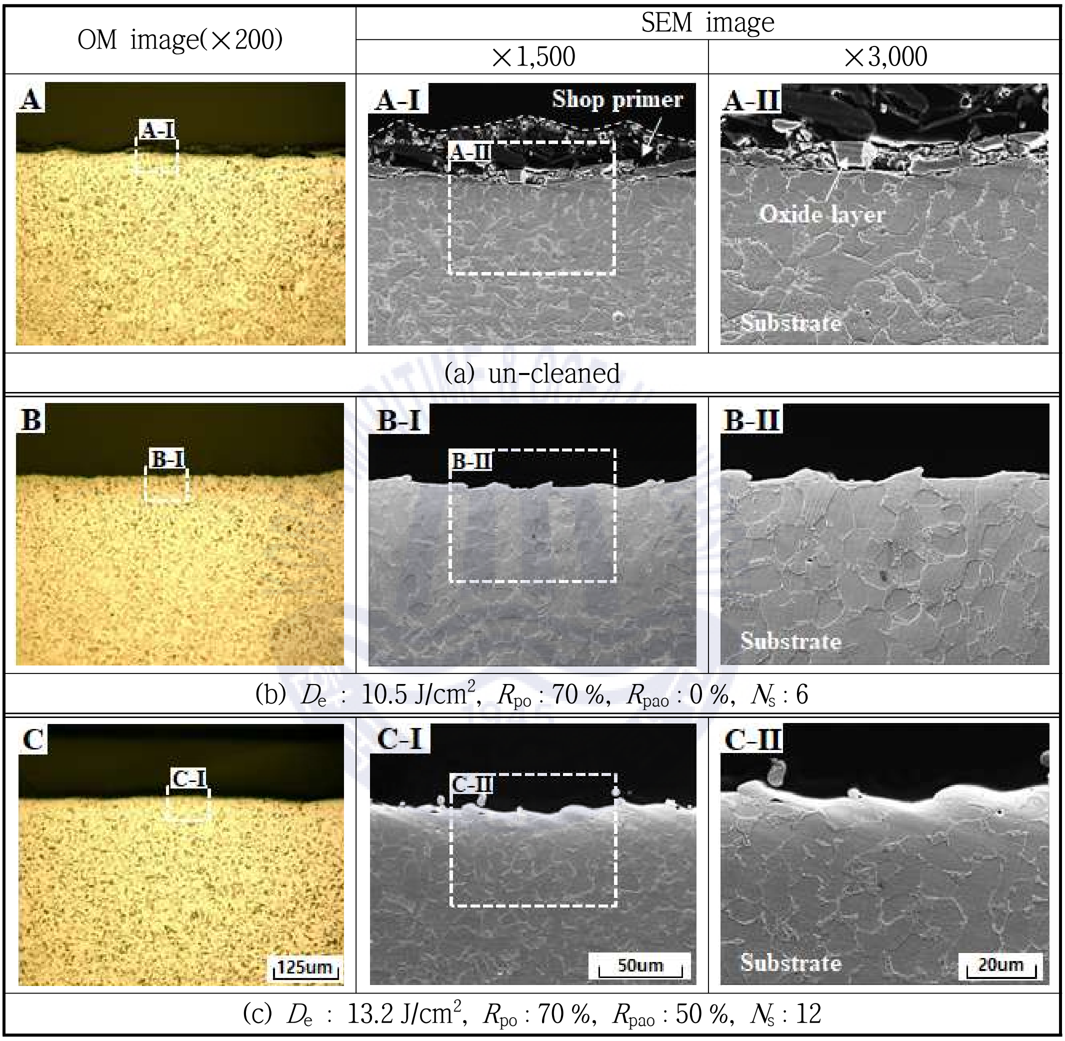

Fig. 4.52 Microstructure of laser cleaned shop primer surface

Chapter 5 Conclusion

In this study, to improve the in-field applicability, laser cleaning was applied to epoxy and shop primer paints used in actual ships using a Q-switching fiber laser with an average power of 100 W. As a fundamental experiment, various laser cleaning characteristics according to the laser process and material parameters applied were identified, and optimal conditions for achieving an efficient laser cleaning were derived.

The results are summarized as follows.

1. As a result of analyzing the laser cleaning characteristics according to the number of scans during the laser cleaning of an epoxy paint, the thickness of the paint and oxide layer decreased as the number of scans increased. The roughness of the specimen before laser cleaning was 2.19 ㎛, whereas the roughness of the painted surface was increased through laser irradiation and then decreased similarly to the that of the base metal when the paint was completely removed. However, the laser irradiation was excessively applied, and thus the base metal was damaged and the roughness increased.

2. As a result of the laser cleaning of epoxy paint according to the pulse and pass overlap rate, as the overlap rate of the laser beam increases, the amount of laser energy irradiated per unit area increases, and thus the paint and oxide layer can be removed with a small number of scans. Thus, damage to the base metal can be minimized.

3. As the energy density increases, the heat input to the material increases, and therefore, the removal amount increases during a single laser scan. Therefore, the number of scans required to remove the epoxy paint and oxide layer was reduced and the roughness according to the energy density

showed a similar tendency.

4. An XRD analysis of the laser cleaned shop primer surface showed that the paint and oxide layer were completely removed with only three scans under the maximum heat input condition with a 70 % pulse overlap, 50 % pass overlap and energy density of 13.2 J/cm^2. Increasing the pulse overlap rate and energy density decreases the laser scan speed, whereas increasing the pass overlap rate increases the number of laser passes irradiated per unit area, thus increasing the heat input to the material. Therefore, it was found that removal effect of the paint and oxide layer was excellent.

5. In a shop primer specimen having a high roughness of 32.28 ㎛ before the laser cleaning, as the laser was irradiated, the roughness decreased because the non-uniform shop primer paint and oxide layer on the surface of the base metal were removed. However, at relatively low overlap rates, damage to the base metal becomes more severe as the number of scans increases, and this tendency is intensified as the energy density increases. By contrast, at a high overlap rate, a gently laser cleaned area with a roughness of 10 to 16.2 ㎛ was obtained regardless of the change in energy density and the number of scans.

6. As a result of examining the optimum laser cleaning efficiency for each paint, an epoxy paint layer of 200 ㎛ in thickness showed the highest efficiency under a high heat input, an energy density of 13.2 J/cm^2, a pulse overlap rate of 70 % and a pass overlap rate of 20 %. In the case of a thin shop primer paint layer with a thickness of 15 ㎛, the most efficient cleaning was possible under an energy density of 10.5 J/cm^2, a pulse overlap rate 70 % and a pass overlap rate of 0 %, in which only the paint and oxide layer can be selectively removed within a short interaction time between the material and laser.

7. As a result of comparing the evaporation characteristics of each paint, it was confirmed that the removal of materials with a relatively low evaporation point was easier during the laser cleaning process of the paint and oxide layer which involves the thermal process and laser ablation. Therefore, the average cleaning efficiency of the epoxy paint was significantly higher than that of the shop primer paint, and the properties of the material significantly influenced the laser cleaning results.

8. As a result of the hardness and microstructure analysis of the laser cleaned specimen under optimum efficiency and maximum heat input conditions, a laser cleaned area without a melting zone or a heat affected zone was obtained. Above results can be used as important data on the application of laser cleaning technology, which has received increased interest in the shipyard industry.

9. Based on this fundamental study, portable laser cleaning equipment with an average power of 100 W will be developed and applied to the field and evaluated regarding its applicability. The paradigm of surface pretreatment in the shipbuilding and offshore industries is thus expected to change.

References

1. Jong Do Kim, So Young Choi, Su Jin Lee, Jeong Suh, 2014. "The Study on Weldability of Boron Steel and Hot-Stamped Steel(Ⅰ)", Trans. Korean Soc. Mech. Eng. A, Vol. 38, No. 12, pp. 1367~1372

2. Jong Do Kim, Eun Jin Lee, Cheol Gyu Kim, 2017. "The Study on Laser Cladding of Heat Resisting Steel Using EuTroLoy 16006 Powder(Ⅰ)", Trans. Korean Soc. Mech. Eng. A, Vol. 41, No. 4, pp. 299-305

3. Ji-Eon Kim, Moo-Keun Song, Jong-Myoung Lee, Jeong-Hoon Hyun, Jong-Do Kim, 2019. "A Study on the Effect of Overlap Rate on Laser Beam Cleaning Characteristics while Cleaning Paint Using a Low Power Pulsed Laser(Ⅰ)", Journal of Welding and Joining, Vol. 37, No. 5, pp. 435-440

4. Ji-Eon Kim, Moo-Keun Song, Jong-Myoung Lee, Jeong-Hoon Hyun, Jong-Do Kim, 2019. "A Study on the Effect of Overlap Rate on Laser Beam Cleaning Characteristics while Cleaning Paint Using a Low Power Pulsed Laser(Ⅱ)", Journal of Welding and Joining, Vol. 37, No. 5, pp. 441-447

5. D.M.D'Addona, S.Genna, A.Giordano, C. Leone, D. Matarazzo, L.Nele, 2015. "Laser Ablation of Primer During the Welding Process of Iron Plate for Shipbuilding Industry", Procedia CIRP 33, pp. 464-469

6. Md. Shamsujjoha, Sean R. Agnew, Mike A. Melia, James R. Brooks, Terry J. Tyler, James M. Fitz-Gerald, 2015. "Effects of laser ablation coating removal (LACR) on a steel substrate:Part1", Surface & Coatings Technology 281, 193-205

7. Q.H. Tang, D. Zhou, Y.L. Wang, G.F. Liu, 2015. "Laser cleaning of sulfide scale on compressor impeller blade", Applied Surface Science 355, pp. 334-340

8. Mohammad Khairul Azhar Abdul Razab, An'amt Mohamed Noor, Mohamad Suhaimi Jaafar, Nor Hakimin Abdullah, Fatanah Mohamad Suhaimi, Mazlan Mohamed, Noraina Adam, 2018. "A review of incorporating Nd:YAG laser cleaing principal in

automotive industry", Journal of Radiation Research and Applied Sciences 11, pp. 393-402

9. A.W, AlShaer, L. Li, A. Mistry, 2014. "The effects of short pulse laser surface cleaing on porosity formation and reduction in laser welding of aluminium alloy for automotive component manufacture", Optics & Laser Technology 64, pp. 162-171

10. Kersten H, Steffen H, Behnke JF, 1996. "Investigations on plasma-assisted surface cleaning of aluminum contaminated with lubricants", Surf. Coat. Technol., Vol. 86-87, pp. 762-768

11. Haboudou A. Peyre P. Vannes AB, Peix G, 2003. "Reduction of porosity content generated during Nd:YAG laser welding of A356 and AA5083 aluminium alloys", Master Sci Eng. A, Vol. 363, No. 1-2, pp. 40-52

12. Dimogerontakis T, Oltra R, Heintz O, 2005. "Thermal oxidation induced during laser cleaning of an aluminium-magnesium alloy", Applied Physics A, Vol. 86, No. 6, pp. 1173-1179

13. R.E. Litchfield, G. W. Critchlow, S. Wilson, 2006. "Surface cleaning technologies for the removal of crosslinked epoxide resin", International Journal of Adhesion & Adhesives 26, pp. 295-303

14. Cooper M, 1998. "Laser cleaning in conservation", London: Butterworth Heinemann

15. F.D.Zhang, H.Liu, C.Suebka, Y.X.Liu, W.Guo, Y.M.Cheng, S.L.Zhang, L.Li, 2018. "Corrosion behaviour of laser-cleaned AA7024 aluminium alloy", Applied Surface Science 435, pp. 452-461

16. M.W.Turner, P.L. Crouse, L. Li. 2006. "Comparison of mechanisms and effects of Nd:YAG and CO_2 laser cleaning of titanium alloys", Applied Surface Science 252, pp. 4792-4797

17. Wang Qiang, Guan Yingchun, Cong Baoqiang, Qi Bojin, 2016. "Laser cleaning of

commercial Al alloy surface for tungsten inert gas welding”, Journal of Laser Applications, Vol. 28, No. 2

18. Abdel-Kareem, O., Harith, M. A., 2008, “Evaluating the use of laser radiation in cleaning of copper embroidery threads on archaeological Egyptian textiles”, Applied Surface Science, Vol. 254, pp. 5854-5860

19. Koh, Y.S., Sarady, I., 2003, “Cleaning of corroded iron artefacts using pulsed TEA CO_2- and Nd:YAG-lasers”, Journal of Cultural Heritage, Vol. 4, pp. 129-133

20. Korenberg, C., Baldwin, A., 2006, “Laser cleaning tests on archaeological copper alloys using an Nd:YAG laser”, Laser chemistry, pp. 1-7

21. Naylor, A., 2000, “Conservation of the eighteenth century lead statue of George Ⅱ and the role of laser cleaning, Journal of Cultural Heritage, Vol. 1, pp. 145-149

22. Sokhan, M., Gaspar, P., McPhail, D.S., Cummings, A., Cornish, L., Pullen, D., Hartog, F., Hubbard, C., Oakley, V., and Merkel, J.F., 2003, “Initial results on laser cleaning at the Victoria & Albert Museum, National History Museum and Tate Gallery”, Journal of Cultural Heritage, Vol. 4, pp. 230-236

23. T. W. Trelenberg, L. N. Dinh, B.C. Stuart and M. Balooch, 2004, “Femtosecond pulsed laser ablation of metal alloy and semiconductor targets”, Applied Surface Science, Vol. 229, pp. 268-274

24. G. Dumitru, V. Romano, H. P. Weber, S. Pimenov, T. Kononenko, M. Sentis, J. Hermann and S. Bruneau, 2004, “Femtosecond laser ablation of diamond-like carbon films”, Applied Surface Science, Vol. 222, pp. 226-233

25. F. Beaudoin, J. Lopez, M. Faucon, R. Desplats and P. Perdu, 2004, “Femtosecond Laser Ablation for Backside Silicon Thinning”, Microelectronics Reliability, Vol. 44, pp. 1605-1609

26. M.W Turner, P.L. Crouse, L. Li, A.J.E. Smith, 2006. “Investigation into CO_2 laser cleaning of titanium alloys for gas-turbine component manufacture”, Applied

Surface Science 252, 4798-4802

27. A. Kumar, M.C. Gupta, 2009. “Surface preparation of Ti-3Al-2.5V alloy tubes for welding using a fiber laser”, Opt. Lasers Eng. 47, pp. 1259-1265

28. A. Kearns, C. Fischer, K.G. Watkins, M. Glasmacher, H. Kheyrandish, A. Brown, W.M. Steen, P. Beahan, 1998. “Laser removal of oxides from a copper substrate using Q-switched Nd:YAG radiation at 1064nm, 532nm, 266nm”, Applied Surface Science 127-129, pp. 773-780

29. Madhukar, Y.K., Mullick, S., Chakraborty, S. S., Nath, A.K., 2013. “Effect of water jet on laser paint removal behaviour”, Procedia Engineering 65, pp. 467-472

30. Hee Dong Lee, 2010, “Anti-corrosion properties of nanocomposite paints”, University of Ulsan

31. 이학렬, 2004. “금속부식공학”, 연경문화사

32. Drazic D., Stojan S., Kulenovic, Z., 2011. “Corrosion protection in shipbuilding”, 14th International Conference on Transport Science ICTS 2011

33. Baek K.K., Chung M.K., Lee H.I., Lee C.H., C.S.Shin Hyundai, 2005. “Effect of retaining preconstruction primer (PCP) on the quality of high performance protective coatings systems”, Nace International

34. Ault J. P., 2011. “Retention of Pre-Construction Primers During Shipbuilding”, SSPC 2011 Conference Proceedings, pp. 1-9

35. Knudsen Ole O., Steinsmo U, Bjordal M, 2005. “Zinc-rich primers-Test performance and electrochemical properties”, Progress in Organic Coatings 54, pp. 224-229

36. Seki Y., Kondou K., Harada O., 2007. “The Third Generation Shop Primer and Japanese Shipbuilding Construction Process”, International Symposium on Shipbuilding Technology, pp. 37-44\

37. Seung-Seok Lee, Joon Hyun Lee, Ik Keun Park, Sung-Jin Song, Man, Yong Choi, 2006. “The Weldability of Primer-Coated Steel for Shipbuilding by CO_2 Laser”, Key Engineering Materials, Vol. 321-323, pp. 1745-1749

38. Hyeyoun Lee, 2014. “Optimization of Hd:YAG Laser Cleaning for Metallic Artifacts Conservation”, Kongju National University

39. 이종명, 2002. “레이저와 청정가공”, 한림원

40. Jung-Han Lee, 2012. “A study on Photothermal and photomechanical ablation characteristics and analysis of 355nm UV laser micromachining”, Pusan National University

41. IL-Young Chung, 2010. “Femtosecond Laser Ablation Characteristics for Industrial Application and Estimation of Processing Quality”, INHA University

42. C. Momma, S. Nolte, B. N. Chichkov, F. v. Alvensleben and A. Tunnermann, 1997. “Precise laser ablation with ultrashort pulses”, Applied Surface Science, Vol 109, pp. 15-19

43. M. E. Fermann, A. Galvanauskas and G. Sucha, 2003. “Ultrafast Lasers: Technology and Applications”, Marcel Dekker

44. Mi-rae Lim, 2016. “Improved ablation efficiency of ultrafast laser by parameter optimization process”, Chungnam National University

45. Jae Yong Oh, 2008. “A study on micro patterning and applications using 355nm UV laser”, Pusan National University

46. B.S. Shin, J.Y. Oh, H. Sohn, 2007. “Theoretical and experimental investigations into laser ablation of polymide and copper films with 355-nm Nd:YVO4 laser”, Journal of Materials Processing Technology, Vol. 187-188, pp. 260-263

47. W. Zhang, Y.L. Yao, 2001. “Microscale Laser Shock Processing-Modeling, Testing and Microstructure Characterization”, Journal of Manufacturing Processes, Vol. 3, No. 2

48. T. Hu, Z. Yao, J. Hu, 2006. “3-D FEM simulation of Laser Shock Processing”, Surface & Coatings Technology 201, pp. 1426-1435

49. 김종도, 김영식, 2012. “알기쉬운 용접·접합공학”, 다솜출판사

50. 김도훈, 2005. “레이저 가공학”, 경문사

51. Mongelli, 2005, “Portable handheld laser small area supplemental coating removal system retrieved from Dayton”, Ohio, United States

52. Metsios, I., Dai, D. C., Chard, S., McComb, T. S., Kwon, Y. K. 2018. “High Pulse Eenergy kW average power nanosecond lasers enable breakthrough in rapid coating removal”, Proc. SPIE: High-power laser materials processing: Applications, diagnostics, and systems VII, Vol. 10525, pp. 1-12

53. Poprawe, R. 2011. “Tailored light 2: Laser application technology”, Berlin, Springer

54. Targowski, P., Ostrowski, R., Marczak, J., Sylwestrzak, M., Kwiatkowska, E. A., 2009. “Picosecond laser ablation system with process control by Optical Coherence Tomography”, SPIE europe optical Metrology, munich, Germany

55. Madhukar, Y. K., Mullick, S., Shukla, D. K., Kumar, S., Nath, A. K., 2012. “Effect of laser operating mode in paint removal with a fiber laser”, Applied Surface Science 264, pp. 892-901

56. Lawrence, J., Minami, K., Li, L., Edwards, R. E., Gale, A. W., 2002. “Determination of the absorption length of CO_2, Nd:YAG and high power diode laser radiation for a selected grouting material”, Applied Surface Science, Vol, 186, No. 4, pp. 162-165

57. Schmidt, M., Li, L., & Spencer, J., 2003. “An investigation into the feasibility and characteristics of using a 2.5 kW high power diode laser for paint stripping”, Journal of Materials Processing Technology, Vol. 138 No. 1, pp. 109-115

감사의 글

석사과정을 입학한지 엊그제 같은데 벌써 2년이라는 시간이 흘러 졸업을 앞두고 있습니다. 석사 학위 청구논문 작성을 마치며 지금까지 저를 응원해 주시고 발전 할 수 있도록 도움을 주신 분들께 감사의 인사를 올립니다.

가장 먼저, 학문은 물론이며 연구자의 자세에 대한 가르침을 주신 존경하는 김종도 지도교수님께 감사인사 드립니다. 연구에 대한 열정과 교수님의 성실함을 본받아 훌륭한 연구자로 거듭날 수 있도록 노력하겠습니다. 더불어 바쁘신 와중에도 예리한 논문심사를 해주시며 논문 전체의 숲을 볼 수 있도록 지도해 주신 이명훈 교수님, 늘 진심어린 조언과 심사로 학문적 도움을 주셨던 강준 교수님께 진심으로 감사드립니다. 더불어 학부 때부터 부족한 저를 너무나도 이뻐해 주셨던 해양플랜트운영학과 조권회 교수님, 이상태 교수님, 이명호 교수님, 이강기 교수님께도 감사인사 드립니다.

다음으로, 연구실 생활에서 어려움이 있을 때 항상 뒤에서 해결해주시고 제 상황을 잘 이해해주시는 송무근 실장님께 감사인사 드립니다. 그리고 입학 후 연구실에 잘 적응 할 수 있도록 많은 도움을 준 박수한 오빠, 김지성 오빠와, 뵐 때 마다 유쾌한 명기훈 오빠에게 감사인사 드립니다. 또 곧 입학할 이기훈 오빠, 정제한 친구에게 응원의 말 전합니다. 연구실의 기둥으로 소중한 조언과 격려를 아끼지 않으셨던 오재환 사장님, 김평수 소장님, 이창제 선배님과, 제 박사과정 진학을 누구보다 응원해 주시는 오상진 이사님, 이종명 박사님께 감사인사 드립니다. 여성 연구자로써 제 롤모델인 이수진 박사님과 항상 발전하기 위해 쉬지 않는 모습을 보여주시는 여준섭 선배님께도 감사인사 드립니다.

레이저 클리닝에 관한 독창적 연구를 할 수 있도록 도움을 주신 대우조선해양 한명수 소장님, 이돈진 부장님, 조연호 연구원님, 현정훈 연구원님과 IMT 최한섭 부장님께 감사인사 드립니다. 표면공학 실험실의 박준무 선배님, 김순호 오빠, 서범덕 오빠, 동기 박기동, 김용성 오빠, 김효진 친구와 NEO 실험실의 김대영 오빠, 양현수 오빠에게도 감사의 말을 전합니다.

마지막으로 물심양면으로 저에게 지원을 아끼시지 않는 부모님과 언니, 형부에게도 감사와 사랑을 표합니다. 지면 관계상 언급하지 못한 많은 분들께도 감사의 말씀 드립니다.

2020년 2월

김지언